Petrography, Geochemistry and Structure of the Timmins area, Ontario

by

CRAIG WILLIAM CHARLES PAYNE

A thesis submitted to the Department of Geological Sciences
in fulfilment of the requirements
for the degree of
Master of Science

BROCK UNIVERSITY

ST. CATHARINES, ONTARIO

OCTOBER, 1978

In Memory of Bruce L. Payne

ABSTRACT

Regional structural analysis of the Timmins area indicates four major periods of tectonic deformation. The D_1 deformation is characterized by a series of isoclinal F_1 folds which are outlined in the study area by bedding, pillow tops and variolitic flows. The D_2 deformation developed the Porcupine Syncline and refolded the F_1 folds about a NE. axis. A pervasive S_2 foliation developed during low grade (greenschist) regional metamorphism associated with the D_2 deformation. The S_2 foliation developed south of the Destor-Porcupine Break. The third phase of tectonic D_3 deformation is recognized by the development of a S_3 sub-horizontal crenulation cleavage which developed on the plane of the S_2 foliation. No mesoscopic folds are associated with this deformation. The S_3 crenulation cleavage is observed south of the Destor-Porcupine Break. The D_4 tectonic deformation is recorded as a subvertical S_4 crenulation cleavage which developed on the plane of the S_2 foliation and also offsets the S_3 crenulation cleavage. Macroscopic F_4 folds have refolded the F_2 axial plane. No metamorphic recrystallization is associated with this deformation. The S_4 crenulation cleavage is observed south of the Destor-Porcupine Break.

Petrographic evidence indicates that the Timmins area has been subjected to pervasive regional low grade (greenschist) metamorphism which has recrystallized the original mineralogy. South of the study area, the Donut Lake ultramafic lavas have been subjected to contact medium grade (amphibolite facies) metamorphism associated with the intrusion of the Peterlong Lake Complex.

The Archean volcanic rocks of the Timmins area have been subdivided into komatiitic, tholeiitic and calc-

alkaline suites based on Zr, TiO_2 and Ni. The three elements were used because of their relative immobility during subsequent metamorphic events.

Geochemical observations in the Timmins area indicates that the composition of the Goose Lake and Donut Lake Formations are a series of peridotitic, pyroxenitic and basaltic komatiites. The Lower Schumacher Formation is a sequence of basaltic komatiites while the upper part of the Lower Schumacher Formation is an intercalated sequence of basaltic komatiites and low TiO_2 tholeiites. The variolitic flows are felsic tholeiites in composition and geochemical evidence suggests that they developed as an immiscible splitting of a tholeiitic magma. The Upper Schumacher Formation is a sequence of tholeiitic rocks displaying a mild iron enrichment. The Krist and Boomerang Formations are the felsic calc-alkaline rocks of the study area which are characteristically pyroclastic. The Redstone Formation is dominantly a calc-alkaline sequence of volcanic rocks whose minor mafic end members exposed in the study have basaltic komatiitic compositions. Geochemical evidence suggests that the Keewatin-type sedimentary rocks have a composition similar to a quartz diorite or a granodiorite. Field observations and petrographic evidence suggests that they were derived from a distal source and now represent in part a turbidite sequence. The Timiskaming-type sedimentary rocks approach the composition of the felsic calc-alkaline rocks of the study area. The basal conglomerate in the study area suggests that the unit was derived from a proximal source.

Petrographic and geochemical evidence suggests that the peridotitic and pyroxenitic komatiites originated as a 35-55% partial melt within the mantle, in excess of 100 Km. depth. The melt rose as a diapir with the subsequent

effusion of the ultramafic lavas.

The basaltic komatiites and tholeiitic rocks originated in the mantle from lesser degrees of partial melting and fractionated in low pressure chambers. Geochemical evidence suggests a "genetic link" between the basaltic komatiites and tholeiites.

The calc-alkaline rocks developed as a result of the increase in PO_2 in the magma chamber. The felsic calc-alkaline rocks are a late stage effusion possibly the last major volcanic eruptions in the area.

ACKNOWLEDGEMENTS

The author wishes to thank Dr. W. T. Jolly and Dr. M. J. Kennedy of the Department of Geological Sciences, Brock University, for their field assistance, comments and suggestions during critical reading of this thesis.

The author also thanks Dr. P. A. Peach for helpful suggestions and critical reading of this manuscript.

Many special thanks to Mr. Mehran Tabatabai, Mr. Medhi Ghorashi-Zadeh and all the other graduate students in the department for many evenings of stimulating geologic discussions.

Many special thanks to Miss Lu-Anne Crysler for the masterful typing job of this manuscript.

Many thanks to Dr. R. G. Roberts of the University of Waterloo, Waterloo, for reading the manuscript and offering helpful comments.

Also, the author gratefully acknowledges the financial support from The National Research Council, Grant A-128 awarded to Dr. W. T. Jolly.

CONTENTS

LIST OF FIGURES

LIST OF TABLES

List of Plates

CHAPTER I
INTRODUCTION

GENERAL STATEMENT

The Timmins area is one of the most productive gold and base metal mining areas of the Canadian Shield. The Timmins area is situated in the western part of the Abitibi Greenstone Belt of the central Superior Structural Province (Fig. 1). The bedrock of the Timmins area consists of Precambrian volcanic, sedimentary and intrusive rocks.

LOCATION

The area of study includes both Tisdale and Deloro Townships (Fig. 2). Timmins, Schumacher and South Porcupine are the largest centres of population. Access to the area is provided by highway, railroad and an airport. In addition, mining and logging activities have produced a number of overgrown trails and roads.

The topography of the region consists of broad east-west trending ridges interspersed with large areas of sand and gravel. The relief of the area is low ranging from 280 to 400 meters A.S.L.

The study area is covered by the Timmins 42 A/6 and Pamour 42 A/11 topographic maps produced by the Survey and Mapping Branch, Department of Energy, Mines and Resources. Detailed locations of sample numbers are given with reference to the one thousand meter, Universal Transverse Mercator Grid.

PREVIOUS WORK

The Timmins area has been prospected and studied for the past seventy-five years. The first recorded geological and prospecting activities began in the late 1800's when Park (1899) noted the occurence of quartz veins

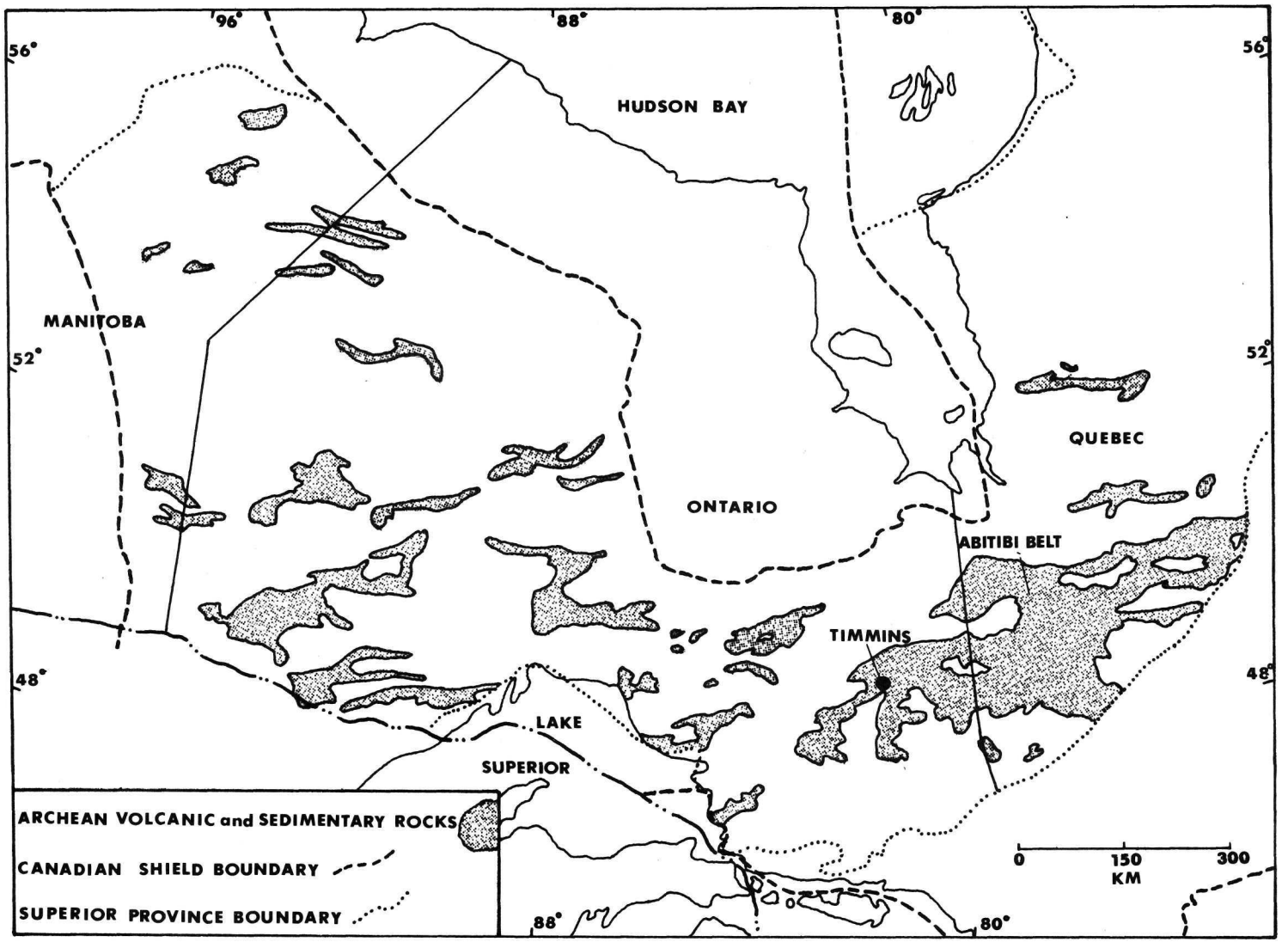
96°
88°
80°
56°
HUDSON BAY
MANITOBA
52°
ONTARIO
QUEBEC
ABITIBI BELT
TIMMINS
48°
LAKE
SUPERIOR
ARCHEAN VOLCANIC and SEDIMENTARY ROCKS
CANADIAN SHIELD BOUNDARY
SUPERIOR PROVINCE BOUNDARY
0
150
300
KM

FIGURE 1

Timmins and Surrounding Area
Location of Study Area

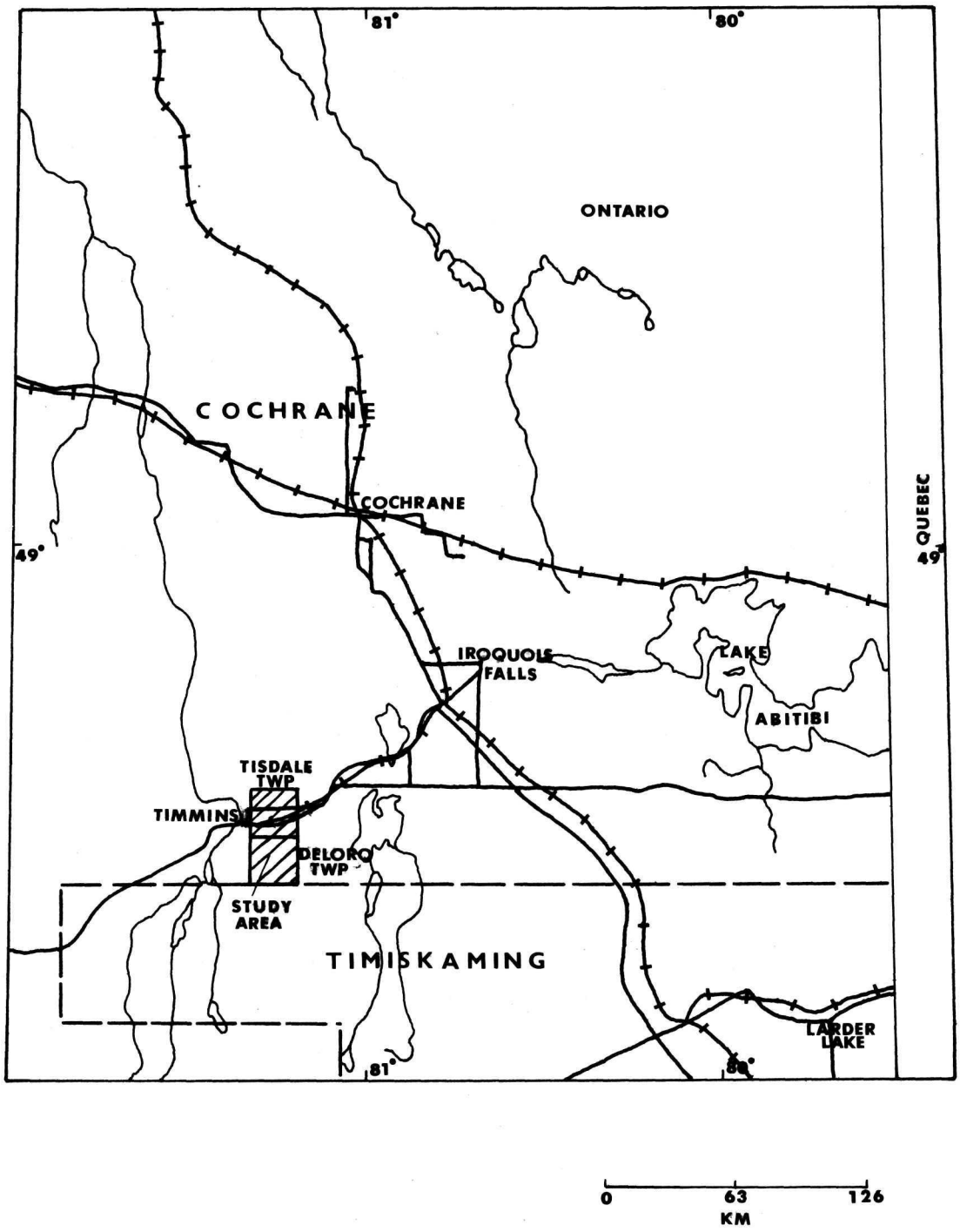

FIGURE 2

in the region which carried traces of gold. Subsequently, in 1909, gold discoveries were made at the present site of the Dome Mine. Further investigation immediately to the west of the Timmins area by Miller (1907) suggested that the volcanic rocks were of Keewatin age. Burrows and Rogers (1910) and Burrows (1911, 1912) published several reports and maps of the Porcupine area. However, in 1915 Burrows reclassified the rocks of the area into: volcanic (Keewatin), sedimentary (Timiskaming), serpentinites (pre-Algoman), granites (Algoman) and diabase dykes (Keweenawan). Further reclassification of the diabase dykes by Burrows in 1924 subdivided them into Matachewan quartz diabase and Keweenawan olivine diabase while the serpentinites became Haileyburian in age. Subdivision of the Keewatin volcanic rocks was first attempted by Graton et al. (1933) using the variolitic marker horizons within the Timmins area. This allowed the correlation of individual and groups of flows throughout the different mine sites. Structural information of the Timmins area reported by Hurst (1936, 1939, 1942) further subdivided the sedimentary rocks into an older (Keewatin) and younger (Timiskaming) series of rocks thought to be separated by an uncomformity. Then in 1948, Dunbar divided the Timmins rocks into the Deloro Group, Tisdale Group, Hoyle Sedimentary Series which is unconformably overlain by the Timiśkaming Series. Conducting underground mapping in several of the mines within the Timmins area, Hogg (1950) placed the serpentinites with the Keewatin lavas using the previously established stratigraphy of Dunbar (1948). Ginn et al. (1964) produced a compilation map with data on the Timmins area. Carlson (1967) working directly to the south of the Timmins area in Ogden, Deloro and Shaw Townships produced a study of the general geology. Ferguson (1956-1958, 1960, 1961, 1962) and Ferguson et al. (1964) produced the most comprehensive study of Tisdale Township which was published in 1968. In that report Ferguson (1968) re-

tained Hursts' (1939) rock classification. Numerous mining geologists have investigated the structure of the Pamour Mine (McIntyre) while Holmes (1964) studied the environment and deposition of gold at the Dome Mine as well as the mines geology. Several geologic field trip guide books have been written on the area by: George (1967), Goodwin et al. (1972), Bright (1973) and George et al. (1975). Pyke (1974, 1975a, b, 1978) studied the area in which he petrographically and chemically differentiated between the Tisdale and Deloro Group rocks which he subsequently subdivided into formations. Pyke retained Dunbars' stratigraphic sequence, however he renamed the sedimentary rocks the Porcupine Group. Pyke also examined the structure of the area. Carnevali (1976) worked extensively on the minor structures of the Timmins area in which he recorded six periods of superposed deformation excluding faulting. Grant (1977) investigated the geochemistry of the Timmins and surrounding area lavas in which he confirmed Pykes' stratigraphic sequence. Roberts et al. (1978) continued Carnevalis' structural analysis of the Timmins area and has described the structures within the Porcupine Syncline.

PURPOSE OF STUDY

The present study was undertaken to investigate and interrelate three major aspects of the Timmins geology:

(a) to investigate on a regional basis the structural history of the Timmins area to determine the sequence of deformational events,

(b) to study the petrography of the different formations of both the Tisdale and Deloro Groups of rocks and their metamorphic history; and,

(c) to investigate the geochemical characteristics

of each formation and their interrelationships.

It is hoped that a better comprehension of these three major aspects of the Timmins geology and their interdependence with each other will aid in the understanding of the area.

GENERAL GEOLOGY

The Timmins area is underlain by an Archean assemblage of low grade supracrustal rocks. The sequence consists of ultramafic to felsic volcanics, clastic sediments (chert and iron formation). These rocks have been complexly folded and faulted and subsequently intruded by sills, dykes and stocks ranging in composition from ultramafic to felsic (Fig. 3).

As mentioned previously, Pyke (1975a, b) has amended the stratigraphic succession of the Timmins area. Based on his field studies and conclusions, the following generalized geologic column is used for the study area (Table 1).

Table 1 Table of Formations (modified after Pyke,1975b)

Cenozoic				Sand, Gravel, Till
				unconformity
Late Precambrian				Diabase Dyke
Archean				Diabase Dyke 4 Periods of Deformation Qtz-Feld Porphyry Dunite-Peridotite
	Porcupine Group	Timiskaming Sedimentary Rock		Greywacke, Slate, Conglomerate
				unconformity
		Keewatin Sedimentary Rock		Greywacke, Slate
				conformity-unconformity
	Tisdale Group	Keewatin Volcanic Rock	Krist Formation	Pyroclastic, Tuff, Lapilli tuff, Fragmental, Brecciated, Porphyritic
				conformity-unconformity
			Schumacher Formation	Mafic to Intermediate Pillowed Flows, minor Fragmental Rocks, Interflow Sediments
			Goose Lake Formation	Ultramafic Flows, Pillowed, Polyhedral Jointing
				(nature of contact unknown) faulted?
	Deloro Group		Boomerang Formation	Intercalated Tuff, Pyroclastic, Brecciated Porphyritic, Iron Formation
			Redstone Formation	Mafic to Intermediate Pillowed, Tuff, Lapilli Tuff, Fragmentals
				relationship unknown
			Donut Lake Formation	Thin Massive Flows

GENERAL GEOLOGY OF THE TIMMINS AREA

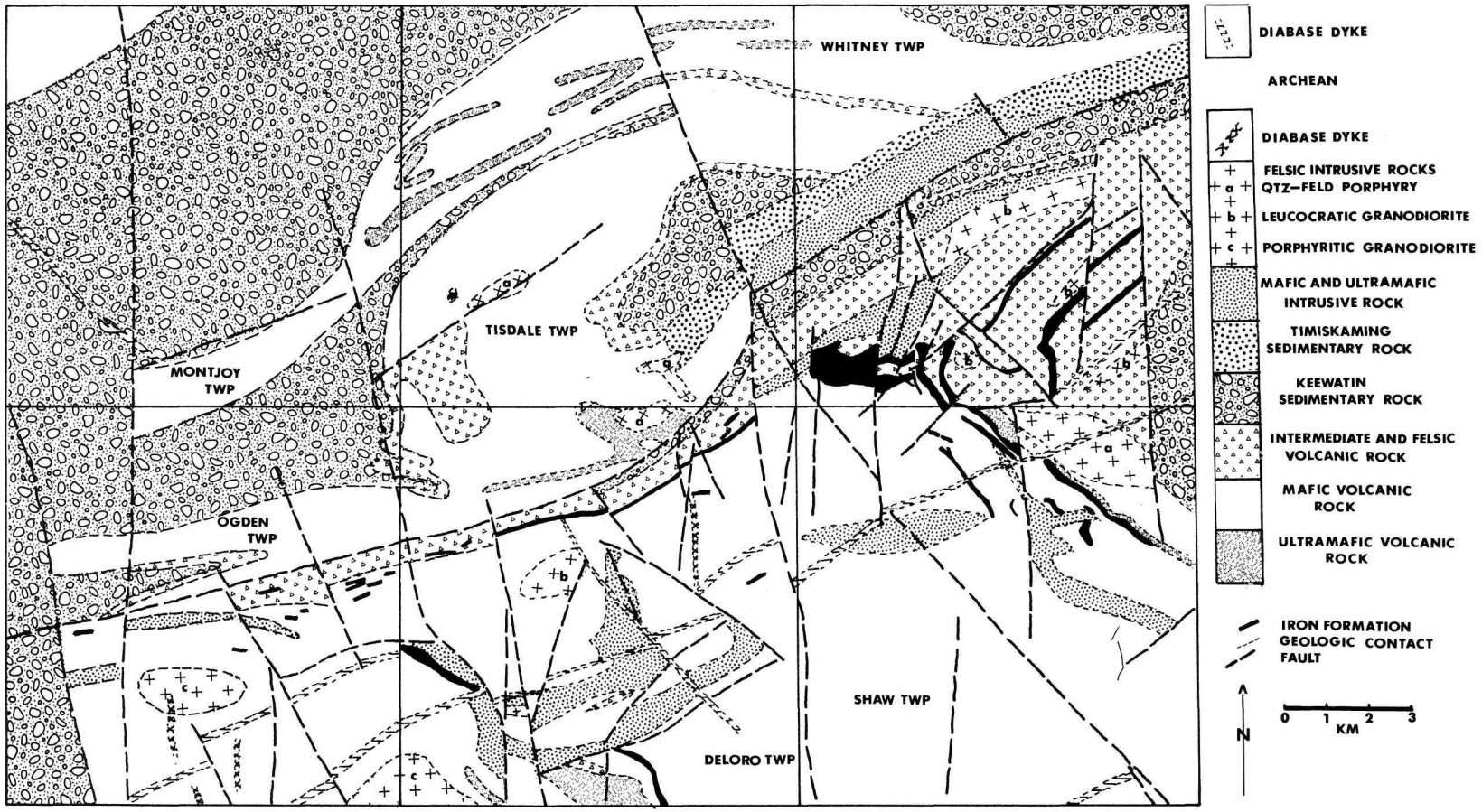

FIGURE 3

The geographic disposition of the formations are presented in Figure 4.

The volcanic rocks are referred to as Keewatin while the sedimentary rocks are referred to as Keewatin-or Timiskaming-type. The terms are used as lithological rather than in a time classification sense.

The Keewatin volcanic rocks are divided into the Deloro and Tisdale Groups structurally separated in the study area by the Destor-Porcupine Break. Pyke (1974, 1975a,b) has further subdivided the groups into six formations; three formations for each group. A geologic map of the study area is presented in Figure 5.

In the study area, the Deloro Group consists of a sequence of ultramafic rocks (Donut Lake Fm.) near Donut Lake, a series of thick, stubby mafic to intermediate commonly porphyritic flows with minor intercalated iron formation (Redstone Fm.) and a series of felsic porphyritic, brecciated, tuffaceous sequences (Boomerang Fm.). Also associated with this group are mafic and ultramafic intrusive rocks.

The Tisdale Group is composed of a well defined succession of ultramafic rocks (Goose Lake Fm.) and dominantly mafic to intermediate pillowed lavas which are intercalated with minor carbonaceous and chemical sedimentary rocks (Schumacher Fm.). Within the Schumacher Formation is a stratigraphically restricted series of variolotic (commonly pillowed) flows. Overlying the Schumacher Formation is felsic pyroclastic, porphyritic, brecciated and tuffaceous sequences (Krist Fm.) Subvolcanic quartz-feldspar porphyry dykes and stocks locally intrude the volcanic pile.

The supracrustal sedimentary rocks (greywacke, slate and conglomerate) are assigned to the Porcupine Group, which has been further subdivided (Pyke, 1975a) into Keewatin and Timiskaming-type rocks in order to explain their uncon-

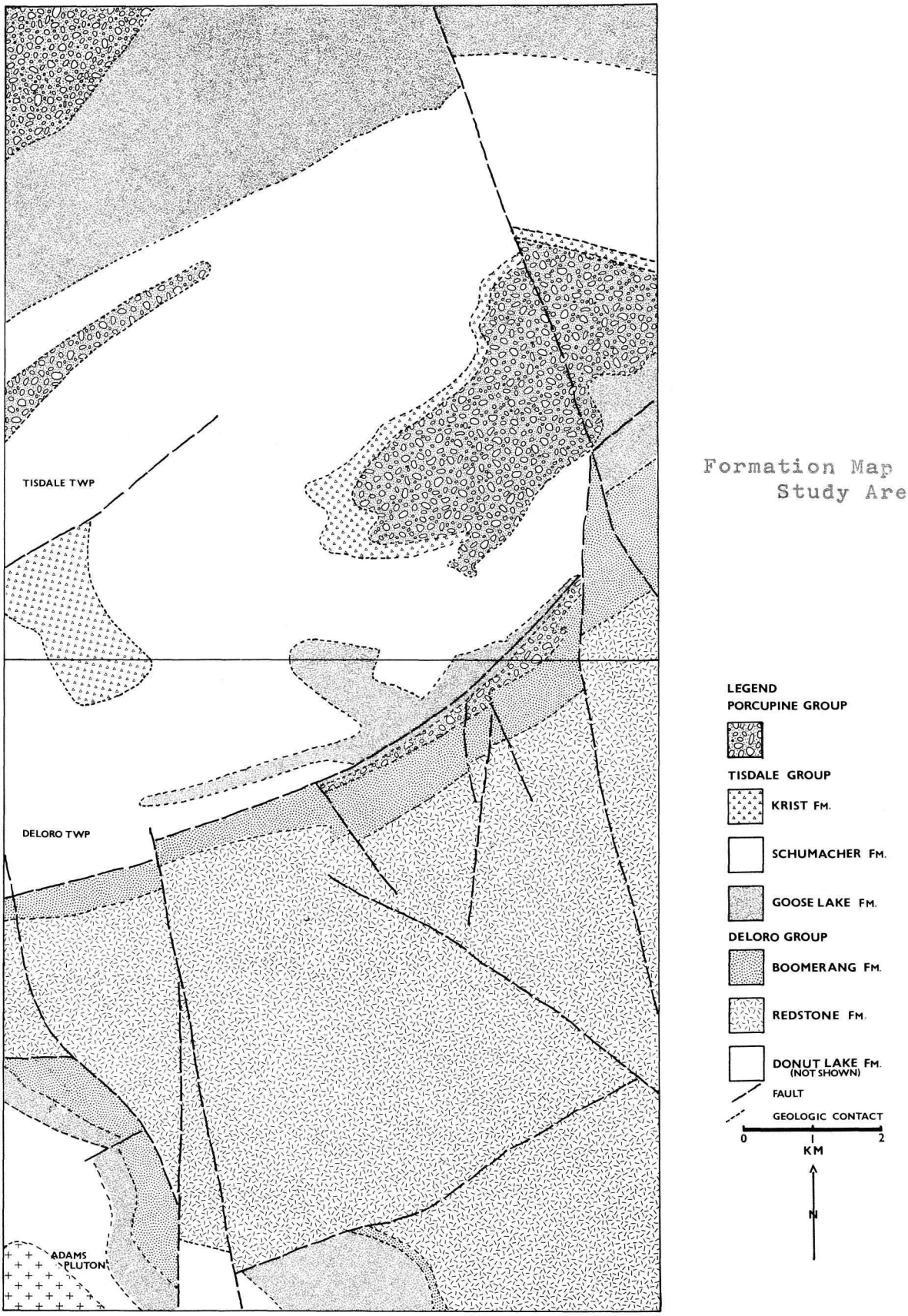

Formation Map of the Study Area

FIGURE 4 (After Pyke, 1974)

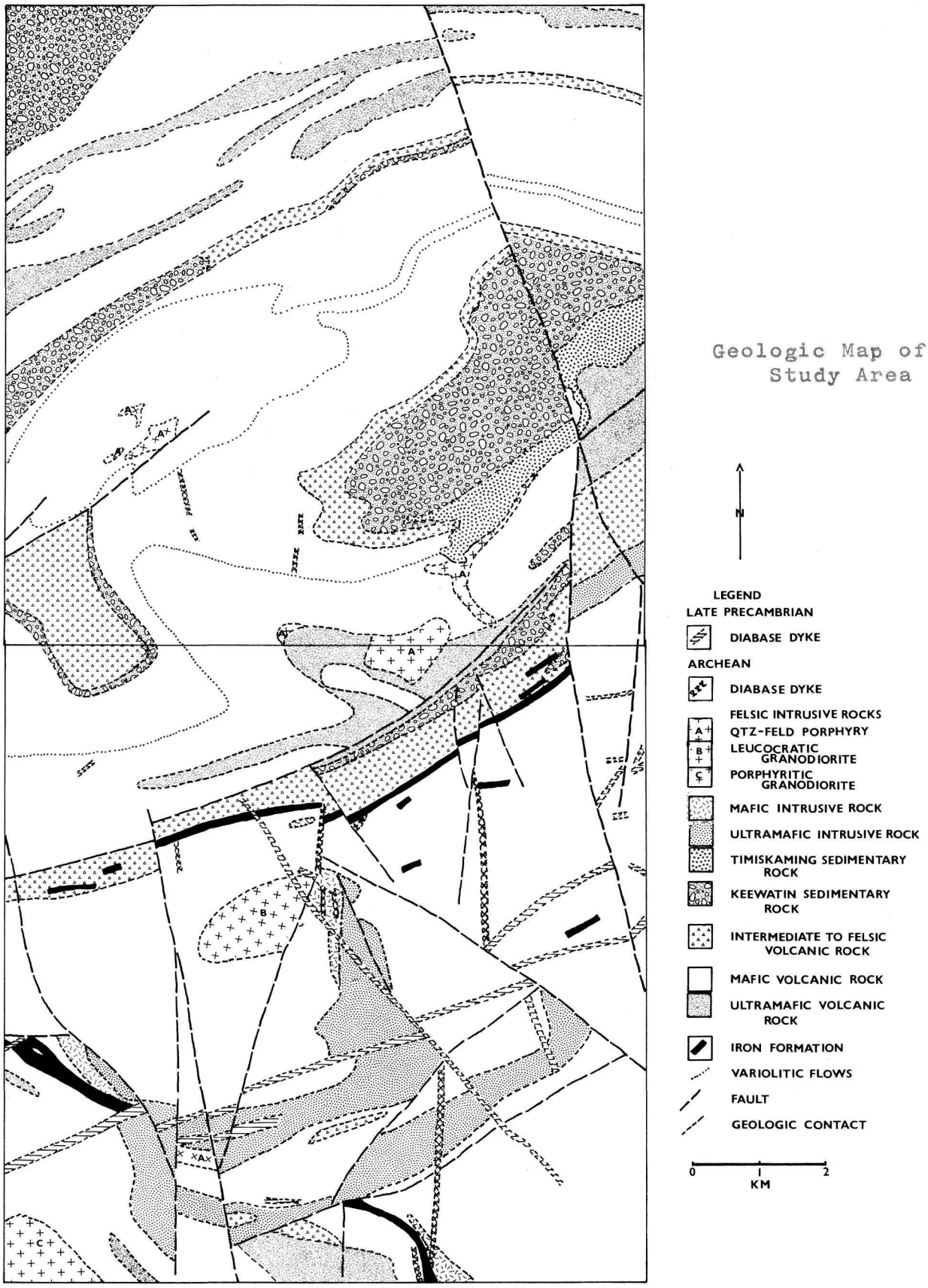

FIGURE 5 (After Pyke, 1974)

formable stratigraphic relations.

North-east to north-west trending diabase dykes of Early to Late Precambrian age transect all other rocks of the region (Pyke et al., 1973; Pyke, 1975a,b).

The bedrock surface of a large portion of the study area is covered by a thick sequence of sand, gravel glacial drift and by swamp.

CHAPTER II
STRUCTURE

GENERAL STATEMENT

The mesoscopic and macroscopic structural features of the Timmins area indicate a polyphase deformational history. The major features are a series of large scale anticlines and synclines refolded to produce a central syncline. Subsequent deformational events resulted in minor changes to the earlier structures.

STRUCTURAL OBSERVATIONS

Prelithification deformational features are observed in the fine-grained sedimentary rocks of the Timmins area. Localized disturbances within the sedimentary rocks are: small scale folding, draping , disruption of bedding, flame structures and scouring. In several localities folding and draping are truncated by disrupted bedding while other localities indicate a gradation into undisturbed bedding. Twenhofel (1950) and Roberts et al. (1978) suggested that these structures are due to sliding and differential loading of the sediments. The differential loading of sediments cause development of folds on the flanks of areas experiencing high load pressures (Cooper, 1943). Field evidence suggests that deformation was contemporaneous with sedimentation because disturbed horizons are overlain by undisturbed beds. In the Timmins area, during sedimentation, disturbances of this sort could have been caused by seismic activity associated with volcanism.

The Timiskaming-type sedimentary rocks unconformably overlie the Keewatin-type rocks in the Timmins area (Burrows 1924; Hurst, 1939; Bass, 1961; Ferguson, 1968; Pyke, 1975a). The unconformity is represented by a conglomerate at the base

of the Timiskaming-type rocks containing fragments of the underlying Keewatin-type sedimentary rocks. Also, a divergence of strike exists at sample location 135, 136 of 36°-40°. Pyke (1975a) suggested that the unconformity is of local importance only and may represent a channel fill environment. However, the map pattern (Fig. 5) suggests that it is more extensive and probably regional. Timiskaming-type sedimentary rocks occur in only the south and south-eastern part of the Porcupine Syncline (Fig. 5). The Timiskaming conglomerate is also in unconformable contact with the Schumacher and Krist Fms. as well as Keewatin-type sedimentary rocks. Field observations at sample locations 135-136 indicate a joint set which is perpendicular to bedding in the underlying Keewatin-type sedimentary rocks. In addition, angular blocks bounded by joint planes were removed and subsequently infilled with conglomerate. This suggests a period of diagenesis and jointing followed by erosion prior to the deposition of the Timiskaming-type sedimentary rocks.

Pebbles in the conglomerate are greywacke, slate, iron formation, dacite porphyry, mafic to intermediate volcanic rocks and minor granitic pebbles (Bass, 1961). The presence of granitic pebbles in the conglomerate suggests a less local source than the other pebbles which are identical to adjacent formations. Carnevali (1976) studied the unconformable contact in detail and geometrically rotated the contact back to a subhorizontal position prior to deposition of the Timiskaming-type rocks. Carnevali concluded that an inclined surface of 39° represented the attitude of the Keewatin-type rocks which he stated is approximate due to the effects of later deformations. This tilting developed an inclined monoclinal surface upon which the Timiskaming-type rocks were deposited. Another conformable-unconformable contact exists between the Krist and Schumacher Fms. (Ferguson, 1968). Where

the stratigraphic section is complete, the Krist Fm. overlies a thin argillite bed. Locally, the map pattern shows that the argillite bed is missing, so that the Krist Fm. lies directly upon the Schumacher Fm. with a presumed angular unconformity (Ferguson, 1968).

PHASE ONE OF TECTONIC DEFORMATION (D_1)

The D_1 tectonic deformation involved the complete sequence of rocks north of the Destor-Porcupine Break (DPB) except the post-Archean diabase dykes. Compressional forces developed a series of isoclinal F_1 folds of which the original attitudes are uncertain. The major series of isoclinal composite folds have wavelengths of 1.0-1.5 km. which vary in their axial trace attitudes due to subsequent deformations. The names and axial traces of the F_1 folds are shown on Fiqure 6. The North Tisdale Anticline is doubly plunging and its axial trace attitude is about 70° NE The North Tisdale Syncline is a complex structure containing felsic pyroclastic rocks (Krist Fm.) and Keewatin-type sedimentary rocks, displaying the conformable-nonconformable contact relationship with the underlying Schumacher Fm. The Central Tisdale Anticline is also a complex structure on whose limbs parasitic folds have developed. The major parasitic folds are: Northern Anticline, Hollinger Anticline, Hollinger Syncline, McIntyre Syncline and Coniaurum Anticline (Ferguson, 1968). Field observations suggest that several fold axial traces are local while others extend for 1-2 Km. The F_1 Vipond Anticline is an arcuate structure in which its axial plane is slightly inclined towards the east. The major F_1 structures are cut by the Burrows Benedict Fault (BBF) to the east. Correlation across the fault is uncertain. A subparallel bedding foliation, S_1 accompanied the F_1 folding in both the Keewatin and Timiskaming-type sedimentary rock.

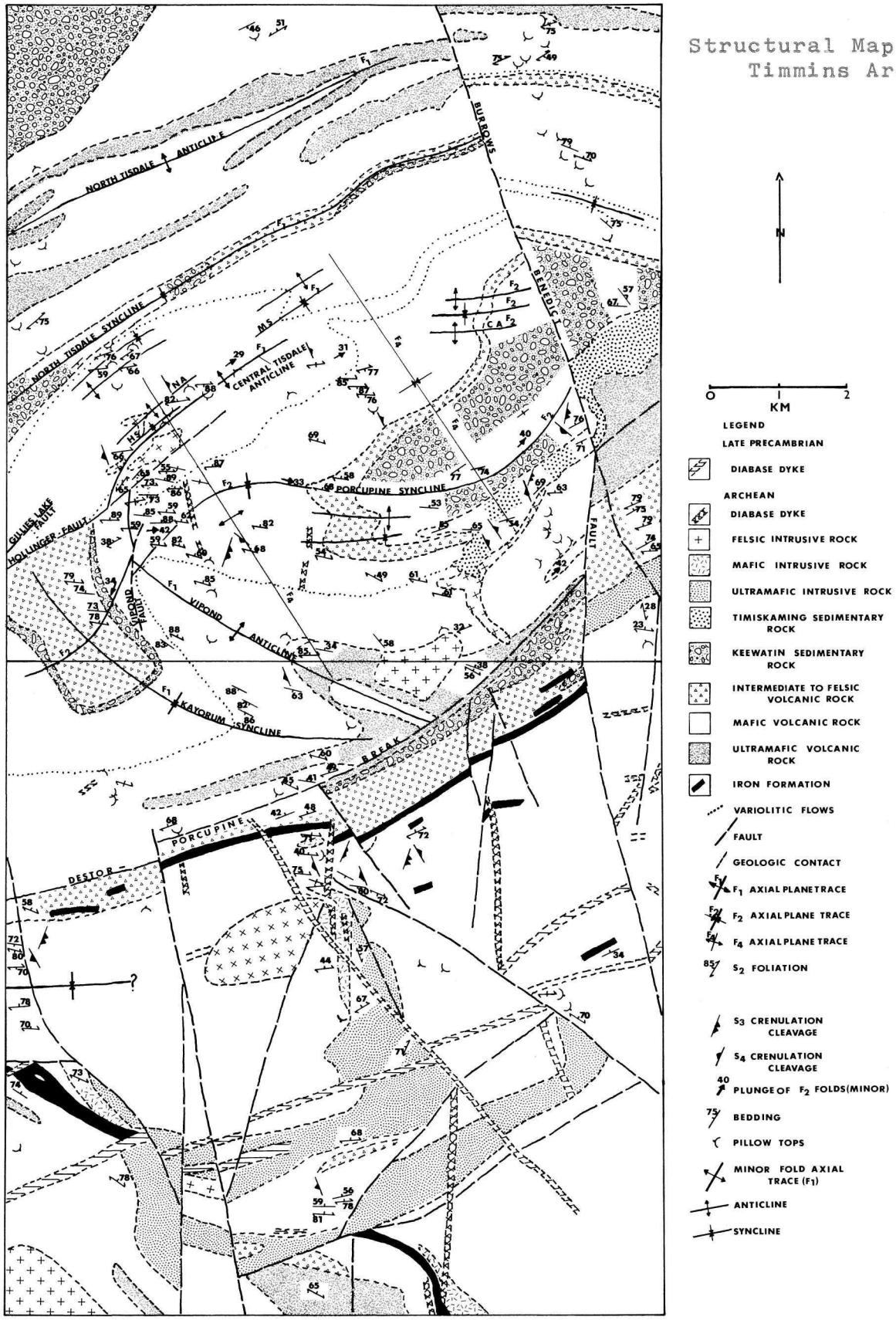

Structural Map of the Timmins Area

FIGURE 6

Alignment of the micaceous (muscovite) material can be traced around the hinge of later F_2 folds. Bedding and pillow tops outline the major anticlines and synclines in the study area (Fig. 6). The apparent reversals of bedding and pillow readings on the limbs of F_1 folds indicate parasitic folding. Continuous variolitic flows are used throughout the Timmins area as stratigraphic marker horizons which also help outline the major F_1 structures (Holmes, 1968; Davies, 1977; Fig. 6).

PHASE TWO OF TECTONIC DEFORMATION (D_2)

The second phase of tectonic deformation was the development of a penetrative S_2 foliation which is axial planar to the F_2 folding. It is well developed in the volcanic rocks both north and south of the DPB. The cross-cutting attitude of the S_2 foliation to the F_1 fold limbs can be observed on Figure 6. Although the S_2 foliation is penetrative in nature, the foliation is not observed in the centre of thick massive flows. The F_2 folding refolded the F_1 structures to produce the Porcupine Syncline. Field observations and map patterns suggest the Porcupine Synclinal axial trace is continuous to the west. The development of the Porcupine Syncline produced a series of mesoscopic anticlinal and synclinal structures in the sedimentary rocks. Bedding facing directions and cleavage-bedding intersections indicate a series of parasitic folds which developed on the major F_2 folds in the Porcupine Syncline (Fig. 7). The axial trace of the parasitic folds parallels that of the larger F_2 folds. Measurement of the plunge attitude of the parasitic folds is 17°-44° NE. Associated with the plunge of the Porcupine Syncline is a stretching lineation L_1 that developed in the Timiskaming conglomerate. Readings of 50 Z and X axes of pebbles were measured according to the method of Ramsay (1967). Average values from the calculations produced a pebble elongation ratio of 3 to 1. However, caution must be taken

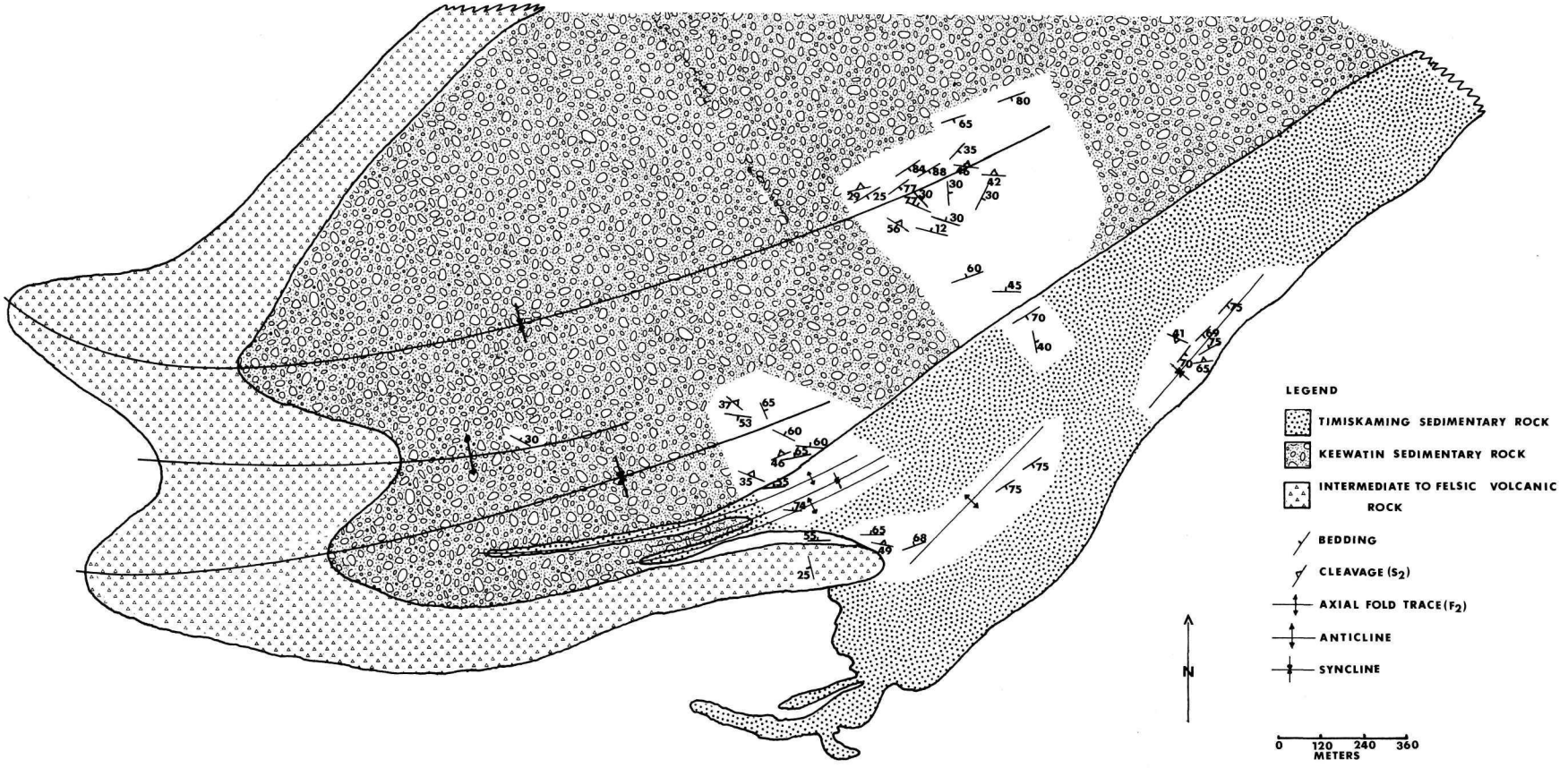

FIGURE 7

Structural Map of the Porcupine Syncline

in using the value since the original pebbles may not have been spherical. Long axis orientation of the pebbles gives an average reading of 47° NE and plunge at 28°. However, plunge measurements west of the Pamour Mine (Hollinger) is to the west. Plunge attitudes on all major F_2 structures are plotted on Figure 6. Plunge directions on the Vipond Anticline change because of its interference pattern with the F_2 Porcupine Syncline. The bell shaped map pattern of the F_1 Kayorum Syncline is caused by its interference with the F_2 Porcupine Syncline. However, the F_1 axial trace of the Kayorum Syncline is truncated by the Hollinger Main Fault (HMF) (Pyke, 1975a; Davies, 1977). Displacement along the HMF is as much as 400 meters (Jones, 1968). The displacement of the HMF and the Gilles Lake Fault intersection is unknown (Jones, 1968). The Vipond Fault and the HMF offset the Vipond Anticlinal axial trace (Pyke, 1975a) of which the displacement is unknown.

THIRD PHASE OF TECTONIC DEFORMATION (D_3)

The D_3 tectonic deformation is recorded as a sub-horizontal S_3 crenulation cleavage which developed on the S_2 foliation. Measurement of the axial plane attitudes of the S_3 crenulation cleavage produced a general reading of 023/27° ESE. The S_3 crenulation cleavage is observed south of the DPB (Fig. 6). The S_3 crenulation cleavage is well developed in the tuffaceous beds, fine grained foliated dacite and pyroclastic lenses. The S_3 crenulation cleavage is obscured somewhat by a well developed S_4 crenulation cleavage in some places (S_4 cleavage which commonly offsets the S_3 crenulation cleavage). In the less ductile material a series of continuous parallel wavy F_3 microfolds developed. This type of microstructure is defined as a crinkle crenulation cleavage (Durney, 1972). Within the more ductile material a

series of microlithons developed separated by microfaults. Williams (1973) defined this as a differential crenulation cleavage. The fine grained pyroclastic material developed a complete series of crenulation cleavages in response to the different mineralogical compositions of the bedding. Field observations and petrographic evidence indicates the S_3 crenulation cleavage overprints the S_2 foliation.

FOURTH PHASE OF TECTONIC DEFORMATION (D_4)

The D_4 deformation was characterized by the development of a series of large, 3 to 4 km. wavelength F_4 folds that refolded the F_2 axial planes (Fig. 6). The attitude of the F_4 folds is NW. The macrostructures are accompanied by the development of a S_4 subvertical crenulation cleavage that is observed overprinting the S_2 foliation. The S_4 crenulation cleavage is observed south of the DPB. Measurement of the axial plane of the S_4 crenulation cleavage produces values of 157/43 E and 158/ 45 W. Associated with the S_4 crenulation cleavage is a fracture cleavage in the sedimentary rocks. It is commonly well developed in the slate interbeds. Ductility contrasts between the slate and greywacke beds deflected the S_4 fracture cleavage to the east. Average attitudes of the S_4 fracture cleavage is 101/47 NE and 099/45 SW.

SUMMARY AND CONCLUSIONS

Field and map observations suggest that the stratigraphic relationships between the Schumacher, Krist, Keewatin and Timiskaming-type rocks range from conformable to unconformable throughout the Timmins area. The regional nature of the unconformities indicate that localized irregularities in topography due to volcanism are only important locally while to explain the regional nature of the unconformities, tectonism must have been active during this period. Previous workers generally agree that a mild to moderate Pre-Timiskaming deformation took place during this time (Graton *et al.*, 1933;

Hurst, 1938; Moore, 1953; Griffis, 1962).

Prelithification deformation is observed as soft sediment folding and slump structures caused by the uneven loading and sliding of the sedimentary rocks (Twenhofel, 1950; Roberts et al., 1978). Disruption of bedding is localized and contemporaneous with sedimentation since bedding directly above the disturbed horizon is not deformed.

The first major period of D_1 deformation developed a series of isoclinally folded rocks. Regional metamorphism may have occurred during this period to the very-low grade (prehnite-pumpellyite facies) (Winkler, 1974). This is supported by the remnant subparallel bedding foliation in the sedimentary rocks associated with the D_1 period of deformation. Further to the east of the study area, textural evidence is observed in the rocks indicating that a very-low grade mineralogy has been overprinted by a regional low grade (greenschist facies) metamorphism (Jolly, 1978). The development of parasitic folding on the limbs of the F_1 folds varies in their axial trace continuation due to subsequent deformational events and lithological differences.

The second tectonic deformation, D_2 resulted in the refolding of the F_1 folds to form the Porcupine Syncline. Associated with the F_2 folding was the development of a pervasive S_2 strain slip foliation which suggest that regional low grade (greenschist facies) metamorphism occurred during this event completely recrystallizing the very-low grade metamorphic textures associated with the D_1 deformation. Field evidence and map patterns suggest that the Porcupine Synclinal axis traverses the entire study area. The development of the S_2 foliation south of the DPB, suggests that movement along the DPB occurred prior to the D_3 deformation since the attitude of the S_2 foliation south of the DPB is not parallel to that north of the DPB. Possibly, the movement along the DPB destroyed the D_1 structures to the

south of it or that movement may have been taken up along existing faults during that time. The S_3 and S_4 crenulation cleavage attitudes are parallel both north and south of the DPB.

The third tectonic deformation, D_3 did not develop any recognizable mesoscopic folding in the study area. The D_3 deformation is characterized by a sub-horizontal S_3 crenulation cleavage which is observed both north and south of the DPB. The S_3 crenulation cleavage is a continuous, wavy set of microfolds that developed on the S_2 foliation.

The development of the fourth tectonic deformation, D_4 culminated in a series of macroscopic (open) folds which have developed a S_4 sub-vertical crenulation cleavage both north and south of the DPB. The F_4 folding has refolded the F_2 axial plane and the S_2 foliation. However, the S_2 foliation was not metamorphically modified by the D_4 deformation. This interpretation of the structural history of the Timmins area varies considerably with previous workers. Recently, Pyke (1975b) produced a structural synthesis of the Timmins area. Pyke (1975b) reported,

> "Isoclinal folding of the ultramafic and mafic volcanic rocks about a north-south axis; folding occurring largely prior to the deposition of the overlying felsic and intermediate volcaniclastic rocks (Krist Fm.) and clastic sedimentary rocks of the upper part of the Porcupine Group. Folding of the metavolcanics and metasediments about a east-west axis giving rise to the Porcupine Syncline."

Pyke believed that this sequence of events accounts for the "doubly plunging" nature displayed by the major structures in the area. It is apparent that Pyke's interpretation is based almost entirely on stratigraphic evidence, which is now modified by the sequence of mesoscopic fabric elements and fold geometry. Further, Pyke concluded that the North Tisdale and Vipond Anticlines are

equivalent and that because the fold pattern developed about a north-south axis prior to the felsic volcanic and sedimentary rock deposition, this effectively moves the major unconformity to the base of the Krist Fm. He further stated that the remaining sequence of felsic and sedimentary rocks were deposited and refolded about a central east-west axis. This interpretation does not explain the joint development in the Keewatin-type sedimentary rocks prior to erosion and Timiskaming sedimentation. It also suggests that the North Tisdale Syncline does not exist. The present investigation of the Timmins structure suggests that the Vipond Anticline and the Central Tisdale Anticline are continuous based on the variolitic marker horizons and the observed interference pattern between the Vipond Anticline and the Porcupine Syncline. Further, the Kayorum Syncline is continuous with the North Tisdale Syncline but the axial trace of the F_1 folds have subsequently been offset by a number of faults (Fig. 6). The major deformational phases, structures and associated metamorphic events are presented in Table 2.

An alternative hypothesis for the weak alignment of muscovite (S_1) is that prior to the D_1 deformation a preferred orientation of clay minerals may have developed during soft sediment deformation and diagenesis. The clay minerals were subsequently recrystallized due to the very low grade (prehnite-pumpellyite) metamorphism to muscovite.

Table 2

Structural and Metamorphic History of the Timmins Area

Phase	Structure	Metamorphism
D_4	S_4 subvertical crenulation cleavage or fracture cleavage; orientation of F_4 axial traces is NNW; wavelength of F_4 folds is 3-4 Km.; S_4 crenulation cleavage is observed south of the Destor-Porcupine Break	
D_3	S_3 subhorizontal crenulation cleavage; no mesoscopic folds observed; S_3 crenulation cleavage is observed south of the Destor-Porcupine Break	
D_2	Penetrative S_2 strain slip foliation or L-S fabric; tectonic development of Porcupine Syncline; axial trace of F_2 folds strike NE.; Porcupine Syncline is continuous to the west; minor, tight to open F_2 folds associated with major F_2 folds	Pervasive Low Grade (Greenschist) Metamorphism
D_1	Weakly developed subparallel to bedding S_1 foliation (recrystallized by subsequent metamorphism; major isoclinal F_1 folds (orientation uncertain); minor parasitic F_1 folds	Very Low Grade (prehnite-pumpellyite) Metamorphism
	Turbidite deposition (Timiskaming-type sedimentary rock) Conglomerate deposition -unconformity- Diagenesis, jointing, uplift, erosion, tilting Soft sediment deformation Turbidite deposition (Keewatin-type sedimentary rocks)	

CHAPTER III
PETROGRAPHY

GENERAL STATEMENT

Petrographic investigation of each formation in the Timmins area, based on a total of 256 thin sections was undertaken to search for primary mineralogy and primary flow or pyroclastic textures, metamorphic mineralogy and textures as an aid in understanding metamorphic grade and secondary mineral assemblages, and in identifying highly altered specimens whose chemical analyses would not be representative of primary lava compositions.

DELORO GROUP

DONUT LAKE FORMATION

Thin section examination of the Donut Lake Fm. ultramafic lavas indicates a different mineralogy in comparison to the ultramafic volcanic rocks in the Timmins area.

Most lavas are medium to fine-grained. Up to 8% olivine is present in several samples but is not generally abundant. In most rocks, olivine occurs as subrounded anhedra exhibiting irregular fractures. Pyroxene, averaging 8% but reaching a maximum of 83%, occurs as rounded to stubby equant grains (Plate 1a). Basal sections, exhibit 87-93° cleavage angles. Most pyroxene is diopsidic in composition as indicated by 2Vs of 58-59°, optically positive and extinction angles ranging from 36 to 44 degrees. Augite is present in small amounts and may be distinguished from diopside by its larger 2V (58-60°) and its lower birefringence. Lath shaped to stubby crystals of hornblende constitute up to 33% of an olivine free rock and averages 8% when present. Many hornblende laths exhibit feathery terminations. The mineral is commonly chloritized. Biotite is rarely present and makes up a maximum of 2% of a rock. It occurs as stubby

shaped grains and is pleochroic in shades of yellowish-brown to brown. Chromium spinel is present in several rocks associated with both olivine and pyroxene. Generally, it is rounded with an opague rim (Cr -rich magnetite?). Rarely, spinel occurs as cubes or octahedral-shaped grains. In plane light, spinel appears dark olive green (picotite) to reddish brown (chromite). The relief of spinel is slightly higher than the surrounding olivine and pyroxene. Spinel never makes up more than 1% of a rock. Feldspar occurs as a minor interstitial mineral.

Alteration minerals make up to 30% of a rock. Anthophyllite-magnesiocummingtonite are most abundant when there is a minimum amount of pyroxene present. The ortho-amphibole occurs as length slow, lath shaped to equant grains with low birefringence, a biaxial positive sign, and when properly orientated parallel extinction (Plate 1b). The mineral exhibits feathery terminations that are commonly altered to chlorite. Chlorite occurs in all samples in varying amounts with a habit ranging from irregular masses to small bladed crystal aggregates. Chlorite replaces amphibole, pyroxene and olivine. Tremolite is present in varying amounts and is rarely observed penetrating altered pyroxene. It may replace the feathery terminations of amphiboles. Minor muscovite occurs interstially in the amphibole rich rocks. Magnetite-ilmenite occur along altered grain boundaries of pyroxene and olivine and as equant grains in unaltered parts of rocks suggesting a primary origin. Olivine alteration is commonly zoned. Magnetite-ilmenite outlines the grain with a serpentine ring along the inside margin while the central part of the grain is olivine or chlorite (Plate 1c). Carbonate is present in several samples commonly occuring in irregular shapes and fills voids or fractures.

PLATE 1

DONUT LAKE FORMATION

a) This photomicrograph is dominated by pyroxene with minor amounts of magnesiocummingtonite (light, centre). One small grain of olivine (light grey, left centre) showing its typical doubly terminated prismatic habit. Polars crossed, X 31.

b) A photomicrograph of a magnesiocummingtonite grain (centre) with a spinel grain situated inside its grain boundaries. The spinel is actually olive-green. An olivine grain exhibiting the diagnostic irregular fracture (left, lower). Pyroxene grain (left, upper). Plane light, X 312.

b_1) This photomicrograph is the same as Plate 1b except rotated 180° with the polars crossed It shows the isotropic nature of the spinel grain and the presence of serpentine (bottom, centre), and an anthophyllite grain (right centre). Polars crossed X 312.

c) A photomicrograph showing magnetite-ilmenite outlining altered grains of olivine and pyroxene. Also serpentine alteration along grain boundaries and within the grains of olivine and pyroxene. Polars crossed, X 125.

PLATE 1

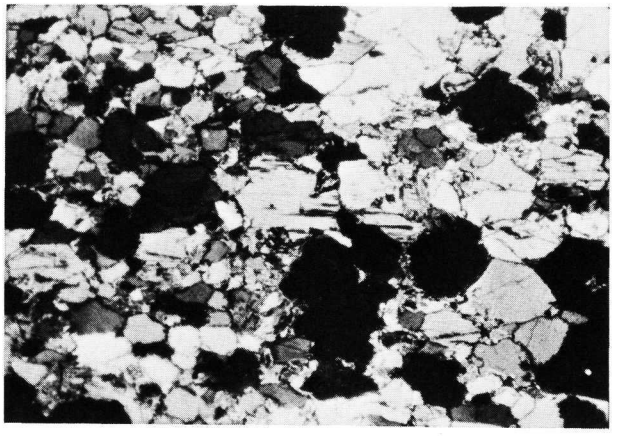

(a)

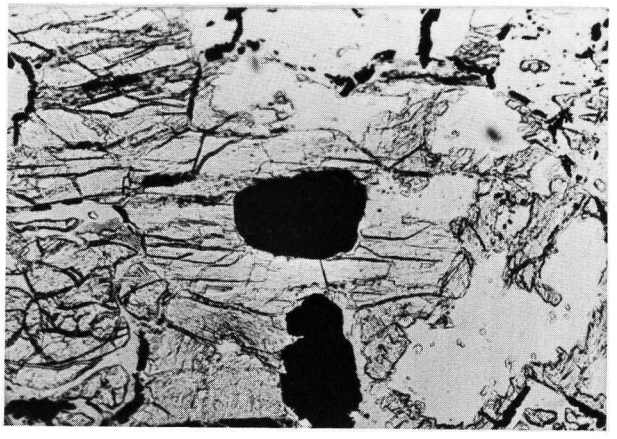

(b)

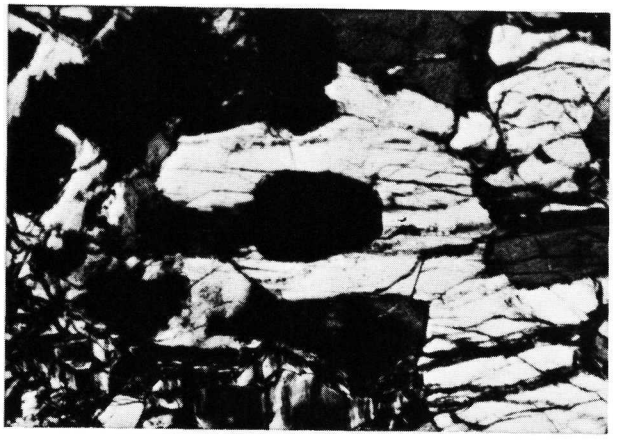

$(b)_1$

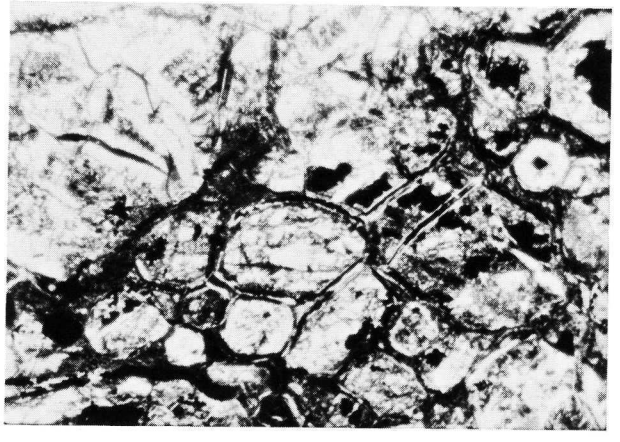

(c)

REDSTONE FORMATION

The Redstone Formation consists of mafic to intermediate volcanic rocks. Intercalated with the volcanic rocks is tuff, lapilli tuff and fragmental lenses. The mafic volcanic flows are commonly pillowed, a few are massive. Field observations indicate most flows pinch out along strike over very short distances. Interlayered iron formation is composed of uniform thinly banded chert, jasper and magnetite. Intermediate lava flows are fine to medium-grained. Pillows were rarely observed in the intermediate flows. Remnants of the original mineralogy are feldspar, quartz, pyroxene and very minor olivine. Most of the volcanic rocks are porphyritic. The feldspar phenocrysts range in size from 0.8 to 1.9 mm. and display ragged lath shapes (Plate 2a). Most have been altered to sericite, chlorite, carbonate and epidote-clinozoisite. Twinning is rarely present, but, a few twins suggest a range in composition from AN_{14} to AN_{32}. There is no preferred orientation to the feldspar laths. Feldspar phenocrysts comprise up to 73% of a rock but the mineral averages 23%. Quartz makes up on average 6%, but ranges a high as 35%. It occurs as strained, rounded phenocrysts or aggregates. Corrosion of quartz grains is common. Pyroxene is rarely observed in the mafic end members (Plate 2b). It is commonly altered to chlorite, epidote-clinozoisite and carbonate. Only one sample contained a grain of partially altered olivine. Rarely, hornblende occurs in the mafic rocks. It is altered to chlorite and/or carbonate. The matrix is composed of fine grained feldspar, quartz, chlorite, sericite, muscovite, actinolite, epidote-clinozoisite, carbonate, sphene, leucoxene, biotite, magnetite, glass and rarely euhedral pyrite. Chlorite is common in the matrix and often forms aggregates of bladed crystals. Epidote-clinozoisite is usually massive but may develop doubly

PLATE 2

REDSTONE FORMATION

a) Photomicrograph showing the porphyritic nature of the Redstone Formation. The phenocrysts are altered and ragged grains of feldspar. Polars crossed, X 31.

b) A photomicrograph showing the remnants of a pyroxene grain (dark grey, centre). The pyroxene grains is surrounded by a matrix of quartz, feldspar, chlorite and epidote-clinozoisite. Plane light, X 31. Plate $2b_1$, Polars crossed, X 46.

c) A photomicrograph showing the relationship between muscovite (right) and the larger grains of actinolite. Actinolite and muscovite are shown in a cross cutting relationship (centre, bottom). Polars crossed, X 125.

PLATE 2

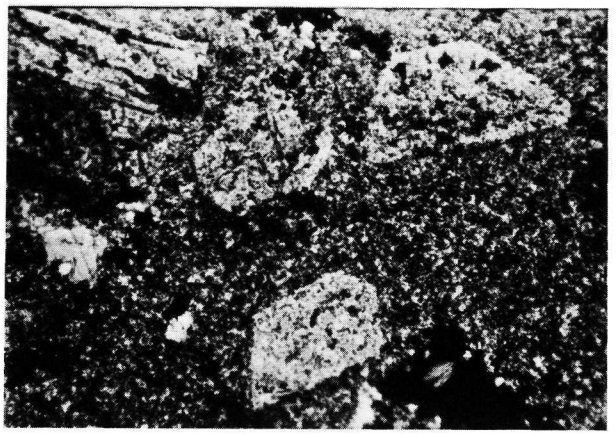

(a)

(b)

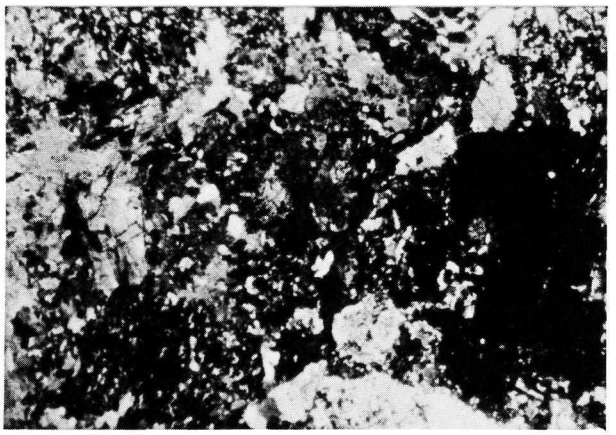

$(b)_1$

(C)

terminated prismatic crystals that are zoned. The relative abundance of epidote-clinozoisite increases as the rocks become more mafic. Muscovite is common and forms small laths or acicular blades. Biotite is rare, and when present exhibits stubby grains. Actinolite is commonly lath to needle shaped. Both muscovite and actinolite cross-cut grain boundaries (Plate 2c). Carbonate occurs as massive to well developed rhombs. It makes up to 60% of a rock, but averages 4%. Feldspar phenocrysts tend to increase in size as the rocks become more felsic. Results from the staining technique of Nold and Erickson (1967) suggest that potassic feldspar is rare.

BOOMERANG FORMATION

The unit consists of intercalated tuffaceous, pyroclastic, brecciated and felsic porphyritic rocks and minor iron formation. The rocks range in colour from dark grey to greenish buff. Evidence of bedding is abundant within the tuffaceous material, which is normally interbedded with course pyroclastic layers containing angular fragmental material ranging in size from 2 to 30 centimeters. The fragments usually weather with higher relief than its surrounding matrix. Original mineralogy is dominated by feldspar and quartz. Feldspar phenocrysts are partly or totally altered to one or more of: sericite, chlorite, saussurite or carbonate. Feldspar occurs as ragged to lath shaped crystals in which the twinning is indistinct (Plate 3a). Feldspar phenocrysts make up to 40% of a sample and average about 23%. Again, the staining technique of Nold and Erickson (1967) suggests that potassic feldspar is absent. Plagioclase compositions are dominatly oligoclase and rarely andesine. Several phenocrysts exhibit preferential sericitization along twin lamellae. Others exhibit rehealing of

PLATE 3

BOOMERANG FORMATION

a) A photomicrograph showing rounded to subangular quartz grains (light grey) and smaller (medium grey) feldspars (centre). The matrix is a mixture of quartz, feldspar, muscovite and sericite. Polars crossed, X 31.

b) This photomicrograph shows part of a quartz grain (dark grey, top centre) that has been fractured and rehealed with quartz and feldspar. Polars crossed, X 31.

c) This photomicrograph exhibits the pressure shadows which are formed on the sides of pyrite grains (black, centre). The pressure shadow is a mixture of quartz, chlorite and sericite. Polars crossed, X 31.

PLATE 3

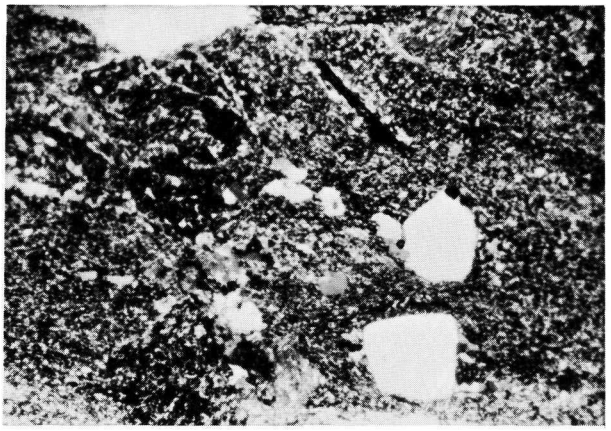

(a)

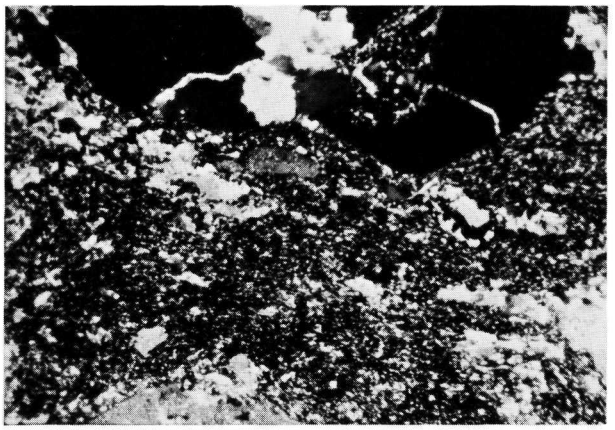

(b)

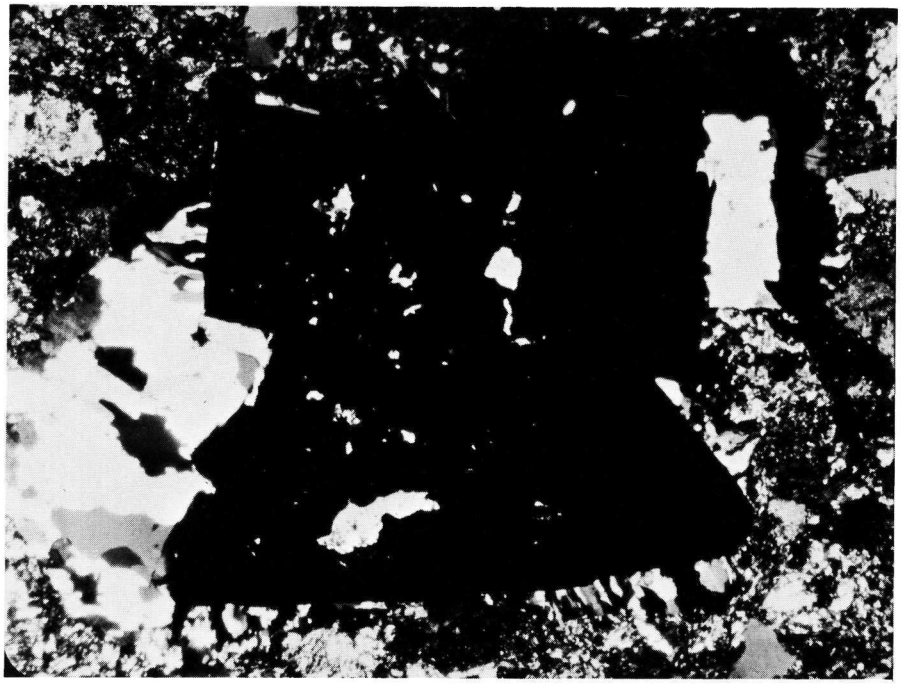

(c)

fractures by carbonate and/or quartz (Plate 3b). Quartz occurs as rounded, often fractured grains. It exhibits undulatory extinction and comprises up to 26% of a sample. The matrix material is an aggregate of fine grained feldspar, quartz, chlorite, carbonate and epidote-clinozoisite. The matrix is usually "dusted" with sericite and clay to produce a light to brown felty appearance. Chlorite is present in all samples and makes up as much as 64% of a fine grained rock. Rarely, aggregates of stubby blades of chlorite are found in the matrix. Muscovite makes up as much as 15% of a rock. It occurs as well developed foliated 0.1 to 0.3 mm. elongate blades. Sphene, zircon and apatite occur within the matrix and average 0.03 to 0.1 mm. in diameter. Leucoxene is associated with or mantling magnetite. Carbonate, quartz, chlorite or feldspar have crystallized along the sides of the euhedral pyrite facing the direction of maximum extension (Spry, 1969). Spry called this extensional feature, "pressure shadows" (Plate 3c). Fragments in the pyroclastic material are a fine grained mixture of feldspar, quartz, chlorite, carbonate, sericite, sphene and muscovite. Several fragments contain altered phenocrysts of feldspar and rounded grains of quartz, indicating that some of the ejecta is of the same mineralogy as the intercalated porphyritic flows.

TISDALE GROUP

GOOSE LAKE FORMATION

The Goose Lake Formation is a series of ultramafic metavolcanic rocks. The total thickness of the unit in the study area is approximately 1500 meters (Pyke, 1975a).

The rocks are generally grey-green to dark green in colour. Most flows contain pillows that range in diameter

from 20 to 80 cm. Rarely, vesicles are observed within the pillows or selvages. The latter are usually darker than the pillow interior. Several flows contain isolated pillows surrounded by massive lavas. These rocks constitute the bulk of the Goose Lake Formation. Ultramafic rocks occur within the formation at two specific stratigraphic intervals (Fig. 5). They are thought to be extrusive because of their concordant nature with the surrounding volcanic rocks and the development of polyhedral jointing (Arndt et al. 1977; Pyke, 1978). The flows are fine-grained, dense rocks ranging in colour from dark blue to black. No spinifex textured flows are observed in the study area.

Microscopic investigation of the ultramafic rocks reveals almost total loss of original mineralogy. Only feldspar and pyroxene are considered original mineralogy. The feldspars rarely exhibit twinning and are altered to chlorite, sericite, carbonate and clay. The pyroxene grains are only seen as irregular outlines in massive chlorite or tremolite. Chlorite is light green to clear in most rocks. It forms irregular masses of stubby shaped grains comprising up to 75% of a rock. Tremolite displays a bladed to acicular habit and may constitute up to 92% of an individual sample. It is most commonly observed with pyroxene where the tremolite is subsequently partially altered to a yellowish-green fibrous amphibole on its feathery terminations. Serpentine is abundant in several samples making up to 69% of the rock. Its habit ranges from stellate to fibrous. The mineral occurs in masses along outlines of previous grain boundaries (Plate 4a). Epidote-clinozoisite occurs as doubly terminated prismatic crystals ranging in size from 0.2 to 0.5 mm. in length. They occur together as aggregates

or zoned crystals. Clinozoisite occurs in the central portion of the grain mantled by epidote. Rarely, biotite occurs as small, pleochroic brown to dark brown grains associated with partially altered pyroxene. Minor amounts of stilpnomelane occur as irregular, moderately pleochroic greenish-brown spindly grains. Carbonate occurs as irregular masses and constitutes up to 15% of a rock. Sphene is rarely observed in the ultramafic rocks. Magnetite-ilmenite is found as small cubic or octahedral grains in the matrix while along pseudomorphed grain boundaries it appears massive. The pseudomorphed outlines are rounded to ovoid or rectangular in shape indicating the former presence of pyroxene and/or olivine (Plate 4b). Magnetite is also present within the rounded pseudomorph as irregular stringers outlining irregular fractures originally present in the olivines. In addition to opaque minerals, pyroxene and olivine pseudomorphs are commonly replaced by combinations of chlorite, tremolite, serpentine and minor talc. Up to 5% prehnite is found in several samples occurring within vesicles or veinlets and is rarely observed replacing the fine grained groundmass. The typical "bow tie" structure is observed along with relatively high birefrigence (Plate 4c). In samples where prehnite is present, veinlets, of chlorite appear to "bleach" the surrounding rock indicating a pre-chloritization origin of the prehnite in the rock (Plate 4d).

The ultramafic rocks are fine-to coarse-grained (cumulate) in thin section. Grains of pyroxene and olivine are now pseudomorphed by magnetite-ilmenite. The presence of sphene in the cumulitic lavas indicates the relative abundance of titanium. Olivine is commonly replaced by chlorite, serpentine, tremolite and talc. Generally, the central portion of the pseudormorph is chlorite while the edges are serpentine (Plate 4e). Pyroxene is commonly

PLATE 4

GOOSE LAKE FORMATION

a) This photomicrograph shows the alteration patterns of serpentine which ranges from stellate to fibrous within altered grains of pyroxene and olivine. Polars crossed, X 125.

b) This photomicrograph shows the pseudomorphic outlines of olivine (rounded to prismatic) and pyroxene (angular). Magnetite outlines the former grain boundaries. Plane light, X 125.

c) A photomicrograph showing the classic "bow tie" structure of prehnite. Polars crossed, X 312.

d) A photomicrograph showing a vein of chlorite (lower, light grey) and how it has bleached the host rock. The upper part of photomicrograph is slightly darker indicating the extent of the bleaching. Plane light, X 125.

e) In this photomicrograph a pseudomorphed grain of olivine has a boundary of serpentine and an interior part of chlorite (left centre). The rest of the photomicrograph is composed of irregular masses of serpentine. Polars crossed, X 312.

f) This photomicrograph illustrates the different alteration patterns of pyroxene. The dominant minerals are chlorite, tremolite and carbonate. Polars crossed, X 125.

PLATE 4

(a)

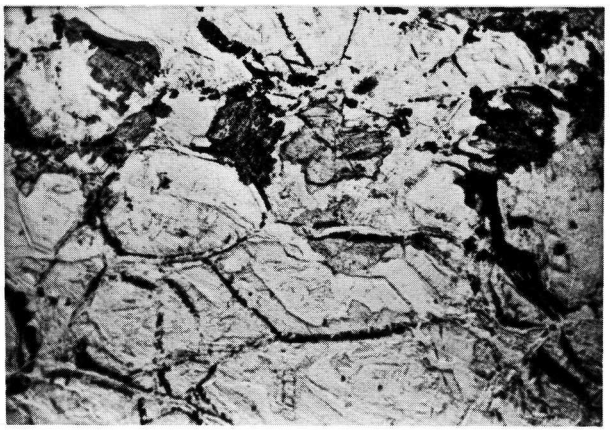

(b)

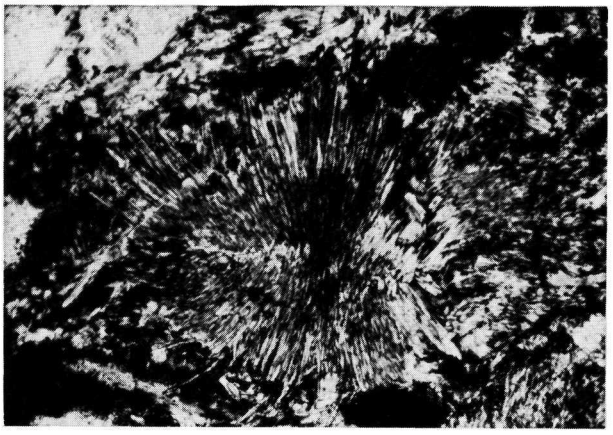

(c)

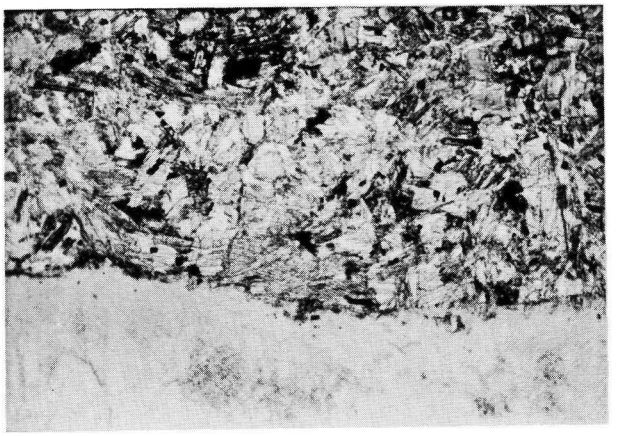

(d)

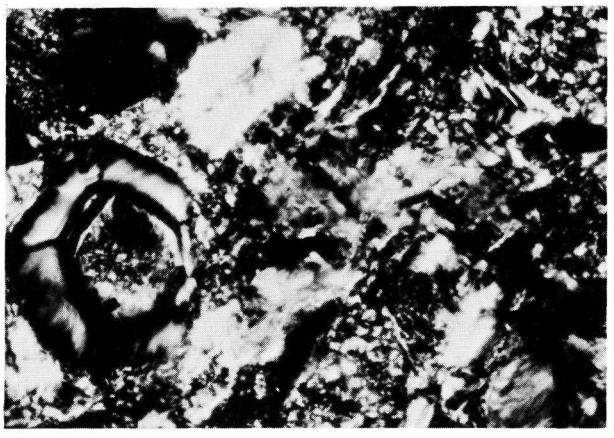

(e)

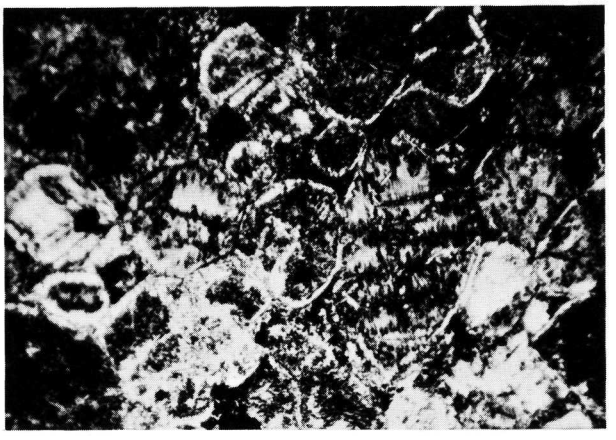

(f)

altered to chlorite, tremolite and carbonate (Plate 4f). Several thin sections display complete development of pseudomorphic pyroxene and olivine. The interstitial material is a mixture of a fine grained chlorite, sphene, with minor feldspar and quartz. Most samples contain small 0.1 to 0.2 mm. isometric grains of spinel. Their rims are partly altered to a chrome bearing reddish iron oxide (Kerr, 1959).

SCHUMACHER FORMATION

The Schumacher Formation consists of mafic to intermediate lava flows with minor intercalated clastic and chemical sedimentary rocks. This unit is host to most of the gold mineralization in the Timmins area. The maximum thickness of the unit in the area of study is about 3100 meters (Pyke, 1975). Several flows appear continuous throughout Tisdale Township. They are the variolitic "marker horizons" which are quite distinct. The variolitic flows contain circular to ovoid shaped white patches set in a dark green matrix. The two major variolitic lavas are known locally as the "V8 and V10B" flows (Jones, 1968; Holmes, 1968).

Generally, the lava flows of the Schumacher Formation can be subdivided into three groups: 1) Thick, massive flows are medium-to coarse-grained and weather green to greenish black. They lack recognizable flow structures but are commonly fractured due to deformation. They do not develop a good foliation. 2) The thinner, structural flows are fine-grained and weather to a buff brown or greenish grey colour. These flows exhibit flow features where there is a crude alignment of feldspar laths. 3) Thin, variolitic flows occur stratigraphically at about the middle of the unit. They are generally fine to medium-grained and are commonly pillowed, as are most of the flows

from this formation.

Original mineralogy of this formation is partly or totally altered. Feldspar makes up 5 to 58% of the rock, averaging 23%. It is lath shaped and rarely twinned. It is partly or totally altered to chlorite, sericite, epidote-clinozoisite or carbonate. When twinning is present, feldspar compositions range from AN_8 to AN_{33}. Generally, flows containing more calcic plagioclase are stratigraphically below the variolitic flows. Rarely, in the course grained flows, pyroxene is observed. Quartz makes up 3 to 34% of the rock and averages 8%. Chlorite occurs as a light to medium green mat in most rocks. Commonly, its habit varies from massive to well developed bladed grains that occur as podular aggregates. Hornblende is usually spotty and is altered to chlorite, epidote-clinozoisite and carbonate. Hornblende is more abundant stratigraphically below the variolitic lavas. It is commonly observed with feathery terminations (Plate 5a). The groundmass consists of a fine- to medium-grained mixture of alteration minerals, the most common being chlorite which may average 42% of a rock. Carbonate is present in nearly all the rocks ranging from trace amounts to 49%. It is massive, irregular or in well developed rhombs. Generally, if the rock is sheared, an increase in carbonate occurs. Epidote is common and increases in amount in the matrix of fine grained lavas. It is found as massive to irregular shaped grains commonly zoned with clinozoisite. Rarely, it is prismatic ranging in size from 0.05 to 0.4 mm. Actinolite is stubby to acicular in habit and may constitute 50% of a rock displaying an inverse abundance with chlorite. Rarely, muscovite (sericite?) is present as small lath shaped grains. Prehnite may be present in vesicles or voids. Prehnite, generally occurs in the upper part of the formation.

Sphene is ubiquitous throughout the formation with a minor increase above the variolitic lavas. It may form as much as 12% of a rock in the upper fine grained mafic lavas. Sphene occurs as rounded masses often altering magnetite-ilmenite. Within the chlorite and epidote-clinozoisite are small (0.01 to 0.2 mm.) euhedral hydrous garnets which range in colour from pink to red. The garnets possibly formed as a result of the silica deficient environment offered by the encompassing chlorite and/or epidote-clinozoisite (Plate 5b). Numerous fractures and microfractures in the rocks are filled with intimate intergrowths of carbonate and quartz (Plate 5c).

The two major variolitic flows in the study area contain white to light-green varioles enclosed in a dark green matrix. Most varioles range in size from 2 mm. to 4 cm. in diameter. The varioles weather in relief compared to the matrix. Varioles range in shape from round, oval or elongate. The lavas are commonly pillowed but some are massive. Varioles increase in abundance towards the pillow selvage.

Microscopic investigation of the varioles indicate complete variability in mineral assemblages. Generally, they have a sharp contact with the surrounding matrix. There are three general types of variolites: unstructured, zoned and monomineralic. The unstructured variole consists of a mixture of carbonate, chlorite, epidote-clinozoisite that is set in feldspar. Normally, the mixture is fine to medium grained. Commonly, small carbonate veinlets cut the varioles (Plate 5d). Zoned varioles show concentric or oval shaped domains of feldspar, carbonate, quartz, chlorite or magnetite-ilmenite. The zoning ranges from simple to complex, depending on the number of minerals present. A typical variole shows a sharp boundary with the matrix, a zone of chlorite, feldspar and euhedral magnetite, and inner

PLATE 5

SCHUMACHER FORMATION

a) This photomicrograph shows hornblende (lower centre) and a lath shaped plagioclase grain (left centre) from the Lower Schumacher Formation. The irregular outline of the hornblende grain is common. $5a_1$ is the same photomicrograph showing the patchy development of the hornblende grain. Plate 5a, plane light, X 125; $5a_1$ polars crossed, X 125.

b) A photomicrograph showing an epidote-clinozoisite grain inside of which small hydrous garnets have developed. $5b_1$ is the same as 5b except in plane light. Plate 5b, polars crossed, X 500; $5b_1$, plane light, X 500.

c) A photomicrograph of a vienlet, showing the intimate intergrowth of quartz and carbonate. Polars crossed, X 312.

d) This photomicrograph shows an unstructured variole (upper, dark grey) with a carbonate grain cross-cutting both matrix and variole. Also the variole shows a sharp contact with the matrix. Polars crossed, X 31.

e) A photomicrograph showing a zoned variole, chlorite (edge) carbonate (light grey inner zone) and a chlorite (centre). Euhedral magnetite laths surround the variole. Sharp contact of variole with matrix. Plane light, X 31.

f) A photomicrograph of a monomineralic variole that is all carbonate. The carbonate exhibits a dendritic growth pattern suggesting that it replaced the original mineralogy. Plane light, X 31.

PLATE 5

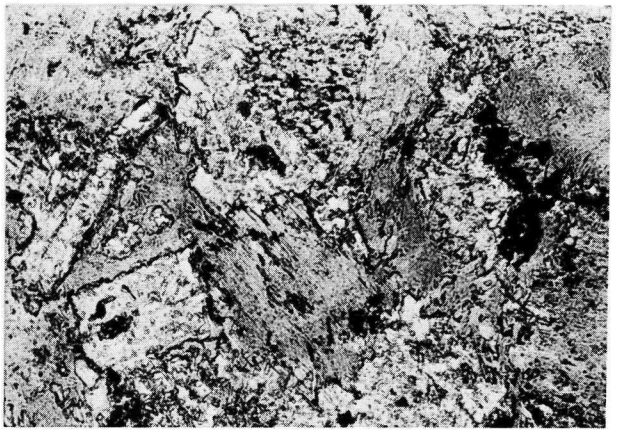

(a)

$(a)_1$

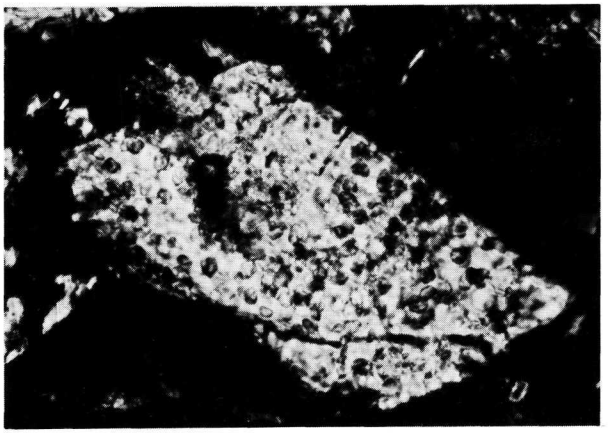

(b)

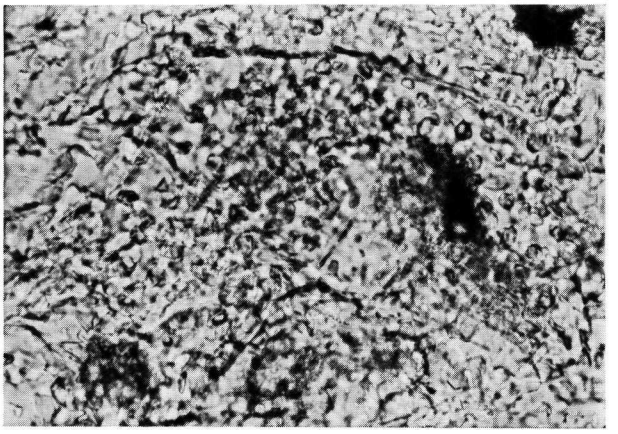

$(b)_1$

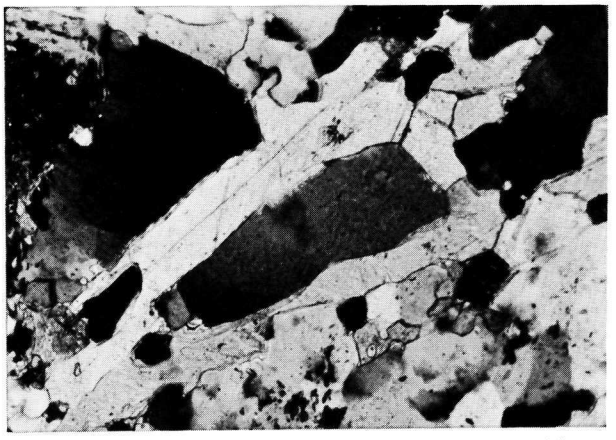

(c)

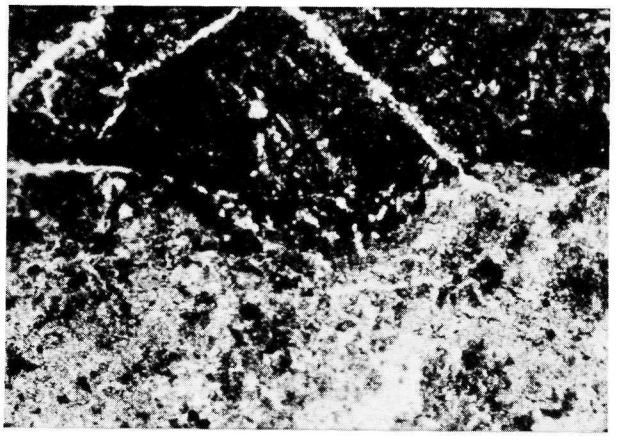

(d)

(e)

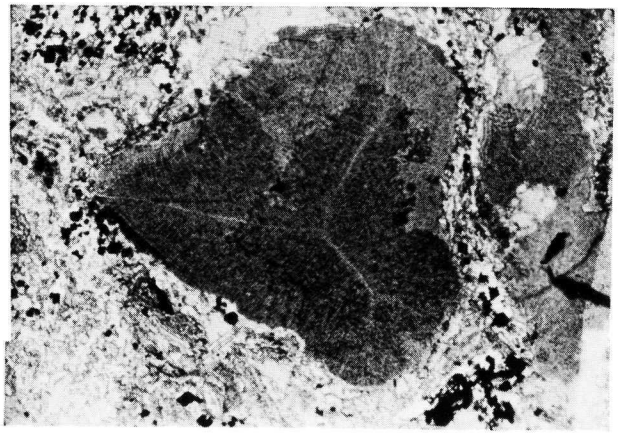

(f)

irregular zones of carbonate and chlorite, an incomplete zone of anhedral magnetite and a centre of carbonate (Plate 5e). Monomineralic varioles are made of either carbonate, chlorite, or an aggregate of quartz grains. This type of variole does not have a boundary of opaque material. Carbonate within the variole may appear dendritic (Plate 5f). The matrix is commonly a fine-grained aggregate of chlorite, epidote-clinozoisite, feldspar, sphene, actinolite and minor carbonate.

KRIST FORMATION

The Krist Formation is a felsic pyroclastic unit containing tuff, lapilli tuff, fragmental layers, porphyritic lenses and brecciated zones. The maximum thickness of the unit in the study area is 360 meters (Ferguson, 1968). Drill hole data indicates that the felsic unit overlies a fine-grained, carbonaceous sedimentary greywacke-slate sequence (Ferguson, 1968). When the sedimentary rocks are absent the Krist Formation unconformably overlies the Schumacher Formation (Buffam, 1948; Hogg, 1950). Buffam suggests that the upper part of the Schumacher Formation including the sediments that underlie the Krist Formation have been deformed and faulted prior to the deposition of the Krist Formation, because they are truncated against it. The volçanoclastic breccia consists of fragments ranging in size from 1 to 25 cm., with an average of 8 to 10 cm. The fragments range in shape from angular to subangular and are randomly packed supported by the matrix The fragments are made up of porphyritic material containing feldspar and quartz-feldspar, also minor mafic volcanics, tuff and chert. The fine to medium-grained matrix is composed of quartz, feldspar, sericite, chlorite, carbonate, muscovite, biotite, sphene, apatite, hematite, leucoxene and minor

euhedral pyrite. The porphyritic flows contain 1 to 8 mm. feldspar phenocrysts set in a medium to course grained matrix (Plate 6a). The feldspar phenocrysts are sericitized and/or chloritized. The staining technique of Nold and Erickson (1967) revealed no potassic feldspar. The angular to sub-rounded lathshaped feldspars have compositions determined by the Fogue method, ranging from albite to oligoclase. Their index is slightly higher than quartz. Rarely, sericite and carbonate preferentially altered the twin lamallae in the feldspar. Several feldspar and quartz phenocrysts are fractured, and subsequently, rehealed with quartz and albite. The quartz phenocrysts are rounded, strained and free of alteration. The matrix is generally a mixture of fine-grained granulated feldspar, quartz and chlorite with minor carbonate, lath shaped muscovite, actinolite, biotite, irregular masses of sphene, apatite, leucoxene and euhedral pyrite.

PORCUPINE GROUP

The Porcupine Group has been subdivided into two lithologic units, namely Keewatin and Timiskmaing-type sedimentary rocks according to the stratigraphic sequence of Pyke (1975).

KEEWATIN-TYPE SEDIMENTARY ROCKS

Keewatin-type sedimentary rocks constitute the lowermost part of the Porcupine Group. It is mainly composed of greywacke-slate couplets. No conglomeratic units are exposed in the study area. The unit is best exposed north of the Dome Mine and north of South Porcupine (Fig. 5). The metasedimentary rocks are in contact with the underlying Krist or Schumacher Formations. The thickness of the Keewatin-type rocks is about 900 meters (Ferguson, 1968). The major lithology of the Keewatin-

type sedimentary rock is a fine to medium-grained sandstone with a fine-grained matrix (greywacke) which ranges in colour from buff brown to grey. Bed thickness ranges from less than a centimeter to three meters. Macroscopically visible beds commonly extend across outcrops. Some exposures are composed of alternating beds of greywacke and slate or rarely siltstone. Graded bedding is commonly observed in the greywackes. The contacts of the individual greywacke beds are sharp and well defined with local flame structures and flute casts used to determine the top of beds. Macroscopically, the greywacke-slate couplets indicate a textural immaturity due to the angular nature of feldspar and quartz grains (Plate 6b). Mineralogic immaturity is also indicated by the relatively fresh feldspars. There are three major components of the framework: quartz, feldspar and rock fragments. Quartz makes up between 10 to 78% of a rock and averages 25%. Generally, there are two types of quartz grains: single and polycrystalline grains. Blatt (1967) suggests that the degree of polycrystallinity may reflect the history of the grain. Polycrystalline quartz with more than six domains (magnetization of constant value characteristic of the mineral composition and temperature) is more likely to be derived from a metamorphic rather than an igneous source. Rarely does this type of quartz occur, suggesting an igneous origin of the quartz. Most quartz grains are angular to subrounded, monocrystalline, exhibiting strained extinction. The angular feldspar grains are generally smaller than the quartz grains and are rarely twinned. Staining techniques suggest no potassium-rich feldspar is present. The corroded, untwinned grains are commonly altered to chlorite, sericite, muscovite, carbonate and clay. Determinations of the anorthite composition using twinned plagioclase yielded albite-oligoclase. The final component

of the framework are rock fragments, constituting 8 to 20% of the rock and averaging 14%. Mafic volcanic rock fragments make up a major part of the identified lithic components. Mafic fragments are characterized by the greater abundance of chlorite and plagioclase laths that are not seen in the felsic matrix. The more felsic fragments can be identified by the diffuse outline of their boundaries. Also scattered chlorite grains and phenocrysts of quartz and feldspar set in a matrix of fine-grained quartz and feldspar identify thefragments. Other minor amounts of muscovite, biotite, sphene, euhedral pyrite aggregates of magnetite and leucoxene, epidote-clinozoisite, carbonate and apatite are present in the matrix. The matrix can make up to 40% of a rock. Commonly, it suspends the framework to prevent grain to grain contact. The matrix is gradational between a dense, medium-grained intergrowth of chlorite, muscovite, quartz and feldspar and with fine-grained quartz and feldspar with minor chlorite and muscovite. The slates appear to be recrystallized to chlorite, muscovite, quartz, feldspar and biotite with minor euhedral pyrite, sphene and magnetite.

TIMISKAMING-TYPE SEDIMENTARY ROCKS

Timiskaming-type rocks consist of greywacke, slate and conglomerate. The best exposures of this unit are located east of the Dome Mine and north of South Porcupine. Ferguson (1966) estimated the thickness of the unit at 460 meters. The lower most part of the unit is a pebble to boulder polymictic conglomerate. A section measured north of South Porcupine attained a thickness of 48.5 meters. Higher in the succession, localized lenses of conglomerate are interbedded with greywacke. The conglomerate is poorly sorted and the clasts range up to 72 cm. in diameter. Most

pebbles are angular to subangular and rarely rounded. Most clasts are of volcanic origin but some are sedimentary or granitic in composition. The mafic volcanic clasts are distinguishable by their medium to dark grey-green colour on a fresh surface. Subsequent weathering of the iron bearing constituents have oxidized the fragments surface to a rusty orange colour. The felsic volcanic fragments are generally medium grey in colour and commonly, quartz phenocrysts are present. Locally, angular to subangular greywacke and slate fragments are common.

Microscopic investigation of the fragments proved them to be extensively altered. Smaller mafic clasts are commonly opaque. Alteration of the fragments produced chlorite, sericite, epidote-clinozoisite, sphene, muscovite, carbonate and clay. The course to fine-grained matrix consists of debris similar in composition to the larger clasts. The supporting matrix is a mixture of quartz, feldspar, chlorite, carbonate, muscovite, sphene, epidote-clinozoisite, leucoxene and rarely euhedral pyrite. Locally, the matrix is intensly foliated. The ratio of matrix to framework varies significantly but the rock is framework supported (Plate 6c). Locally, the finer pebble horizons show a crude stratification indicating tops to the south. No imbrication or cross stratification is observed in the conglomerate. Lenses of graded greywacke are interbedded with conglomerate. The contact of the conglomerate with the underlying rocks is undulating but generally sharp. Massive greywacke and greywacke-slate couplets make up the rest of the formation. The greywackes have sharp lower contacts, and locally show graded bedding. The framework consists of feldspar, quartz and volcanic rock fragments. Rarely, graphic intergrowths of feldspar and quartz are observed (Plate 6d). The matrix is composed

PLATE 6

a) KRIST FORMATION

b) KEEWATIN-TYPE SEDIMENTARY ROCK

c) TIMISKAMING-TYPE SEDIMENTARY ROCK

d) TIMISKAMING-TYPE SEDIMENTARY ROCK

a) A photomicrograph showing rounded and fractured grains of quartz (bottom, centre) while the feldspar phenocrysts are altered and no twinning is visible. Polars crossed, X 31.

b) This photomicrograph is an example of the Keewatin-type sedimentary rocks showing rounded quartz grains (light grey) and angular plagioclase laths (dark grey, right centre). The matrix is fine grained quartz, feldspar sericite, and chlorite. Polars crossed, X 125.

c) This photomicrograph is an example of the Timiskaming-type sedimentary rocks showing altered plagioclase grains (top centre) and quartz grains (bottom centre). Polars crossed, X 125.

d) This photomicrograph shows an intergrowth of quartz and feldspar which formed in response to the low grade (greenschist) metamorphism. Polars crossed, X 312.

PLATE 6

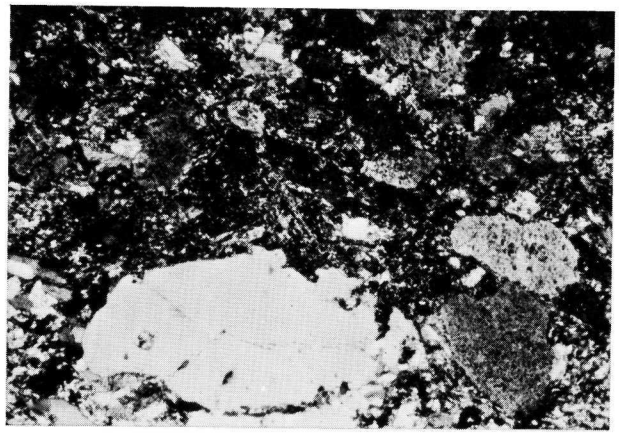

(a)

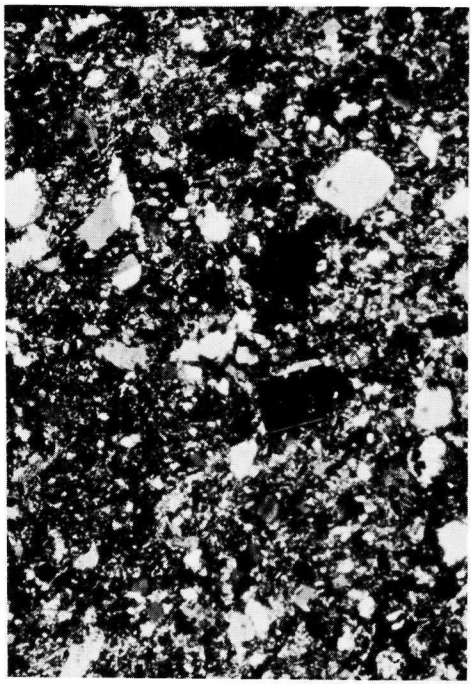

(b)

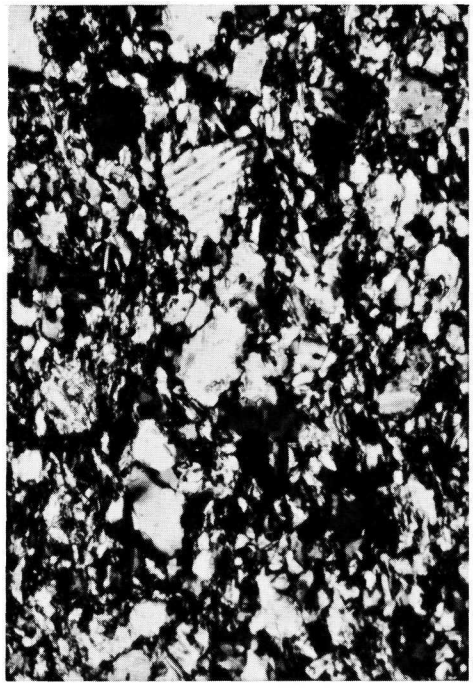

(c)

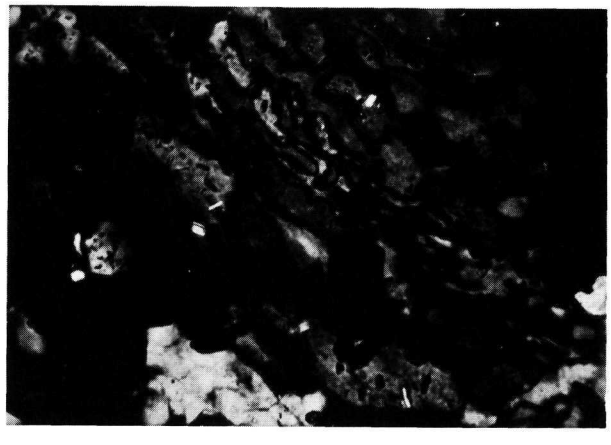

(d)

of fine-grained feldspar, quartz, chlorite, carbonate, muscovite, biotite, sericite, sphene, epidote-clinozoisite, irregular masses of leucoxene and pyrite cubes. The slate interbeds are fine-grained chlorite, quartz, feldspar, biotite, minor sphene, dissiminated magnetite and pyrite cubes. Surrounding the pyrite cubes are pressure shadows which are infilled with quartz, chlorite and carbonate. Bedding is evident in the slate by chlorite-rich bands.

INTRUSIVE BODIES

The ultramafic intrusive bodies studied are located in central Deloro Township (Fig. 5). Hand specimans range in colour from light green to blue-black. A study of Figure 5 indicates a close spatial relationship between the intrusive rocks and faulting. Commonly, fractures ranging from 1 mm. to 8 cm. in width are healed by asbestos. Due to the altered state of the rocks, about 1% pyroxene is present. It is corroded, and contains chlorite and/or serpentine. Commonly, rounded grains of pseudomorphed olivine contain varying amounts of serpentine, chlorite, carbonate, and magnetite. Crystal boundaries of olivine and pyroxene are normally outlined by massive to euhedral grains of magnetite (Plate 7a). Two or more secondary minerals are commonly observed in a zonal arrangement within the pseudomorph of olivine. Pseudomorphed olivine comprises up to 96% of a rock and pyroxene up to 74%. The basal part of the sills is a medium-to course grained cumulate of pseudomorphed olivine and pyroxene. In the cumulitic rocks, serpentine may make up to 97%. It commonly forms small parallel masses along grain boundaries or stellate alignments within pseudomorphed olivine and pyroxene. Serpentine may also form interstitially along grain boundaries (Plate 7b). Chlorite is present in

PLATE 7

DUNITE-PERIDOTITE SILLS

a) A photomicrograph of psuedomorphed pyroxene and olivine grains. They are outlined by massive magnetite. Plane light, X 31.

b) This photomicrograph illustrates how serpentine formed interstitially along grain boundaries (left, upper centre). Polars crossed, X 125.

c) This photomicrograph shows a large spinel grain with small rounded grains containing serpentine (left centre). The spinel grain is party altered (around edges) to Cr-magnetite. Plane light, X 31.

PLATE 7

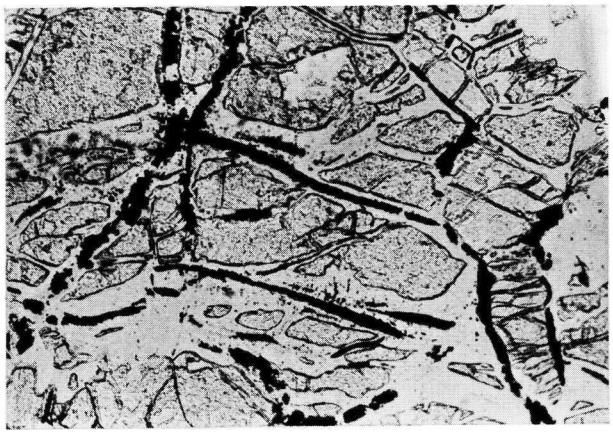

(a)

(b)

(c)

many samples and normally averages about 7% of a rock. Chlorite occurs as bladed aggregates with serpentine in olivine or pyroxene. Carbonate is abundant in several samples or may be totally absent. It occurs as rims around pseudomorphed olivine and pyroxene or is dispersed throughout the rock. Biotite occurs as stubby lath shaped grains and exhibits orangey-brown to brown pleochroism. Biotite never intersects other grain boundaries. Minor amounts of epidote-clinozoisite are scattered throughout the rocks commonly associated with chlorite. Rarely, sphene is present as an alteration product of magnetite, commonly in the cummulitic zones. Olive-green to reddish brown anhedral spinel occurs in most samples. Commonly, its boundaries are opaque suggesting a chrome rich iron oxide. Rarely, olivine pseudomorphs are present within a spinel grain (Plate 7c).

DISCUSSION

The presence of angular feldspar laths, quartz and volcanic rock fragments set in a fine-grained matrix confirm volcanogenic origin and rapid deposition with little chemical weathering of the greywackes. Also, evidence of graded bedding, convolutions and flame structures lend further support for turbidite deposition (Donaldson, 1965; Turner and Walker, 1973). The turbidity currents may have been generated by seismic activity caused by volcanic eruptions in the area. Slate interbeds accumulated during volcanic quiescent periods. Walker (1967) has proposed a criterion for distinguishing a distal or proximal deposition of sedimentary material. Walker stated that thin sharp based beds, fine-grained parallel-sided regular beds, well developed shale horizons between

coarser greywacke beds and graded beds are all indicative of a distal environment. It is believed that the Keewatin-type sedimentary rocks were once more extensive, which is indicated by the features present in the study area that Walker believed are indicative of distal deposition. Also, the absence of a basal conglomerate in the Keewatin-type sedimentary rocks lends further support to the distal environment hypothesis. Prior to the deposition of the Timiskaming-type sedimentary rocks, a period of erosion and tilting is indicated by the presence of an unconformity and the basal conglomerate at the base of the Timiskaming sedimentary rocks (Burrows, 1924; Hurst, 1939; Bass, 1961; Ferguson, 1968; Pyke, 1975a) . The pebble and cobble lithologies of the conglomerate are derived locally (McLaughlin, 1956; Holmes, 1968; Carnevali, 1976). Intercalated with the volcanic rocks in the Timmins area are minor amounts of carbonate rich and chemical sedimentary rocks with minor greywacke beds (Ferguson, 1968; Griffis, 1968; Homes, 1968). The minor amounts of intercalated sediments with the volcanic rocks and the close proximity of all the formations indicates a petrogenetic contemporaneity of the lavas north of the Destor-Porcupine Break. The mineralogic similarity to several of the volcanic formations lends further support to the petrogenetic relationship. The two ultramafic formations Donut Lake (present south of study area) andGoose Lake Formations consist primarily of varying amounts of olivine, pyroxene, feldspar, magnetite and spinel. These minerals are present, or are represented by pseudomorphed grains. Feldspar occurs as an interstitial material which may be primary and/or secondary in origin. Spinel appears olive green with a mantle of reddish Cr-rich magnetite in both formations. The olivine and pyroxene are present in the Donut Lake Formation but is pseudomorphed

in the Goose Lake Formation. The only difference mineralogically between the two formations is the degree of metamorphism.

The Boomerang and Krist Fms. are mineralogically similar. Both formations occur within the Timmins area and consists of tuff, fragmental sequences, porphyritic layers and brecciated zones. The tuffaceous material is fine-grained quartz, feldspar, muscovite, chlorite, sphene and pyrite. Chlorite rich layers occur and represent compositional variations of the original bedding. The porphyritic material contains phenocrysts of lath shaped feldspars and rounded quartz grains set in a fine-grained matrix of feldspar and quartz. Relative mineralogic abundances indicate a similar composition for the two formations.

CHAPTER IV
METAMORPHIC SYNTHESIS

METAVOLCANIC AND METASEDIMENTARY ASSEMBLAGES

Metamorphism of the rocks in the Timmins area developed a consistent secondary mineralogy within each formation in response to chemical homogeneity.

The ultramafic Donut Lake and Goose Lake Fms. have a similar primary mineralogy but subsequent metamorphic conditions have produced different secondary mineralogies.

The Donut Lake Fm. is an elongate body of ultramafic rocks situated within the Peterlong Lake Plutonic Complex (Pyke, 1978; Fig. 8). The contact metamorphic mineralogy is divided into four mineral assemblages each indicative of particular metamorphic conditions (Table 3). The olivine + diopside + hornblende + spinel assemblage indicates high temperature ($700^{\circ}C.$) - low pressure (1 Kb.) conditions (Frost, 1967; Winkler, 1974; Evans, 1977). This assemblage is dominated by diopside with minor olivine, hornblende and spinel. All minerals occur as discrete grains and are never observed in a cross-cutting relationship (Plate 1a). Hornblende occurs as blocky, feathery terminated grains. Spinel appears to surround olivine grains but retains its isometric form. The presence of hornblende and spinel indicates that during high temperature metamorphism aluminous phases develop along with magnesium phases. The presence of magnesiocummingtonite-anthophyllite indicates the second mineral assemblage of diopside + anthophyllite + tremolite + chlorite. This assemblage is rarely observed within the study area and is commonly dominated by magnesiocummingtonite. The anthophyllite-magnesiocummingtonite rich rocks do not contain any iron rich minerals (magnetite-ilmenite) since the iron is incorporated into the amphibole structure. Olivine is never observed in the same rock with anthophyllite. Only minor diopside is observed. The presence of talc

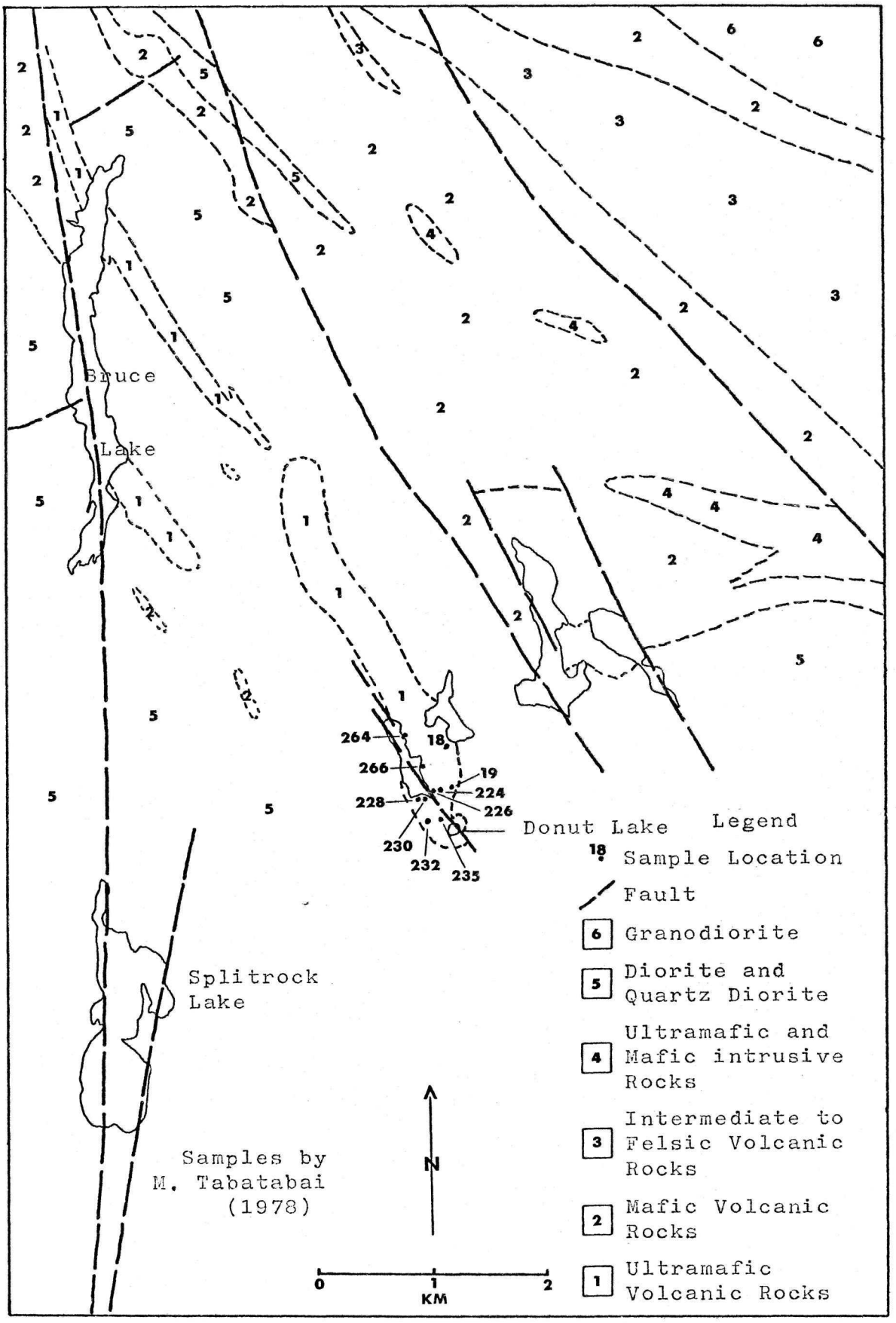

Generalized Geologic Map of the Donut Lake Area

Figure 8

indicates the third mineral assemblage of olivine + diopside + talc + tremolite + chlorite. Olivine and diopside are commonly pseudomorphed by tremolite, chlorite and minor serpentine and outlined by magnetite. Talc occurs interstitally and commonly cross-cuts grain boundaries. Chlorite is patchy in appearance and is associated with talc. The chlorite-talc association indicates the co-existence of aluminous (chlorite) and non-aluminous (talc) phases together. The most common assemblage is olivine + diopside + serpentine + tremolite and chlorite. Serpentine has partly replaced most olivine and diopside and is commonly rimmed by magnetite. Tremolite and chlorite alter diopside and show cross-cutting relations.

Magnetite is present in most rocks except those rich in amphibole. Due to the diadocheity of Mg^{+2} and Fe^{+2}, the iron is preferentially incorporated into the anthophyllite followed by olivine , antigorite , tremolite , diopside , and talc (Trommsdoff and Evans, 1972). The amount of iron available is dependant on the original composition and the degree of serpentinization. Initially, the available iron from serpentinization changes from the ferrous to ferric state on formation of magnetite (Fe^{+2} Fe^{+3} O_4). If total serpentinization of the rock takes place, about 66% of the iron is changed to Fe^{+3} thus limiting the amount of available iron in the Fe^{+2} state to be substituted in other minerals. The lack of magnetite in anthophyllite rocks indicates the iron was preferentially incorporated into its structure rather than forming magnetite.

Initially, metamorphism of the Donut Lake Formation reached the medium grade (amphibole facies) Winkler (1974) with minor development of aluminous hornblende and anthophyllite. The rocks subsequently exhibit retrogressive mineral adjustment followed by hydration to produce the extensive serpentinization now observed in the lavas.

The Goose Lake Formation is totally metamorphosed with only minor pyroxene cores indicating original mineralogy. Most rocks contain serpentine, chlorite, tremolite, magnetite, carbonate and talc all of which, in part, have replaced olivine and pyroxene now outlined by magnetite. The dominance of serpentine throughout the formation associated with chlorite indicates that small amounts of CO_2 were present during metamorphism (Winkler, 1974). The only aluminous minerals present are chlorite and spinel. The consistency of the secondary mineralogy throughout the formation with the dominance of chlorite indicates low grade (greenschist facies) metamorphism (Winkler, 1974). The absence of intrusive rocks in the area suggest regional metamorphism.

Mafic to intermediate volcanic rocks (Schumacher Formation) exhibit the metamorphic assemblage of chlorite + epidote-clinozoisite + actinolite + quartz which is indicative of low grade (greenschist facies) metamorphism (Winkler, 1974) (Table 3). Also, the presence of the mineral assemblage chlorite + epidote-clinozoisite + hornblende + quartz is observed which is also included as greenschist facies metamorphism. Previously, the two main criteria for separating greenschist facies from amphibolite facies is: a) an increase in alumina content of the amphiboles namely the jump from actinolite-tremolite to hornblende (5% Al_2O_3) and b) the anorthite content (albite-oligoclase) composition for greenschist facies rocks while for the amphibolite facies, anorthite contents greater than An 20 is used (Miyashiro, 1961; Hyndman, 1972; Liou, et al., 1974). The use of hornblende in this classification is in fact contradictory since it exists with plagioclase compositions in the oligoclase range. Winkler (1974) has subsequently subdivided the low grade field into two which is divided on the basis of albite-oligoclase and actinolite, tremolite-hornblende. Within

the study area, the lower Schumacher Fm. is dominantly oligoclase-hornblende while the upper part is actinolite-albite with both containing abundant chlorite and epidote-clinozoisite (Table 3).

The felsic volcanic rocks and the sedimentary rocks of the study area contain a metamorphic assemblage of chlorite, muscovite, actinolite, epidote-clinozoisite reflecting low grade (greenschist facies) metamorphism (Turner, 1968; Winkler, 1974) (Table 3). Chlorite is common in most rocks and the finer-grained beds within the slate are completely chloritized. Muscovite and actinolite occur as lath shaped grains commonly embaying feldspar phenocrysts. Epidote-clinozoisite commonly alter feldspar phenocrysts and may occur as euhedral crystals associated with massive chlorite.

In many samples of serpentinized dunite and peridotite in the study area the original mineralogy is preserved by pseudomorphs of serpentine after olivine and pyroxene. The dominance of serpentine in the intrusive rocks indicates low CO_2 concentrations, because if CO_2 is available, serpentine will be altered to magnesite + quartz or magnesite + talc (Winkler, 1974). Along fractures and faults crossing the dunite-peridotite rocks, carbonate + talc + quartz is common due to the accessability of carbonate rich fluids which moved along the fractures.

TABLE 3

Metamorphic Paragenesis of the Timmins Area Rocks

Medium Grade (Amphibolite Facies)	olivine + diopside + hornblende + spinel
	diopside + anthophyllite + tremolite + chlorite
Low Grade (Greenschist Facies)	chlorite + epidote-clinozoisite + hornblende + oligoclase + quartz + sphene
	chlorite + epidote-clinozoisite + actinolite + albite + quartz + sphene
	chlorite + epidote-clinozoisite + muscovite + actinolite + albite + quartz
	chlorite + tremolite + talc + carbonate
	chlorite + tremolite + serpentine

SUMMARY

The rocks of the Timmins area have adjusted to regional low grade (greenschist facies) metamorphism. The Donut Lake Formation has been metamorphosed to medium grade (amphibolite facies) and subsequent retrogressive and hydration changes have further altered the rocks.

CHAPTER V
GEOCHEMISTRY

GENERAL

Prior to any chemical investigation of the lavas, an understanding of possible primary and secondary chemical variation processes must be investigated. Generally, there are three types of process which obscure original lava compositions: 1. primary variations 2. metamorphism and volatization and 3. spilitization.

PRIMARY VARIATIONS

Primary variations of major oxides and trace elements within individual lava flows have been investigated by Dalrymple and Hirooka (1965), Watkins and Haggerty (1965), Sato and Wright (1966), McDonald (1967), Evans and Moore (1968), Watkins et al.(1970), Hart et al. (1971) and Pearce and Birkett (1974). Primary physical factors causing variation of elements in lavas is the thickness of the individual extrusive, which is directly related to cooling time, hence the extent to which fractionation within the flow proceeds. Cooling time and volatization effect the grain size and An content of the plagioclase (Evans and Moore, 1968). Subaerial or subaqueous extrusion produce different confining pressures which may effect element variations. Lavas that are subaerially extruded are not effected by large confining pressures that a lava would experience nearby the Mid Atlantic Ridge. Extrusion of lavas experiencing large confining pressures inhibits S^{-2} separation from the magma thus no SO_2 formation. If the lava is extruded subaerially, S^{-2} may separate from the melt to form SO_2 and escape (degasing). The situation may in fact be directly related to the minor development of minerals containing

Fe, Zn, Cu and Ni since all these element have a strong affinity for S^{-2}.

Internal variations of elements can, in part, be attributed to fractional crystallization of one or more mineral phases. If the flow is ultramafic or basaltic in composition olivine and/or pyroxene crystals may settle due to density differences in which MgO, FeO, Ni, $\pm$CaO in part, will be preferentially enriched in the lower part of the flow. Late in the formation of olivine and pyroxene, plagioclase may become trapped with the denser crystals and sink removing SiO_2, Al_2O_3, CaO, K_2O, Ba and Rb (Hart et al., 1971; Pearce and Birkett, 1974). During initial cooling of a lava flow high oxygen fugacity can develop as a result of the dissociation of water causing a relative enrichment of iron and titanium and enhancing the erratic behaviour of the alkali elements(Watkins and Haggerty, 1965; Sato and Wright, 1966; McDonald, 1967). Depletion of the alkali elements occurs in the central part of the flow with relative enrichment occuring stratigraphically higher due to late stage migrations of magmatic liquids (Dalrymple and Hirooka, 1965; Watkins et al., 1970; Hart et al., 1971). Following the work of Watkins et al., (1970), the most erratic elemental components are Na_2O, K_2O, Rb and Ba. The relatively immobile elemental components are Al_2O_3, TiO_2, Fe_2O_3, MgO, CaO, P_2O_5, Cr, Ni, and Sr while SiO_2 is the least mobile.

SECONDARY ALTERATION

REGIONAL METAMORPHISM

During low grade regional metamorphism, major oxides are redistributed in basic volcanic rocks (Smith, 1968; Smith, 1969; Cann, 1970; Jolly and Smith, 1972; Floyd and Winchester, 1975; Smith and Smith, 1976). Commonly, variations are the result from the segregated development of CaO rich mineralogies

which appear to develop separately from those which incorporate Fe^{+2}, Fe^{+3}, Na^{+}, K^{+} and Mg^{+2} (Smith, 1968; Jolly and Smith, 1972). Smith (1968) reported that major oxide variation is directly related to the lithological domains where, CaO is most erratic, MnO, TiO_2, P_2O_5 appear random, FeO, Na_2O, K_2O, MgO vary concordantly, SiO_2 varies erratically and Al_2O_3 which shows the least variation. Mn^{+2}, Ti^{+4} and P^{+5} are not readily incorporated into minerals such as epidote-clinozoisite, chlorite, albite-oligoclase, hornblende or actinolite which are products of low grade metamorphism. Thus these elements remain relatively constant in their proportions. Trace elements are also redistributed during regional low grade metamorphism. The lease mobile elements are: Ti, P, Mn, Y, Zr, Nb and Cr (Hart, 1969; Philpotts et al., 1969; Cann, 1970; Hart and Nalwalk, 1970; Floyd and Winchester, 1975; Smith and Smith, 1976). The addition of volatiles during metamorphism may also effect element concentrations within the rocks. The major volatile components are H_2O, CO_2, SO_2, N_2, SO_3 and S_2 . These components may make up between 5 to 15% of certain metamorphic minerals which may cause a dilution problem when considering whole rock analyses. This problem in part, may be minimized when chemical analyses are considered on a volatile free basis.

SPILITIZATION

Numerous hypotheses for the formation of spilites have been reviewed by Vallance (1965). The process of spilitization effects the distribution of elements within basic volcanic rocks in which Na_2O and CaO show the most erratic behaviour while SiO_2, Fe_2O_3, MgO and TiO_2 show only minor redistribution. Al_2O_3 is consistent between pillow cores and selvages (Vallance, 1965; Hart, 1970).

SUMMARY

Relatively immobile elements must be used for the classification of original magmatic characteristics of volcanic rocks. In this study, TiO_2, Al_2O_3, Zr, FeO, MgO and Ni will be used for the classification of volcanic rocks from the Timmins area. Also, scatter diagrams will be used in which the elemental components are plotted against MgO.

GEOCHEMICAL SYNTHESIS

GENERAL STATEMENT

Geochemical study of the volcanic rocks within the Timmins area was undertaken along selected traverses in order to sample a complete section through the lavas (Figs. 8,9).

The mafic to felsic volcanic rocks have been subdivided into classes based upon their weight percent SiO_2. The class divisions have been adopted from Jakes and White (1971) as follows:

Class	SiO_2 (wt. %)
Basalt	52
Basaltic Andesite	52-56
Andesite	56-52
Dacite	62-70
Rhyolite	70

The ultramafic rocks have been subdivided on the basis of their weight percent MgO. The class divisions have been adopted from Arndt *et al.* (1977) as follows:

Class	MgO (wt. %)
Peridotitic Komatiite	20
Pyroxenitic Komatiite	20-12
Basaltic Komatiite	12

Although, SiO_2 is used to subdivide the mafic to felsic lavas into their respective classes, several disadvantages are apparent. Because several different volcanic rock suites are found in the area, the mafic classes of rock overlap in scatter diagrams due to equivalent SiO_2 contents.

Several volcanic rock suites have higher silica relative to the mafic components, such as calc-alkaline mafic rocks which contain more magnesium than tholeiitic equivalents. Thus all variation diagrams are plotted against MgO which is progressively depleted towards the

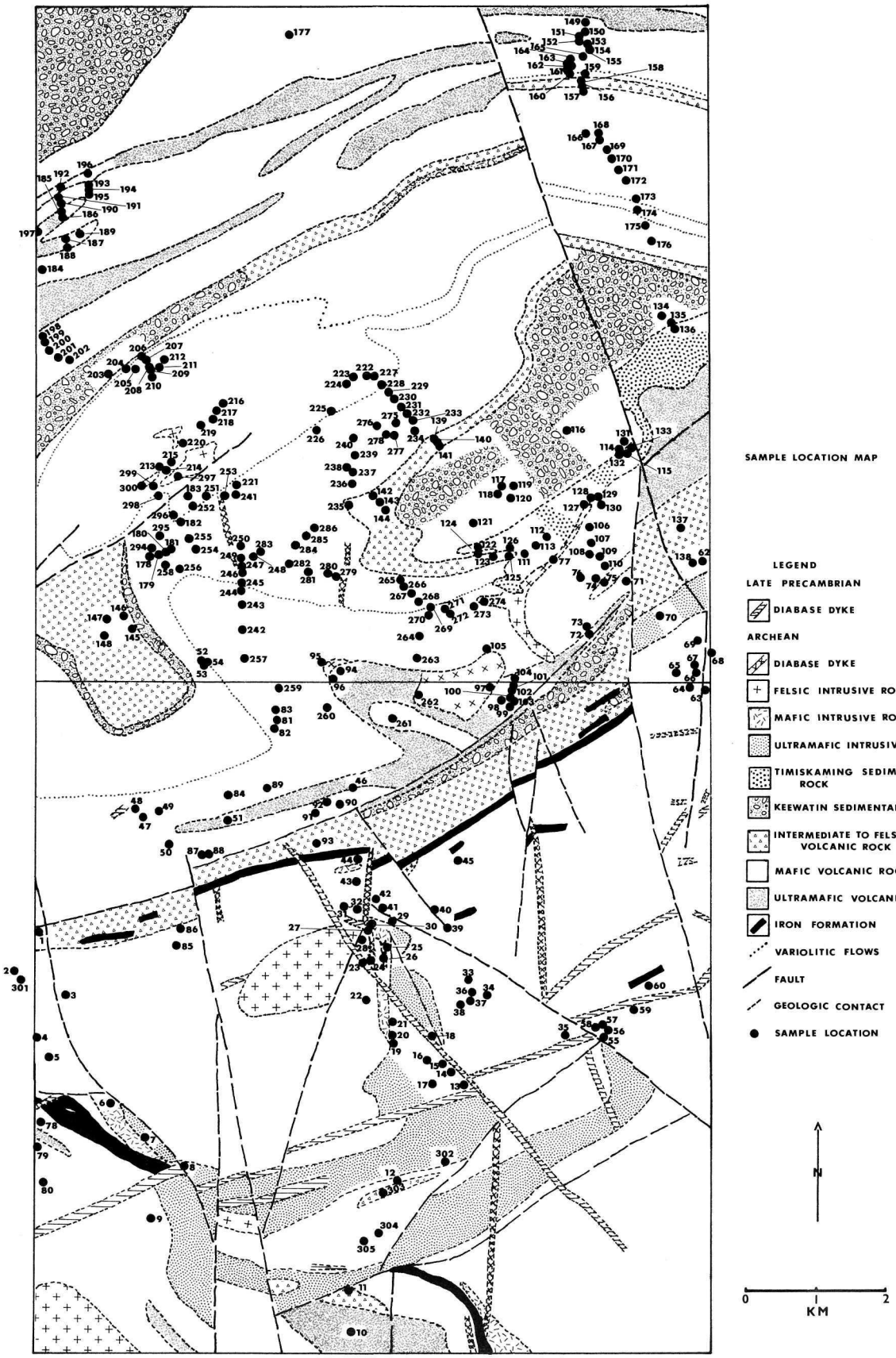
SAMPLE LOCATION MAP
LEGEND
LATE PRECAMBRIAN
DIABASE DYKE
ARCHEAN
DIABASE DYKE
FELSIC INTRUSIVE ROCK
MAFIC INTRUSIVE ROCK
ULTRAMAFIC INTRUSIVE ROCK
TIMISKAMING SEDIMENTARY ROCK
KEEWATIN SEDIMENTARY ROCK
INTERMEDIATE TO FELSIC VOLCANIC ROCK
MAFIC VOLCANIC ROCK
ULTRAMAFIC VOLCANIC ROCK
IRON FORMATION
VARIOLITIC FLOWS
FAULT
GEOLOGIC CONTACT
SAMPLE LOCATION
N
0
1
2
KM

FIGURE 9

felsic end members. Due to the uncertainty of the oxidation state of iron caused by primary variations, metamorphism, oxygen fugacity and volatiles, iron is treated as FeO* (total). When constructing petrologic diagrams with the use of Fe_2O_3; it is assumed to be equal to the weight percent of TiO_2 of the sample plus 1.5% as suggested by Irvine and Baragar (1971).

All lavas are hypersthene or quartz normative, trending from compositions with dominant normative olivine towards minor corundum in the felsic rocks. Some of the peridotite samples contain nepheline in the norm indicating undersaturation with respect to silica (Appendix I).

CLASSIFICATION

A ternary diagram was produced using zirconium, titanium and nickel (ZTN) for the classification of the three major volcanic rock series. The diagram is developed using available published geochemical data from Archean greenstone belts. Generally, the ZTN diagram is analogous to that of the AFM diagram but does not suffer from metasomatic effects inherent in the latter. Zirconium is similar in behaviour to that of the alkali elements which become progressively enriched during fractionation (Rankama and Sahama, 1950; Taylor and White, 1965; Smith and Smith, 1976) and Geochemical Tables pp. 249-250. Titanium resembles FeO* in deportment becoming enriched in the tholeiitic intermediate members while exhibiting systematic depletion during fractionation in the calc-alkaline series (Rankama and Sahama, 1950; Myashiro and Shido, 1975). Nickel is used because of its' diadochy with magnesium which is systematically depleted during fractionation (Gast, 1968). The ZTN diagram, (Fig.10) suggests that each volcanic series develops its' own distinct

Figure 10

LEGEND

Calc-alkaline

△	Hallberg, Johnston and Bye (1976)	(23)
□	Jolly (unpublished data)	(44)
○	Naqvi and Hussain (1973)	(15)

Tholeiitic

⬢	Nesbitt and Sun (1976)	(4)
●	Hallberg, Carter and West (1976)	(5)
■	Jolly (unpublished data)	(37)
▲	Naqvi and Hussain (1973)	(6)

Komatiitic

⬡	Hallberg, Carter and West (1976)	(11)
▼	Nesbitt and Sun (1976)	(19)
▽	Jolly (unpublished data)	(7)
	Total	171

TiO_2 expressed in wt%.

Zr expressed in ppm

Ni expressed in ppm

The ZTN Diagram of Archean Volcanic Rocks

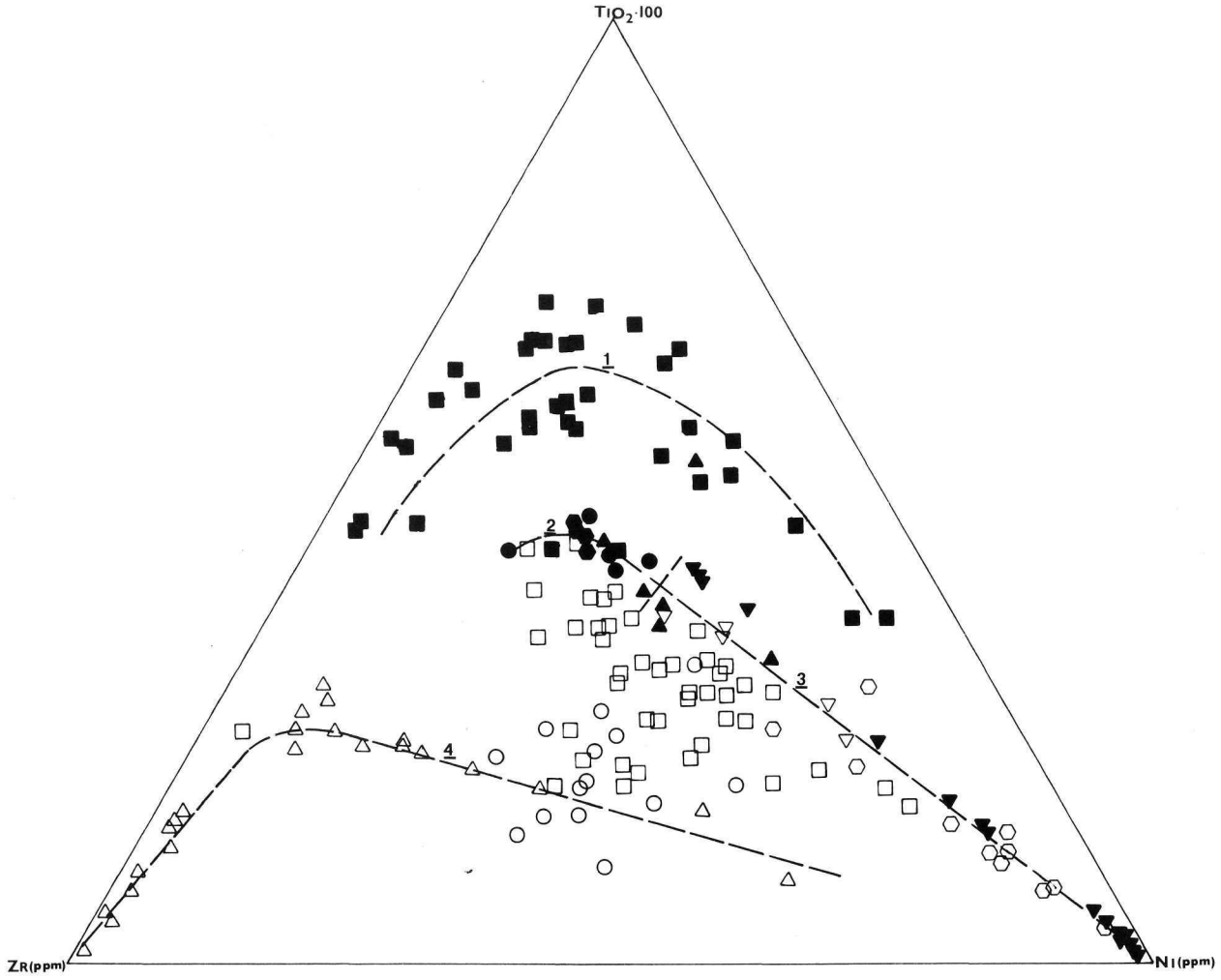

FIGURE 10

trends. Trends one and two are tholeiitic, three is komatiitic and four is calc-alkaline. The area between trend lines 3 and 4 suggest that mafic calc-alkaline rocks plot close to but under line 3 while the more felsic calc-alkaline rocks plot close to trend line 4. The Chitaldrug volcanic rocks from India are reported to represent tholeiitic meta-basalts (Naqvi and Hussain, 1973). The Chitaldrug volcanic rocks plotted on the ZTN diagram suggests that the mafic end members of the suite are both tholeiitic and basaltic komatiites in nature but the intermediate to felsic rocks are calc-alkaline in character and approach the felsic Marda Volcanic complex trend line 4.

The ZTN plot (Fig. 11) of the volcanic rocks from the Timmins area separates them into their respective suites. The komatiitic rocks (trend line 3) are Donut Lake and Goose Lake Formations which plot close to the nickel apex. The Lower Schumacher Formation is a series of basaltic komatiites while the upper part of the Lower Schumacher is tholeiitic in character. The variolitic flows separating the Upper and Lower Schumacher Formations suggest a felsic component associated with these lavas. The variolitic flows occur on the tholeiitic trend lines (1, 2) towards the felsic end members. The Upper Schumacher Formation exhibits tholeiitic trends while the base of the Upper Schumacher appears in part transitional from basaltic komatiite to tholeiitic falling above the basaltic komatiite trend line 3. The Redstone Formation is calc-alkaline in nature and suggests that the mafic end members of the formation exhibit both tholeiitic and basaltic komatiite characteristics. The Krist and Boomerang Formations are classified as felsic calc-alkaline volcanic rocks similar in nature to the Marda Complex (Hallberg et al. 1976). Classification of the Timmins area volcanic rocks are presented in Table 4.

Figure 11

LEGEND

TISDALE GROUP

▲ Krist Formation

○ Upper Schumacher Formation

● Variolitic Flows

□ Lower Schumacher Formation

■ Goose Lake Formation

DELORO GROUP

▽ Boomerang Formation

▼ Redstone Formation

⬡ Donut Lake Formation

⬢ Dunite-Peridotite

Major Oxides expressed in weight percent

Trace Elements expressed in parts per million

The ZTN Diagram of Volcanic Rocks from the Timmins Area

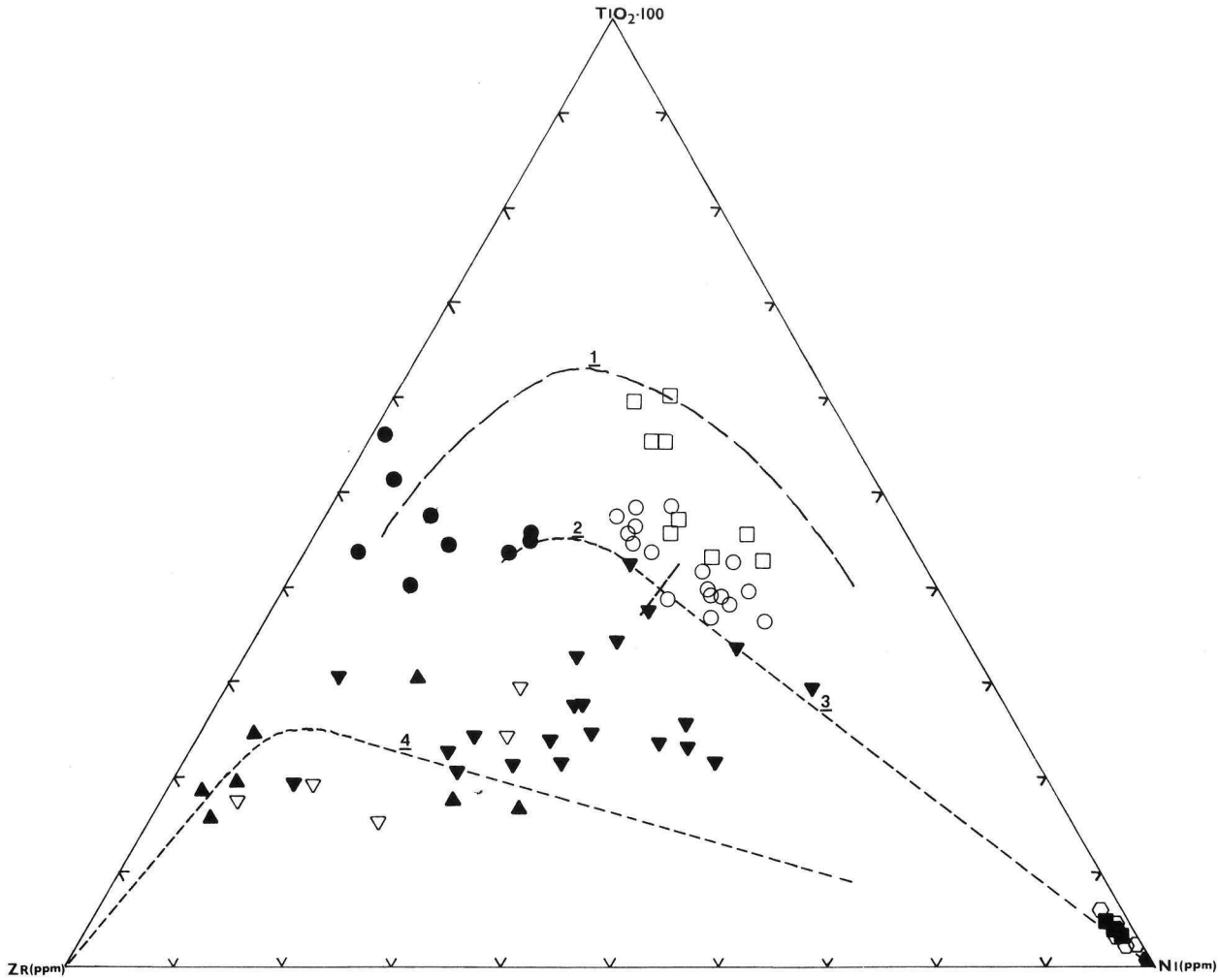

FIGURE 11

TABLE 4

Formation	Classification of Volcanic Rock
Krist Formation	Calc-alkaline
Upper Schumacher Formation	Tholeiitic
Variolitic Flows	Tholeiitic
Lower Schumacher Formation	Basaltic Komatiite; Tholeiitic
Goose Lake Formation	Komatiite
Boomerang Formation	Calc-alkaline
Redstone Formation	Calc-alkaline (Transitional?)
Donut Lake Formation	Komatiite

GEOCHEMISTRY OF TIMMINS AREA LAVAS
KOMATIITIC LAVAS
(DONUT LAKE, GOOSE LAKE FORMATIONS)

Appendix I contains the analyses of the komatiitic rocks from the Timmins area. The komatiitic rocks can be further subdivided on the basis of MgO content according to Arndt et al., (1977). Peridotitic komatiites have MgO contents greater than 20%, pyroxenitic komatiites contain MgO contents between 20 to 12% and basaltic komatiite with MgO less than 12%.

Generally, Figure 12a-s indicates that S, Sr, TiO_2, SiO_2, Al_2O_3, Na_2O, K_2O, Ba and Zr are progressively enriched while MgO, FeO*, Rb, Ce and Ni are continually depleted towards the less mafic basaltic komatiites. CaO is enriched in the pyroxenitic komatiites while depleted in the basaltic komatiites. Depletion of MnO occurs in the pyroxenitic komatiites while it is enriched in the basaltic komatiites. Sulphur is enriched early in the pyroxenitic komatiite rocks at 18% MgO but is then continually depleted. The most ultramafic peridotitic komatiites are commonly medium to coarse grained cumulitic rocks rich in olivine. Normative calculations yield olivine compositions ranging between $Fo_{(77-85)}$ suggesting low iron concentrations inthe olivine. The pyroxenitic komatiites yield normative olivine compositions ranging between $Fo_{(72-76)}$. Peridotitic komatiites range in Al_2O_3 values from 4 to 6.8% while the pyroxenitic komatiites range from 6.5 to 9.5%. The difference in alumina values is in part due to the presence of minor hornblende, feldspar and chlorite in the pyroxenitic komatiites while they are absent in the peridotitic komatiites. Average CaO/Al_2O_3 ratios for the Goose Lake and Donut Lake Formations are 1.0 and 1.05 respectively. The values are similar to those of Nesbitt and

Figure 12a-s

LEGEND

TISDALE GROUP

▲ Krist Formation

○ Upper Schumacher Formation

● Variolitic Flows

□ Lower Schumacher Formation

■ Goose Lake Formation

DELORO GROUP

▽ Boomerang Formation

▼ Redstone Formation

⬡ Donut Lake Formation

⬢ Dunite-Peridotite

Major Oxides expressed in weight percent

Trace Elements expressed in parts per million

NB. (All subsequent diagrams use the same symbol format as presented above, unless otherwise specified).

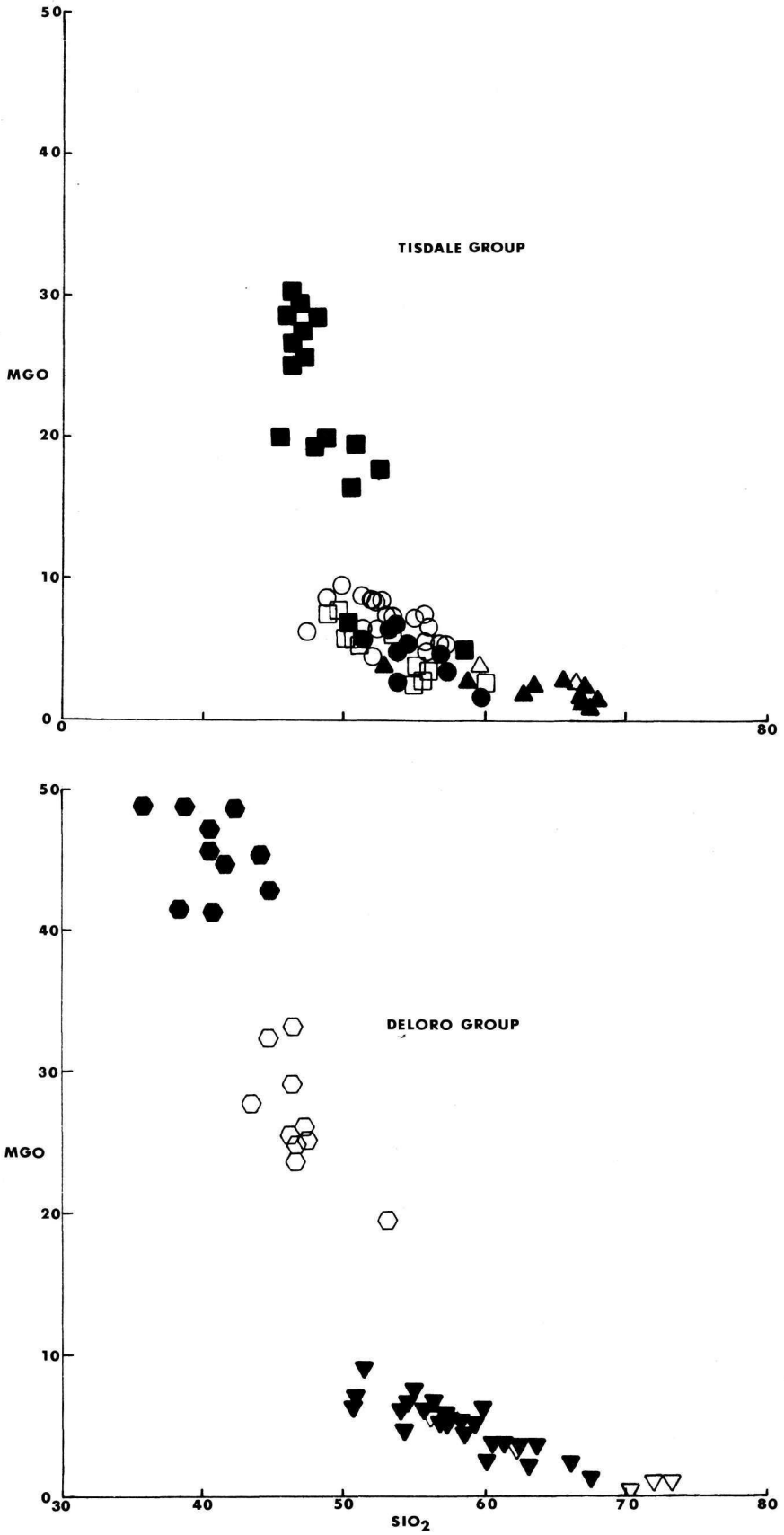
TISDALE GROUP
MGO
50
40
30
20
10
0
0
80
DELORO GROUP
MGO
50
40
30
20
10
0
30
40
50
60
70
80
SIO2

FIGURE 12 A

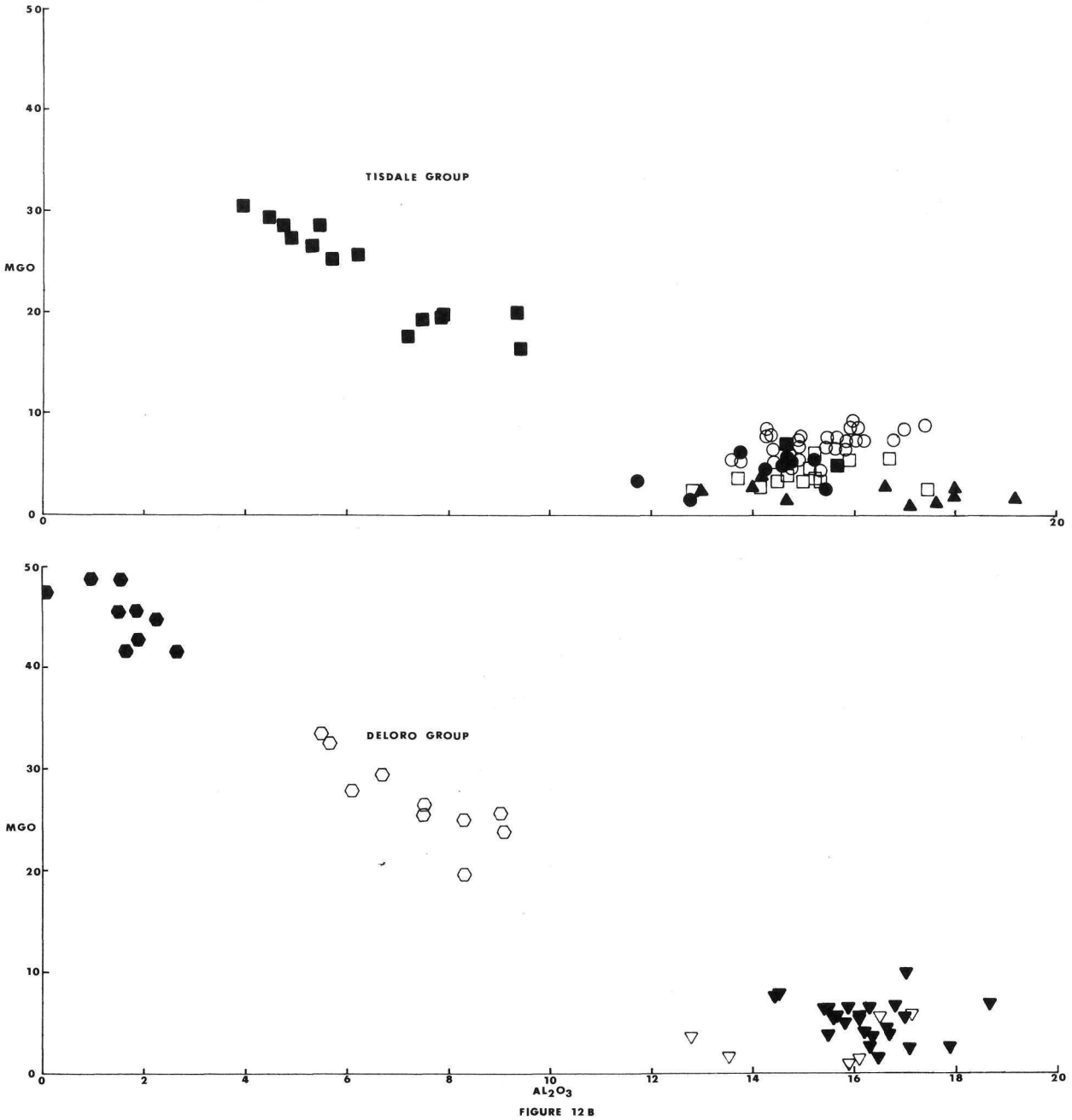

FIGURE 12 B

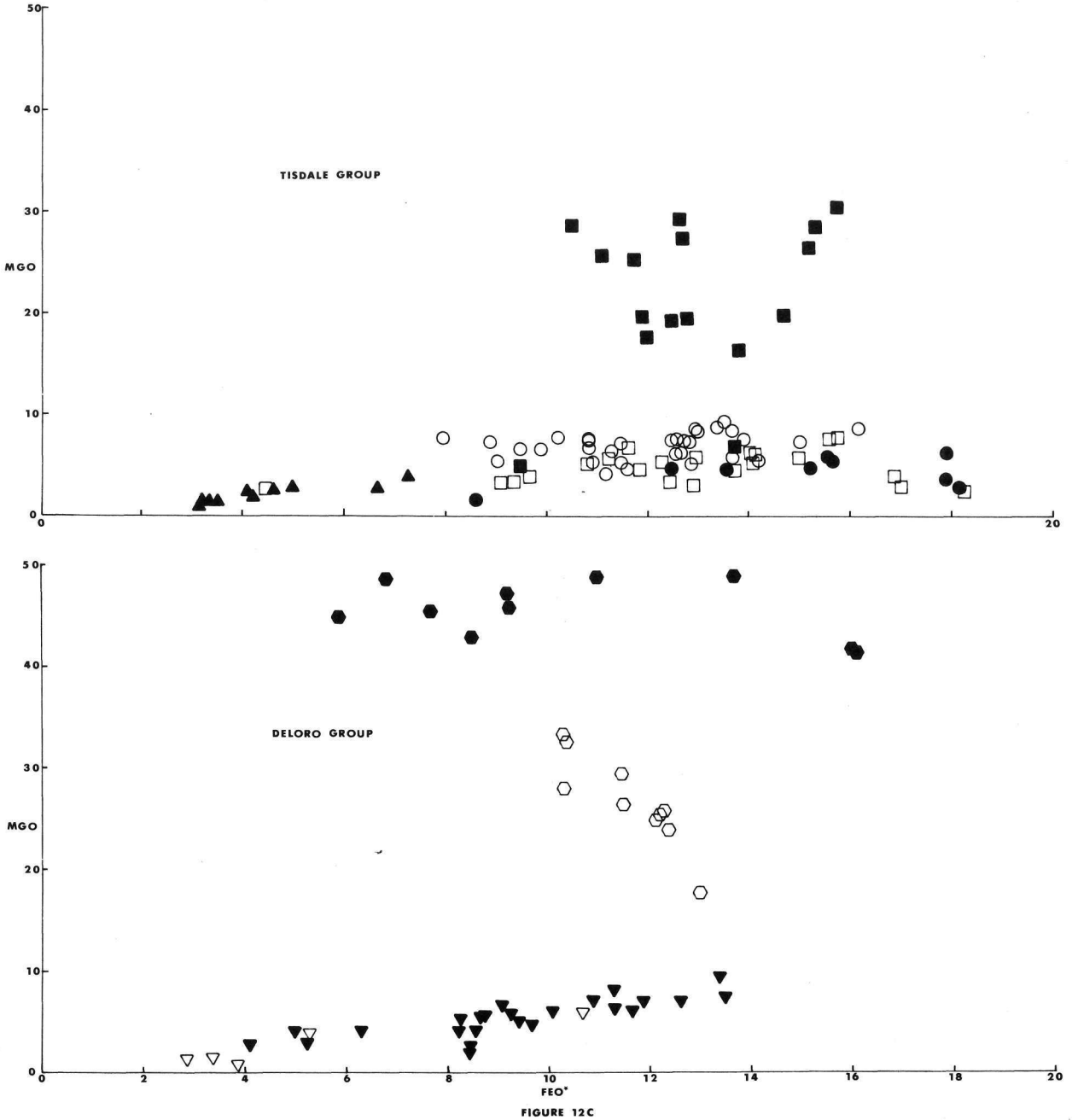

FIGURE 12C

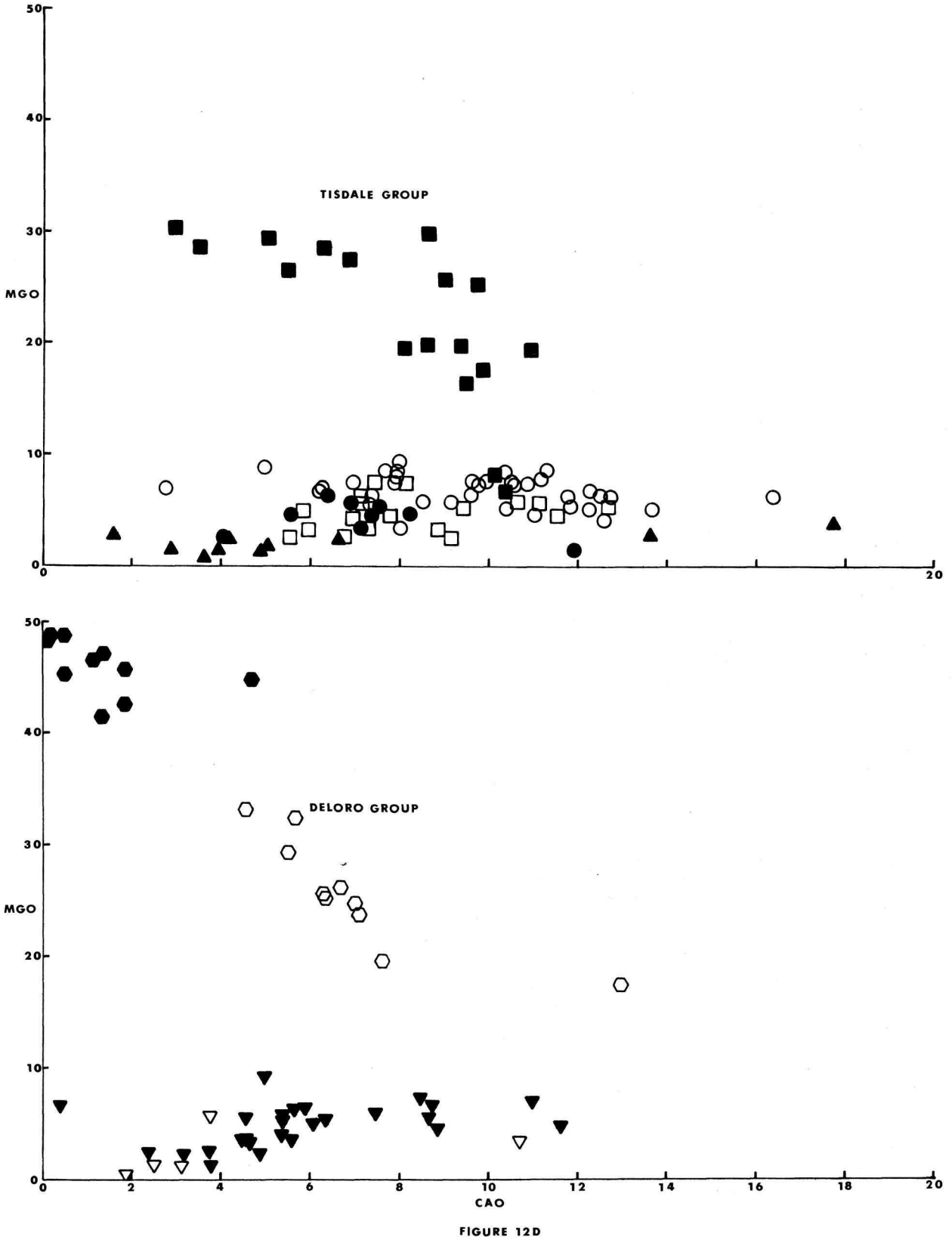
TISDALE GROUP
MGO
DELORO GROUP
MGO
CAO
0
10
20
30
40
50
0
2
4
6
8
10
12
14
16
18
20

FIGURE 12D

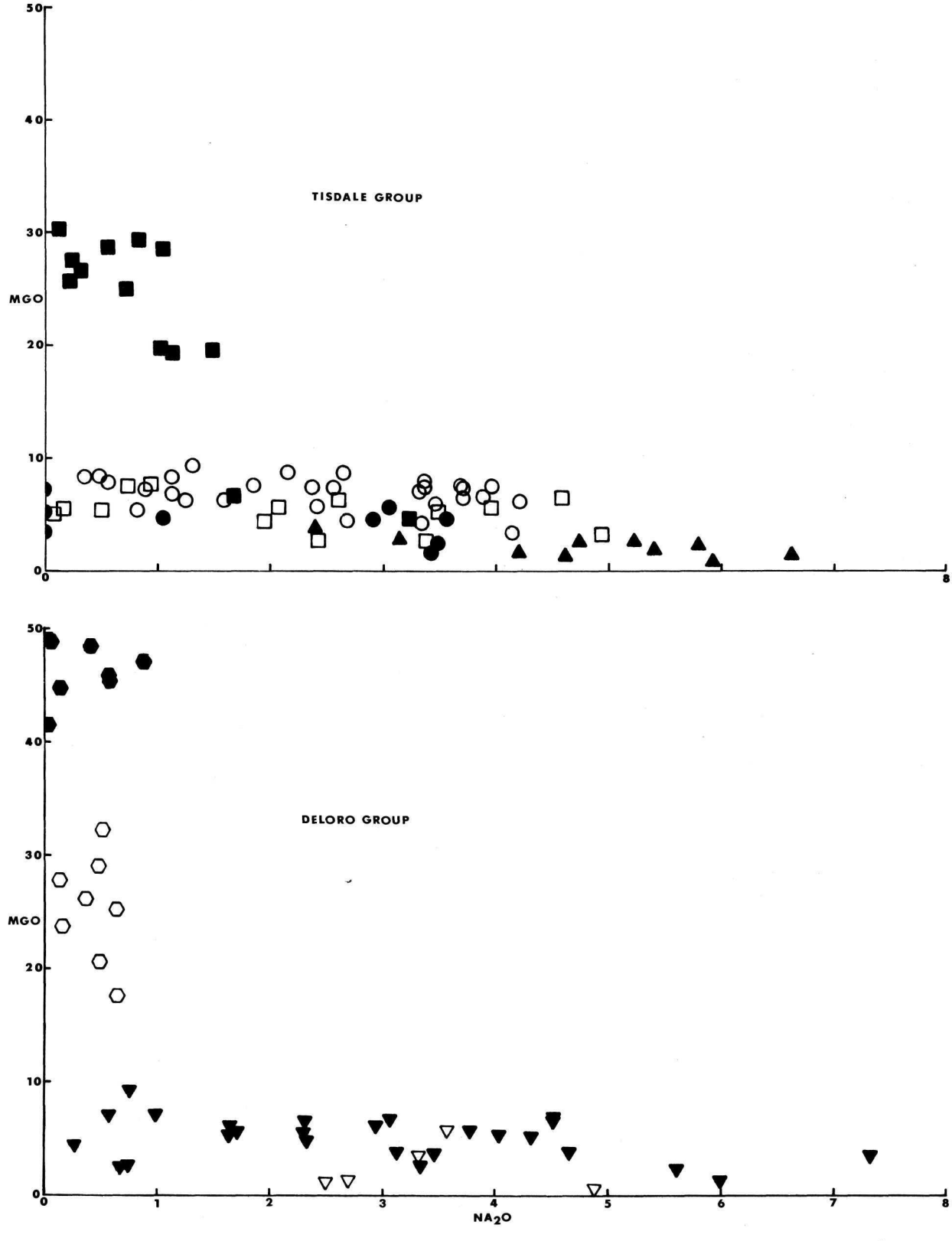
TISDALE GROUP
MGO
50
40
30
20
10
0
0
8
DELORO GROUP
MGO
50
40
30
20
10
0
0
1
2
3
4
5
6
7
8
NA2O

FIGURE 12E

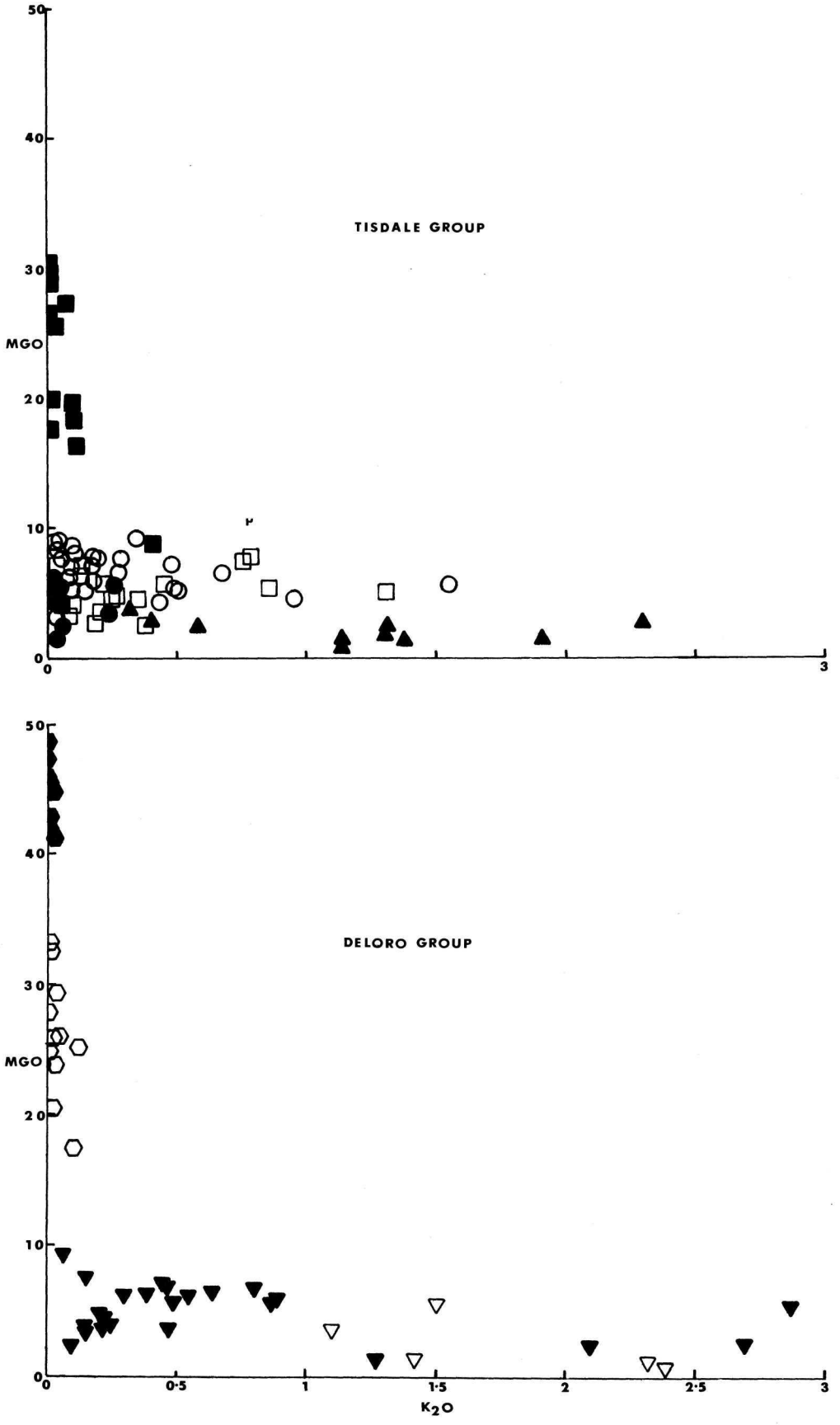
TISDALE GROUP
MGO
50
40
30
20
10
0
0
3
DELORO GROUP
MGO
50
40
30
20
10
0
0
0·5
1
1·5
2
2·5
3
K_2O

FIGURE 12F

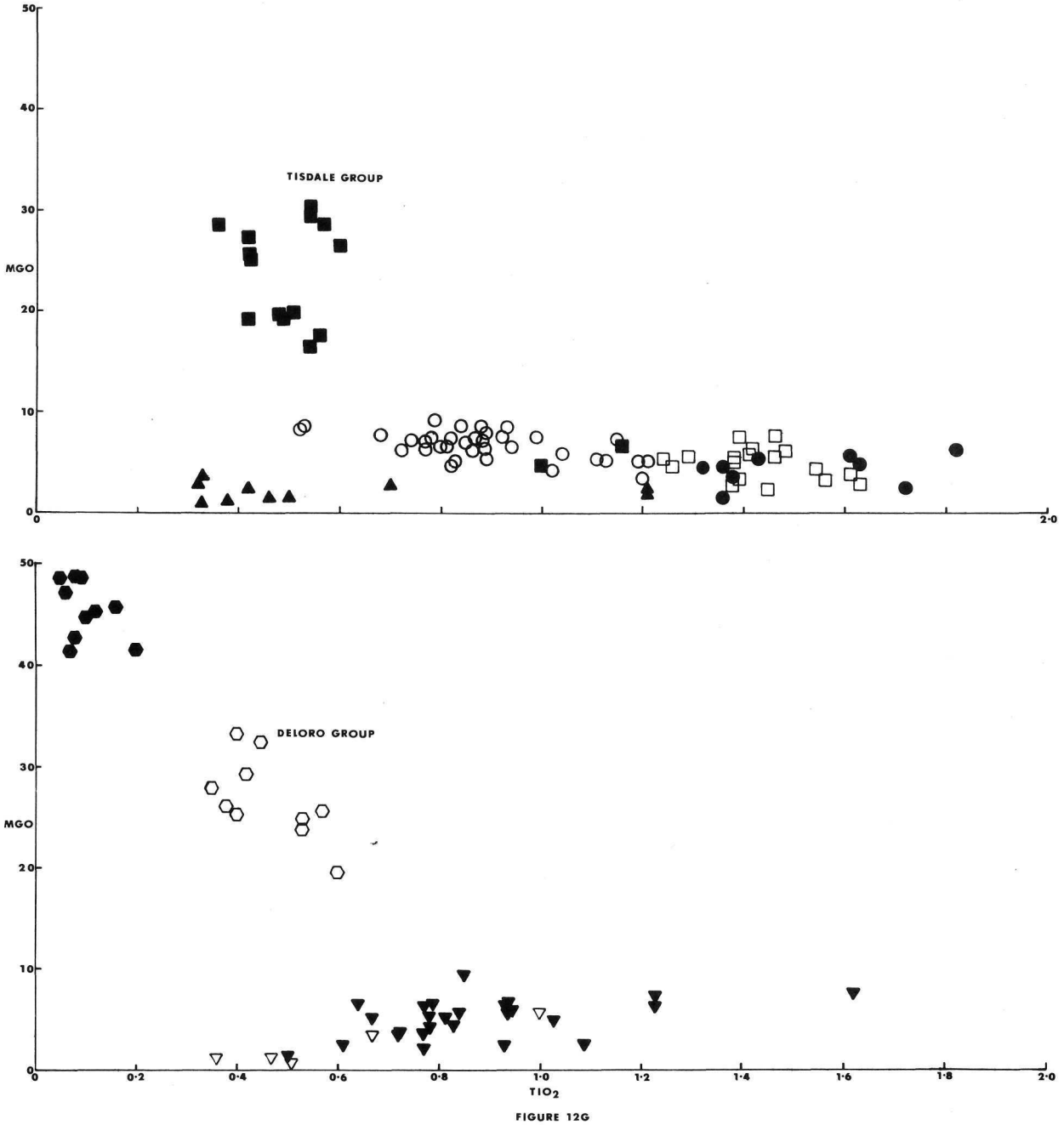
TISDALE GROUP
DELORO GROUP
MGO
TiO_2
0
10
20
30
40
50
0·2
0·4
0·6
0·8
1·0
1·2
1·4
1·6
1·8
2·0

FIGURE 12G

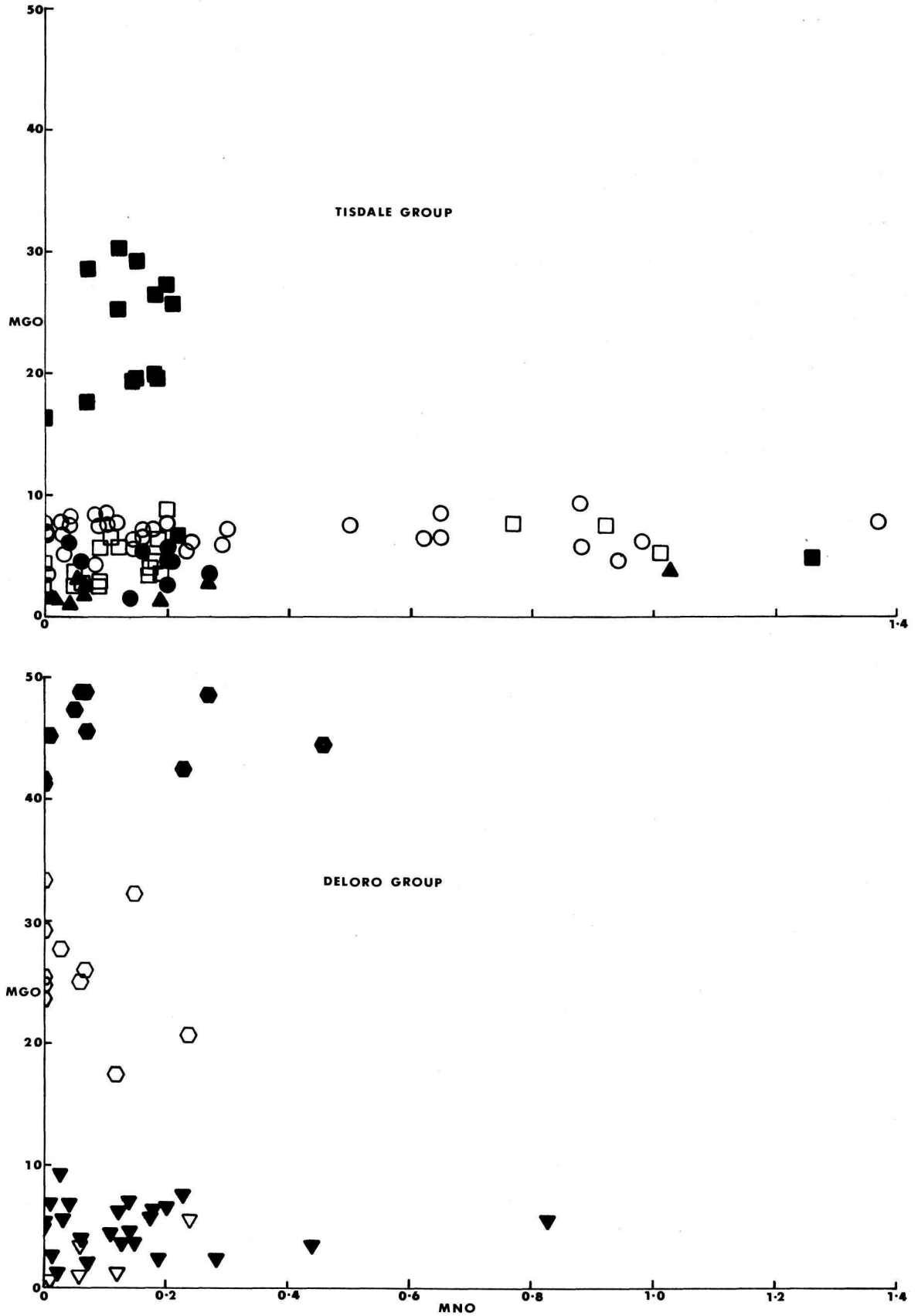
TISDALE GROUP
MGO
50
40
30
20
10
0
0
1·4
DELORO GROUP
MGO
50
40
30
20
10
0
0
0·2
0·4
0·6
0·8
1·0
1·2
1·4
MNO

FIGURE 12 H

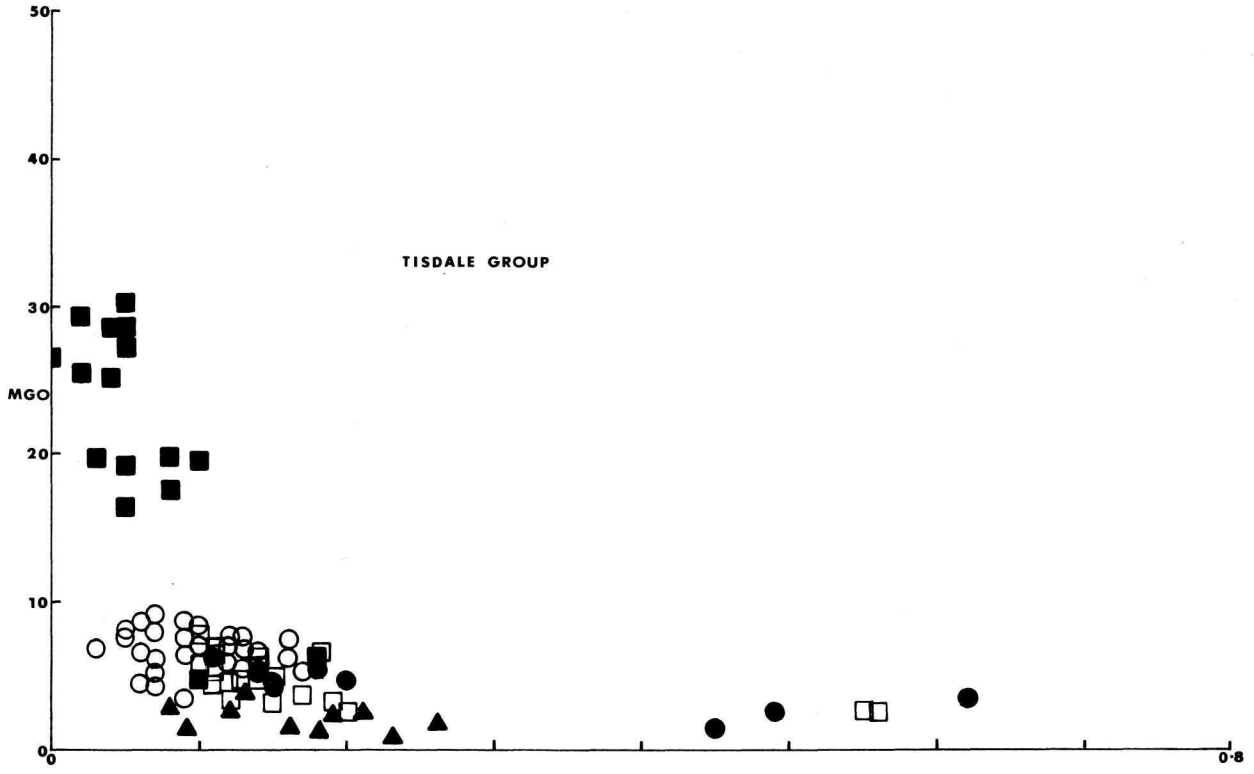
TISDALE GROUP
MGO
50
40
30
20
10
0
0
0·8

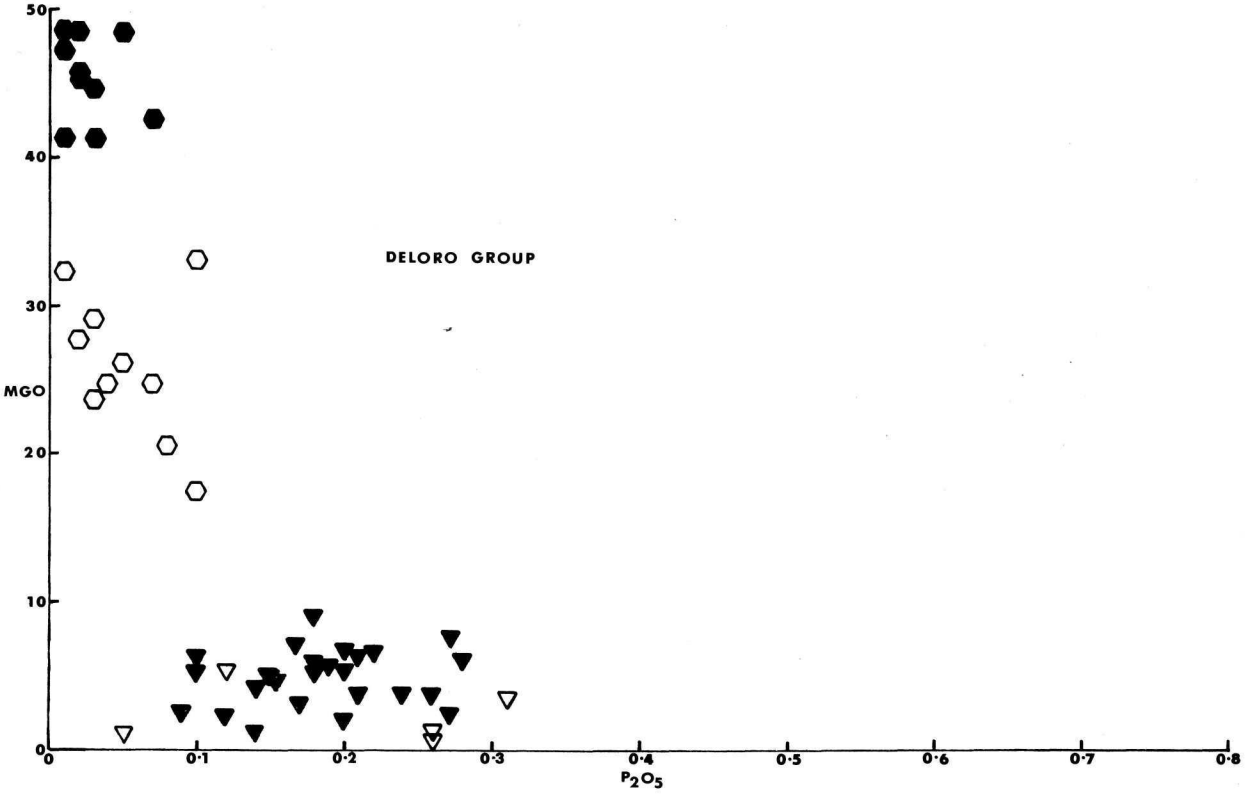
DELORO GROUP
MGO
50
40
30
20
10
0
0
0·1
0·2
0·3
0·4
0·5
0·6
0·7
0·8
P_2O_5

FIGURE 121

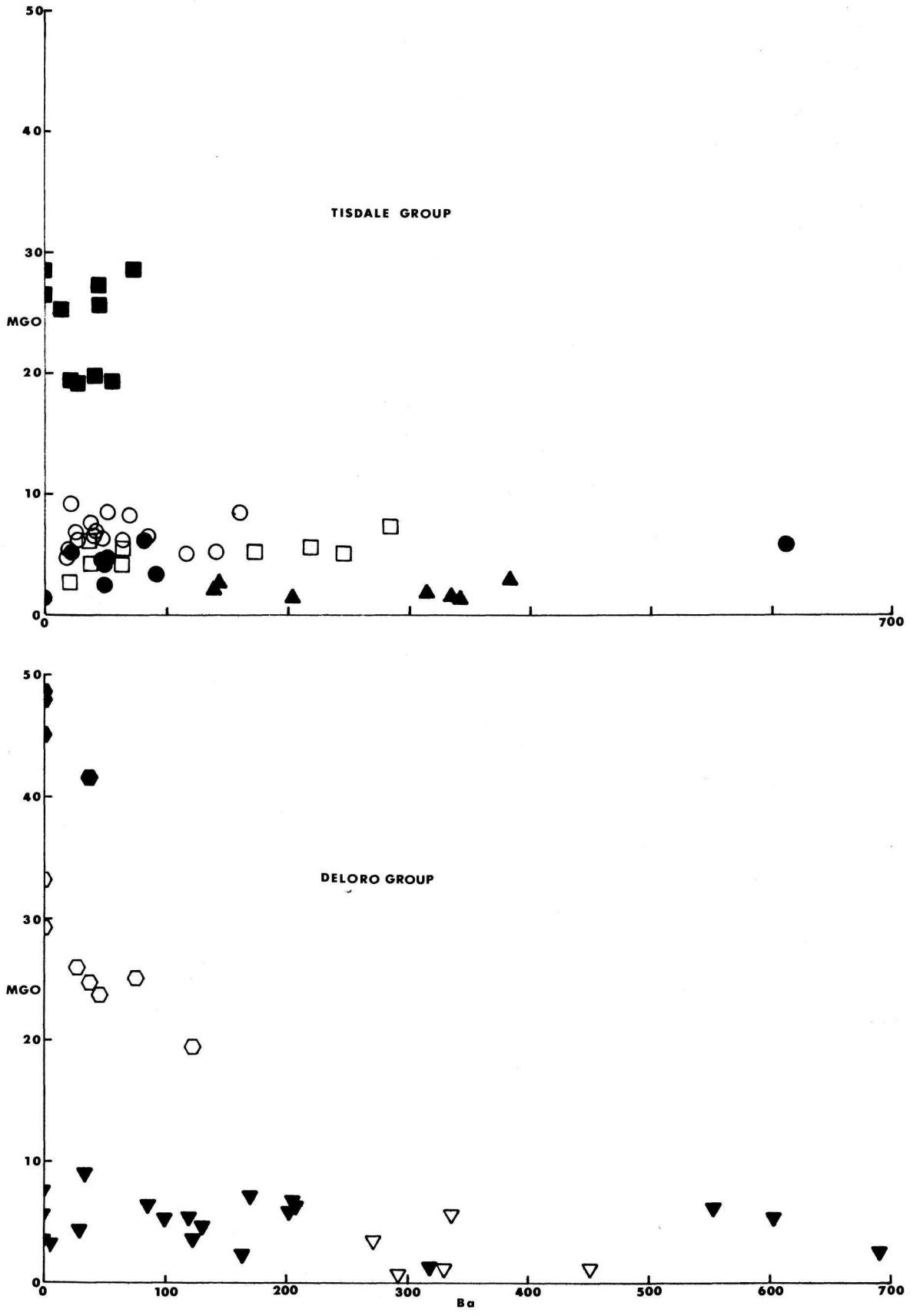
TISDALE GROUP
MGO
50
40
30
20
10
0
0
700
DELORO GROUP
MGO
50
40
30
20
10
0
0
100
200
300
400
500
600
700
Ba

FIGURE 12J

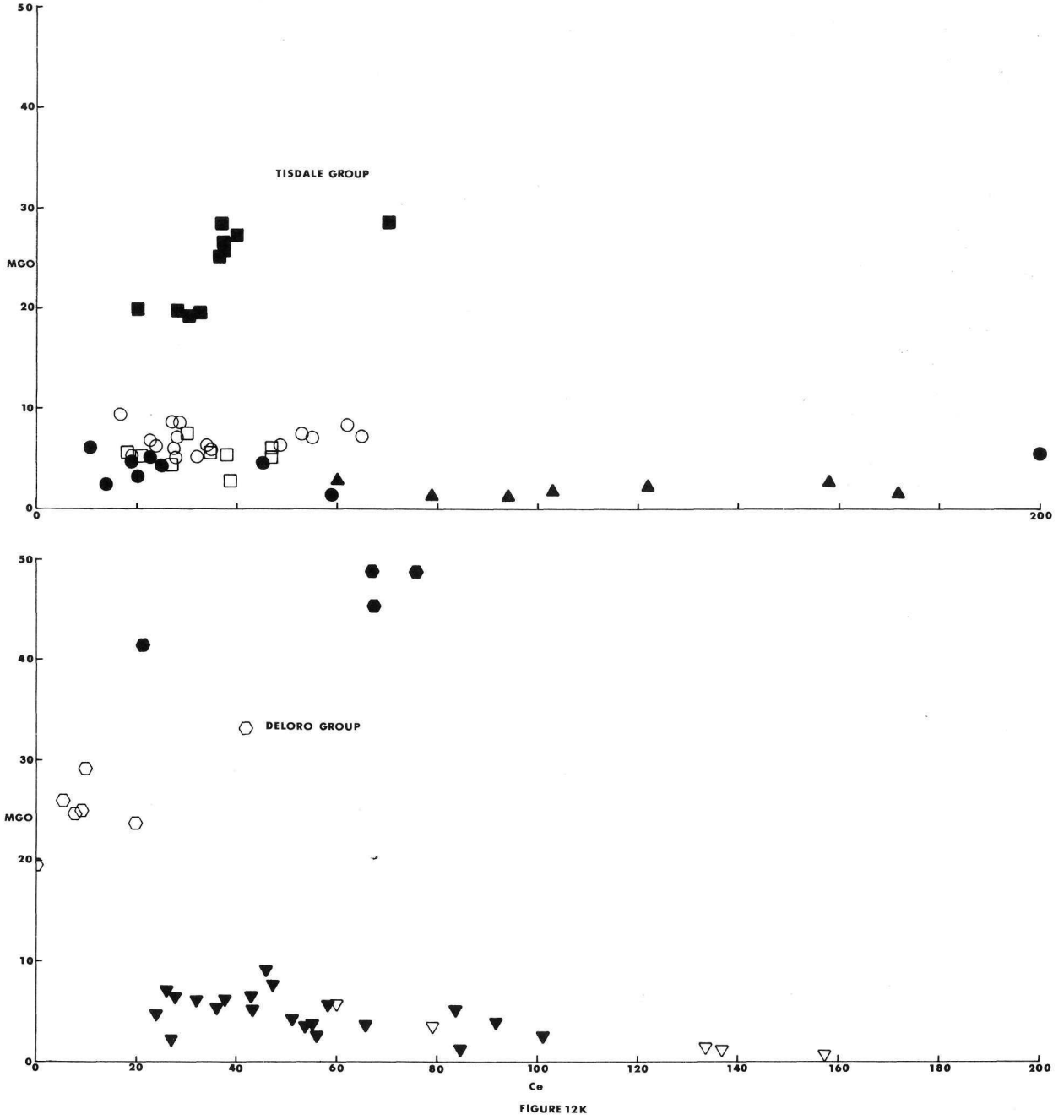
TISDALE GROUP
MGO
50
40
30
20
10
0
0
200
DELORO GROUP
MGO
50
40
30
20
10
0
0
20
40
60
80
100
120
140
160
180
200
Ce

FIGURE 12K

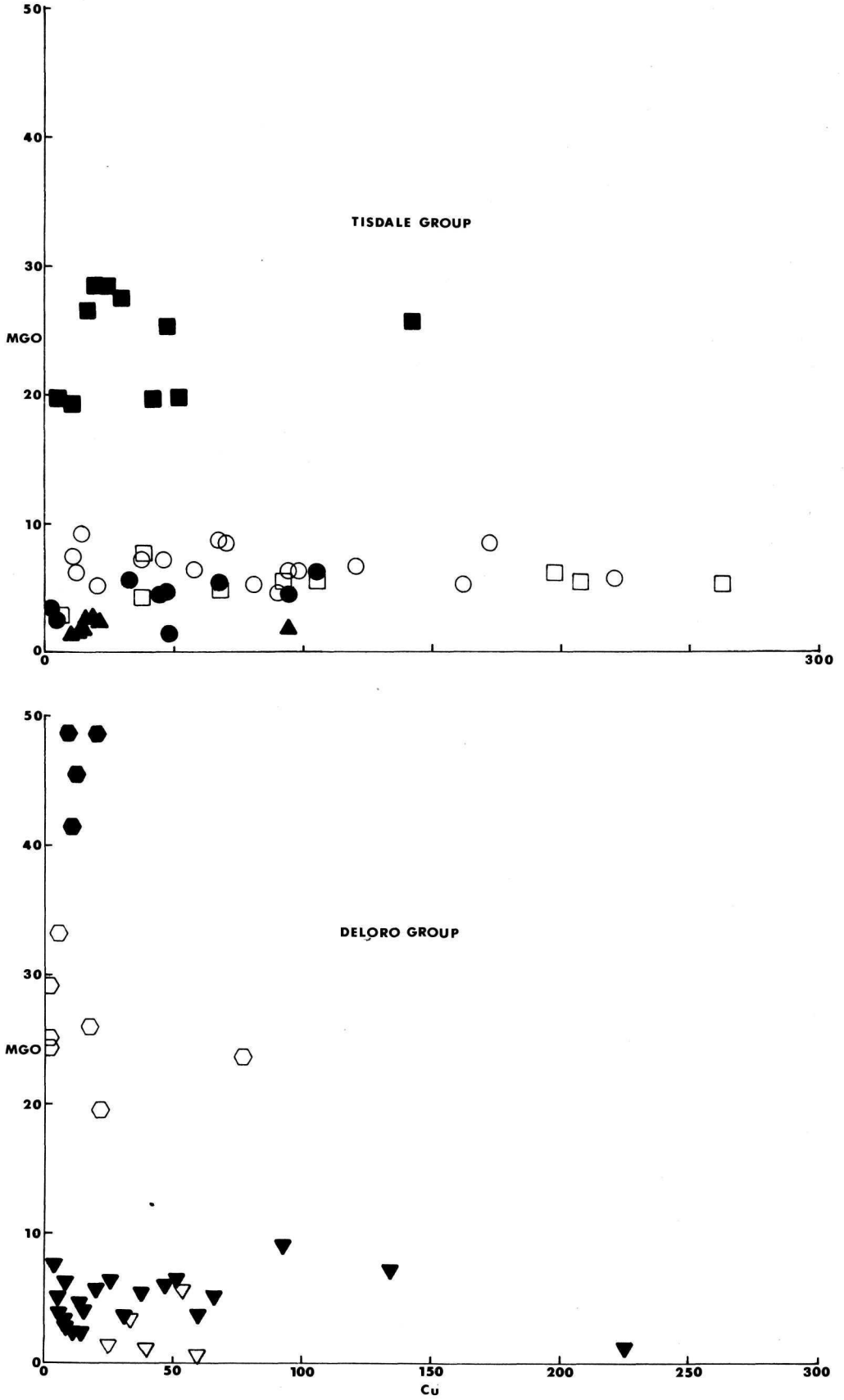
TISDALE GROUP
MGO
50
40
30
20
10
0
300
DELORO GROUP
MGO
50
40
30
20
10
0
50
100
150
200
250
300
Cu

FIGURE 12L

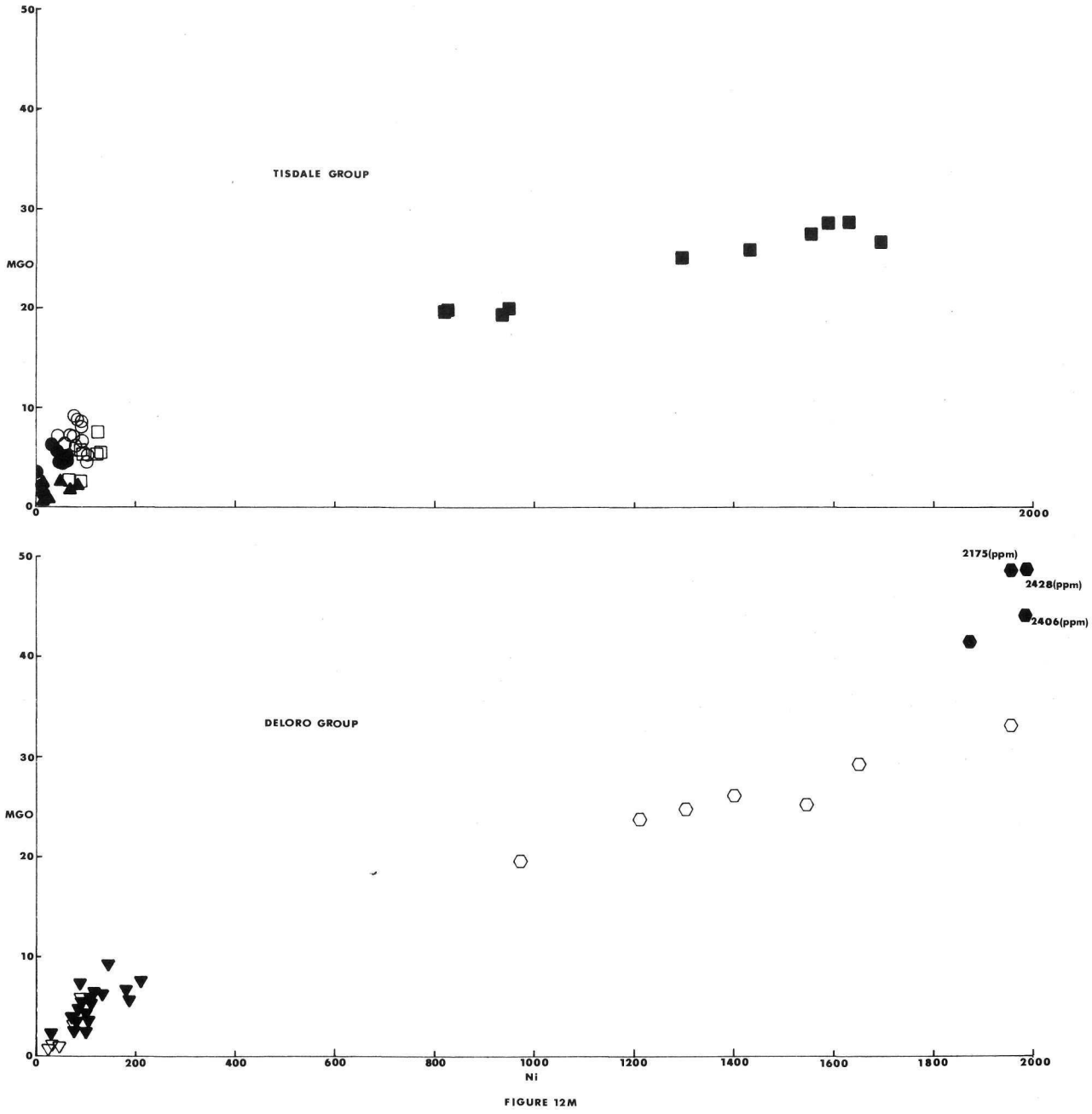
TISDALE GROUP
MGO
50
40
30
20
10
0
0
2000
DELORO GROUP
MGO
2175(ppm)
2428(ppm)
2406(ppm)
50
40
30
20
10
0
0
200
400
600
800
1000
1200
1400
1600
1800
2000
Ni

FIGURE 12M

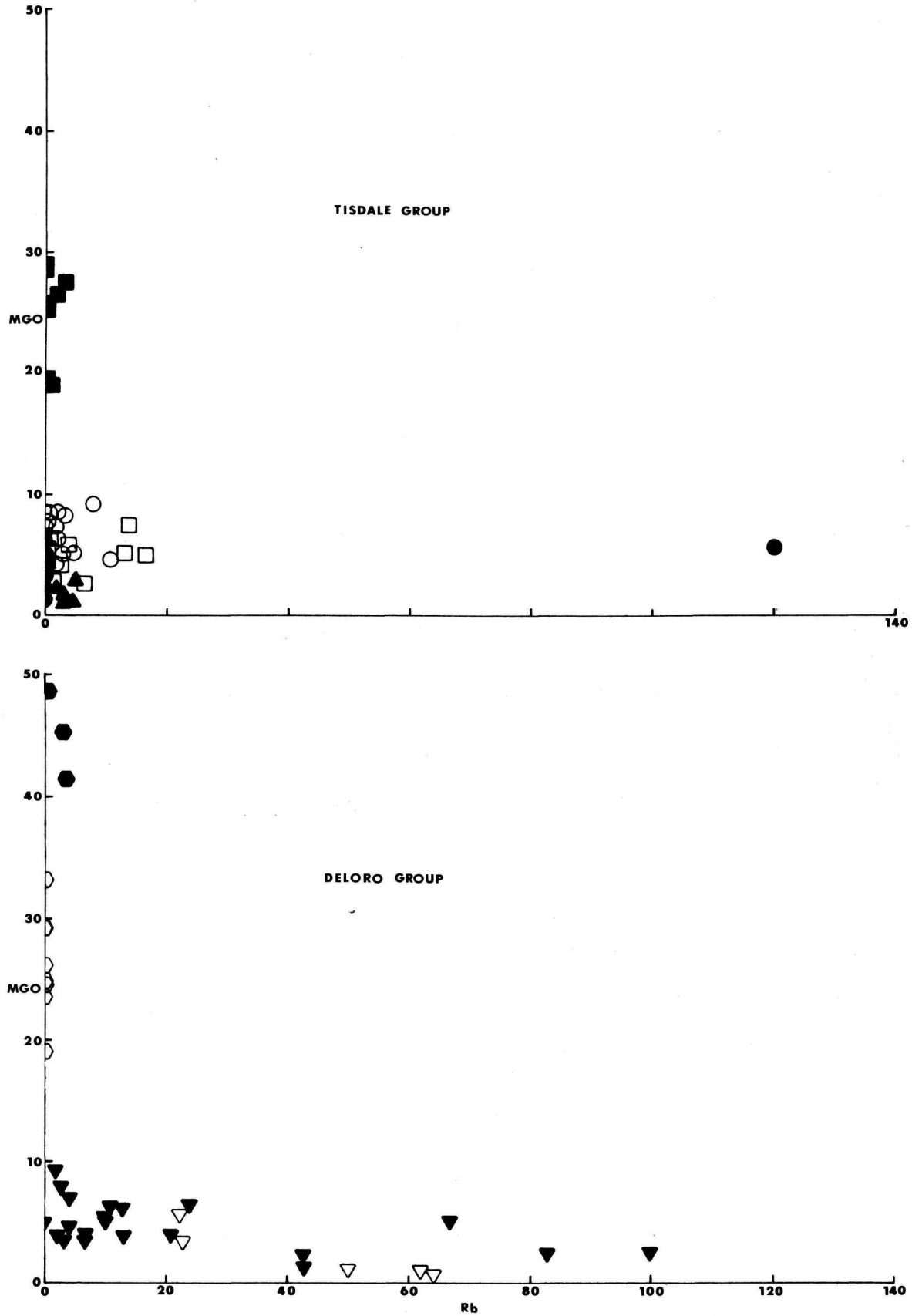
TISDALE GROUP
MGO
50
40
30
20
10
0
0
140
DELORO GROUP
MGO
50
40
30
20
10
0
0
20
40
60
80
100
120
140
Rb

FIGURE 12N

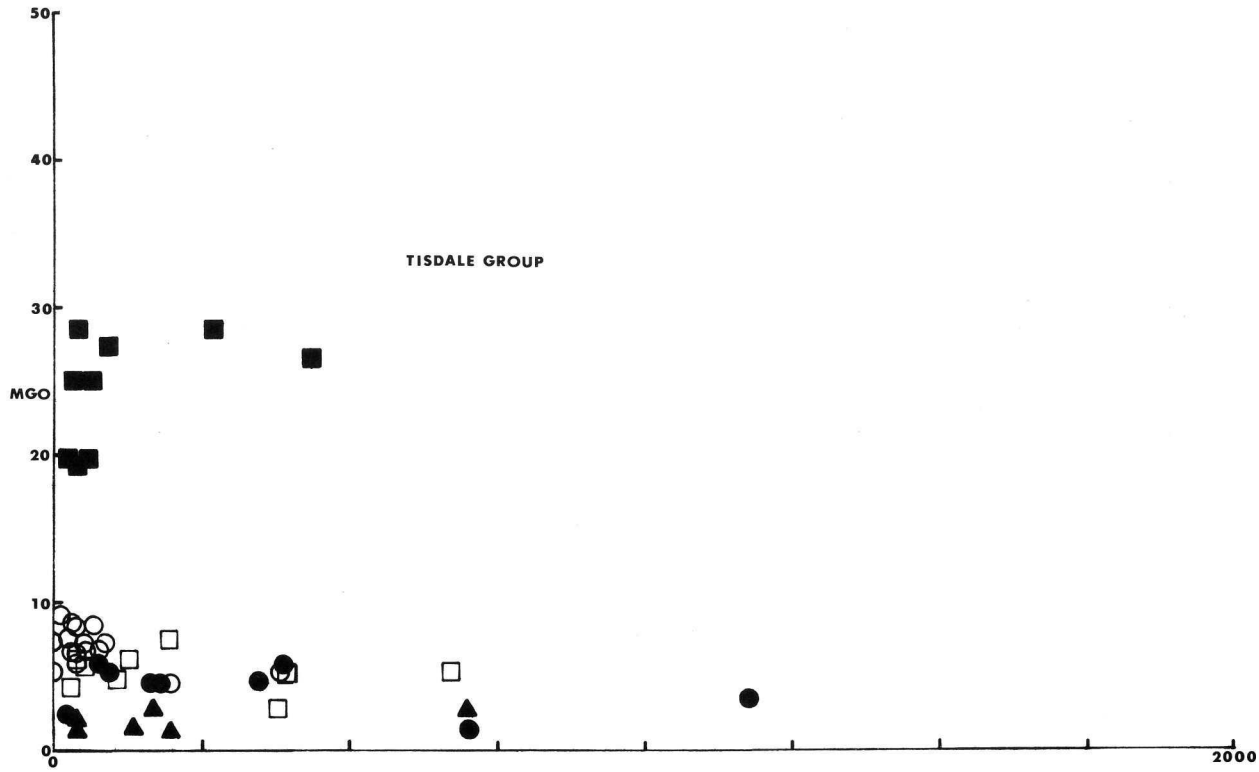
TISDALE GROUP
MGO
50
40
30
20
10
0
0
2000

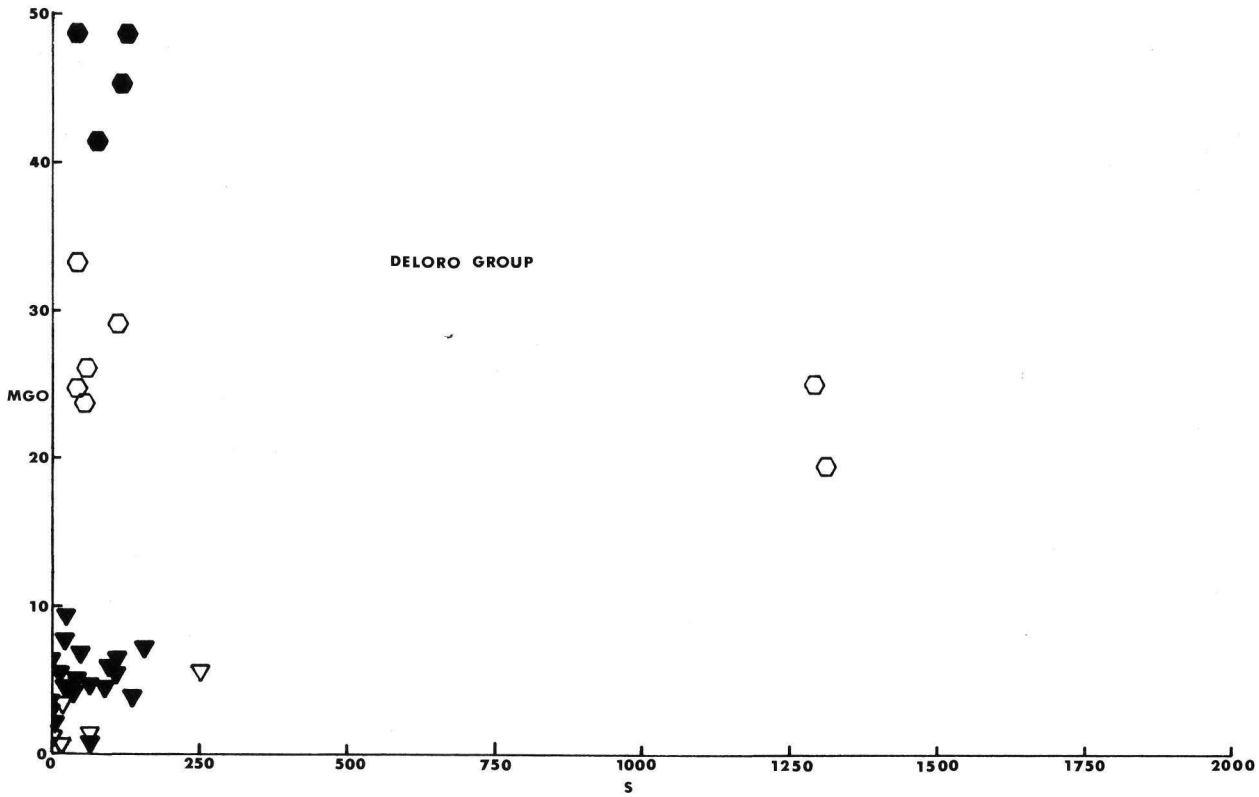
DELORO GROUP
MGO
50
40
30
20
10
0
0
250
500
750
1000
1250
1500
1750
2000
S

FIGURE 120

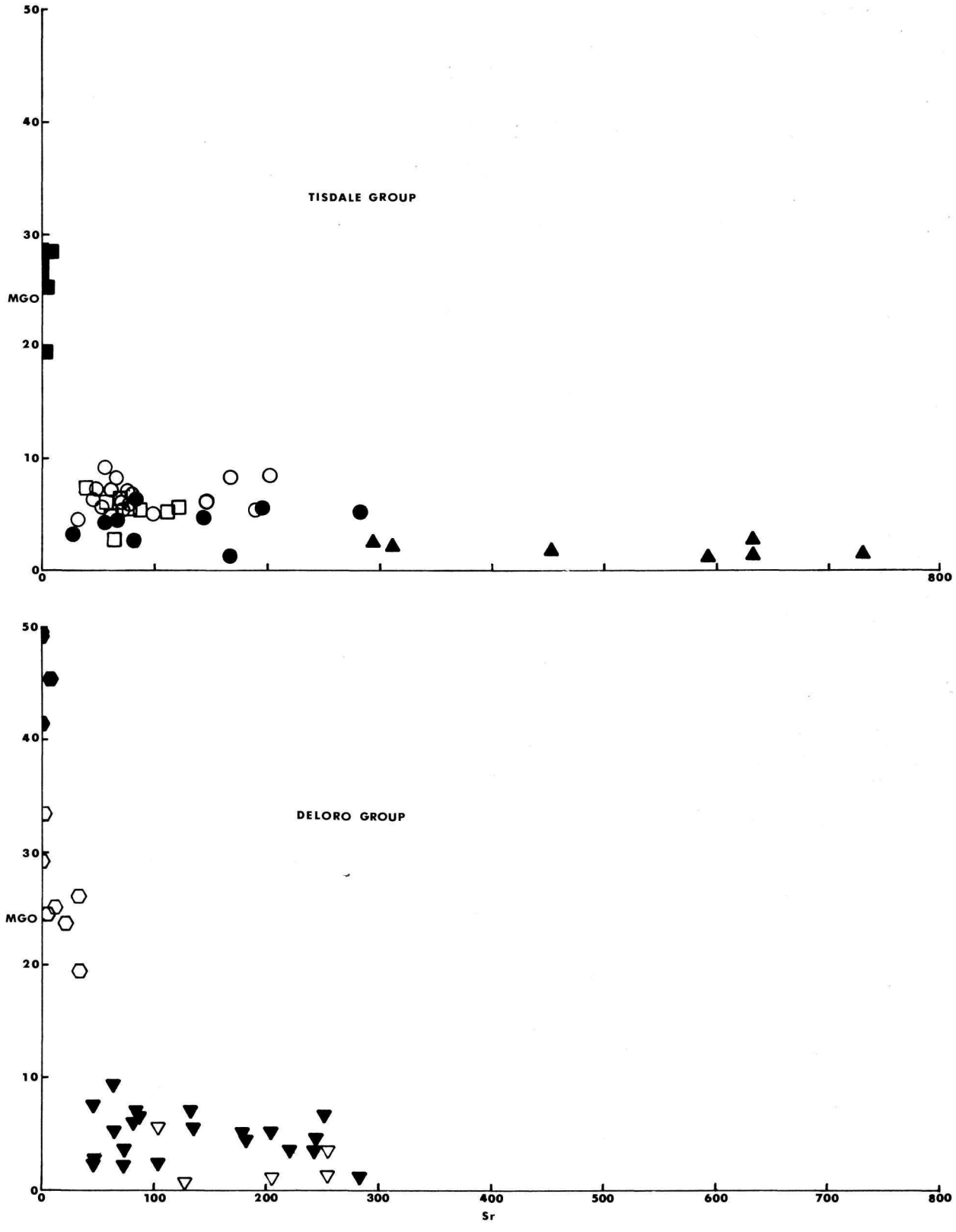
TISDALE GROUP
MGO
50
40
30
20
10
0
0
800
DELORO GROUP
MGO
50
40
30
20
10
0
0
100
200
300
400
500
600
700
800
Sr

FIGURE 12P

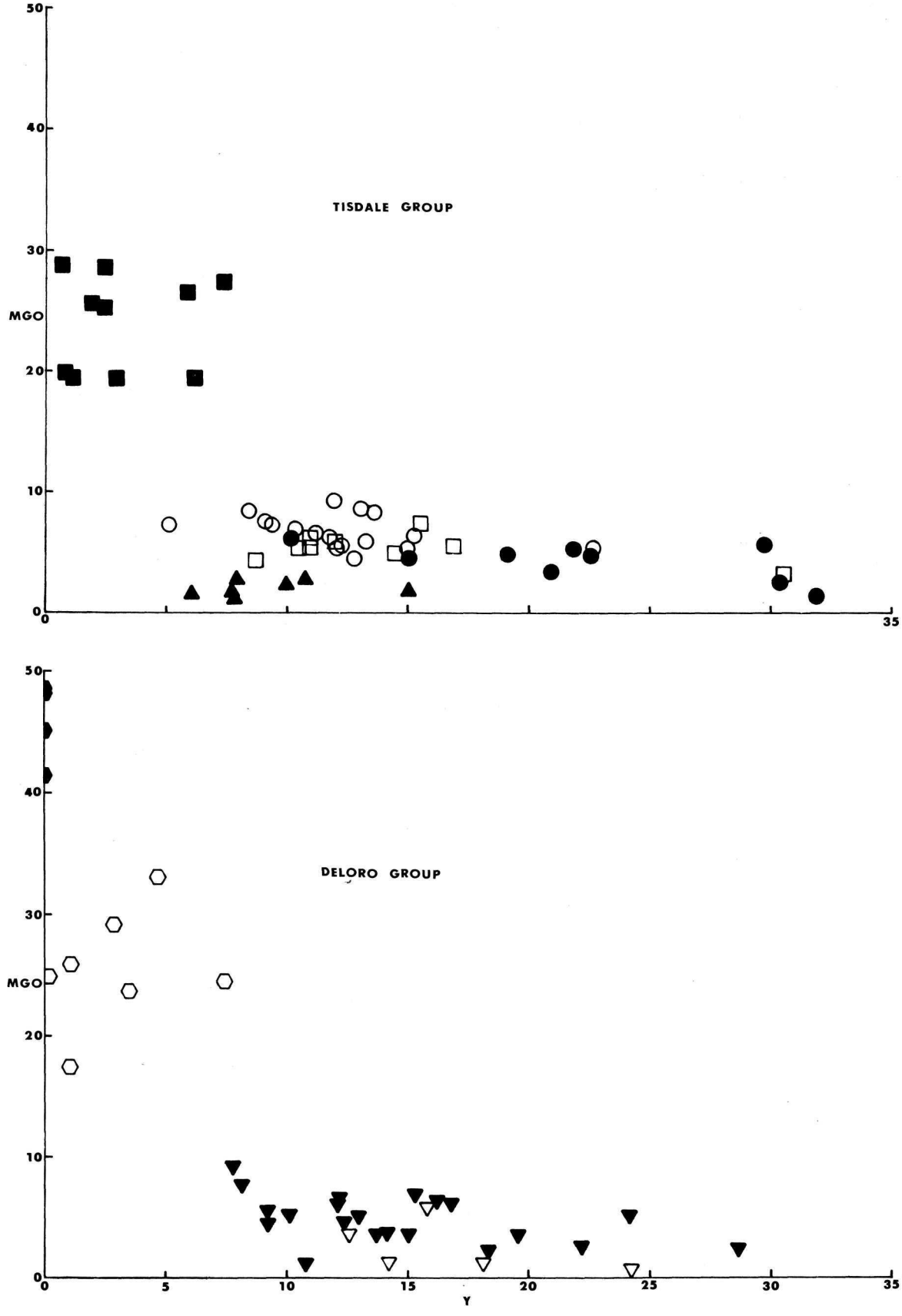
TISDALE GROUP
MGO
50
40
30
20
10
0
0
35
DELORO GROUP
MGO
50
40
30
20
10
0
0
5
10
15
20
25
30
35
Y

FIGURE 12Q

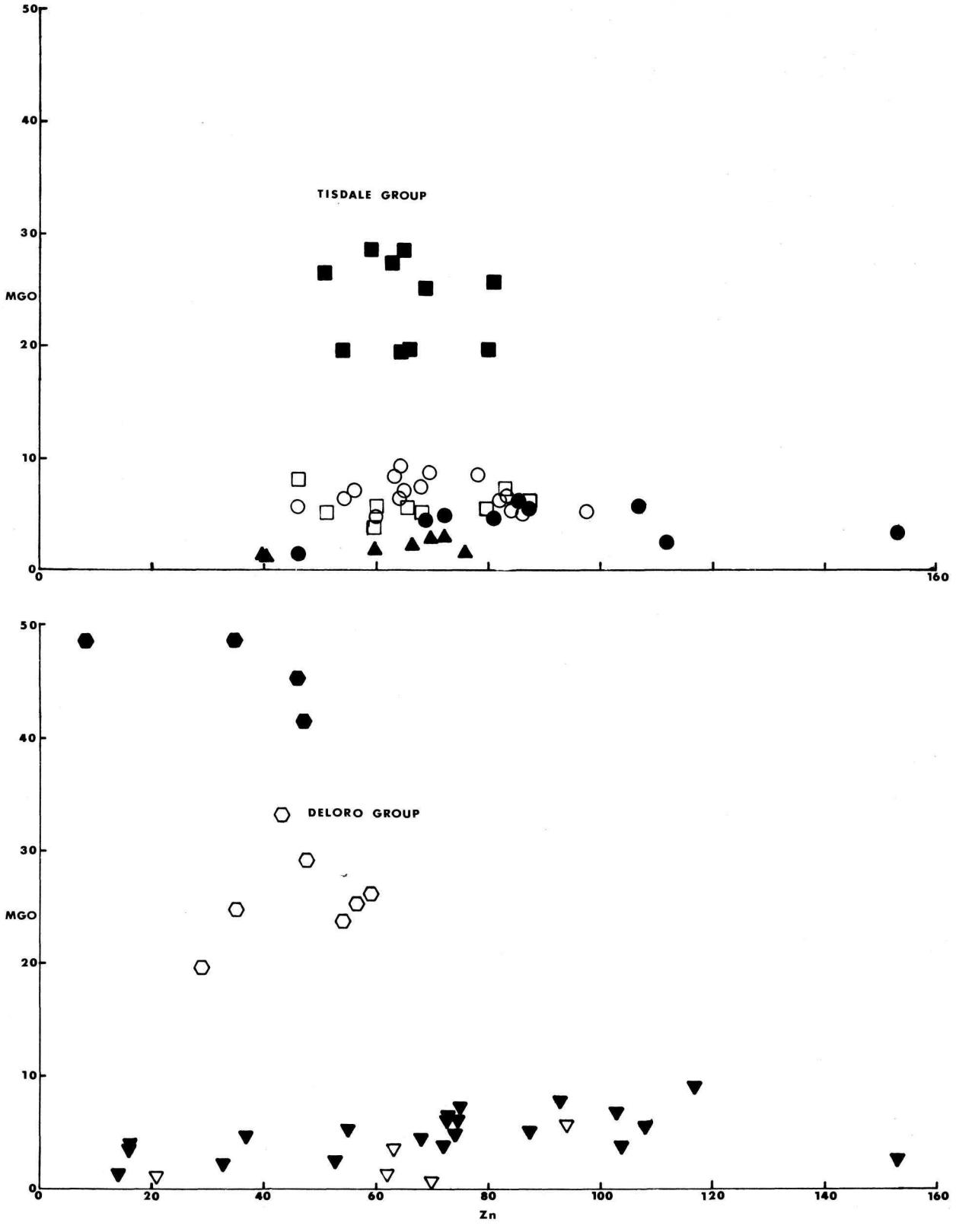
TISDALE GROUP
DELORO GROUP
MGO
Zn
0
10
20
30
40
50
60
80
100
120
140
160

FIGURE 12R

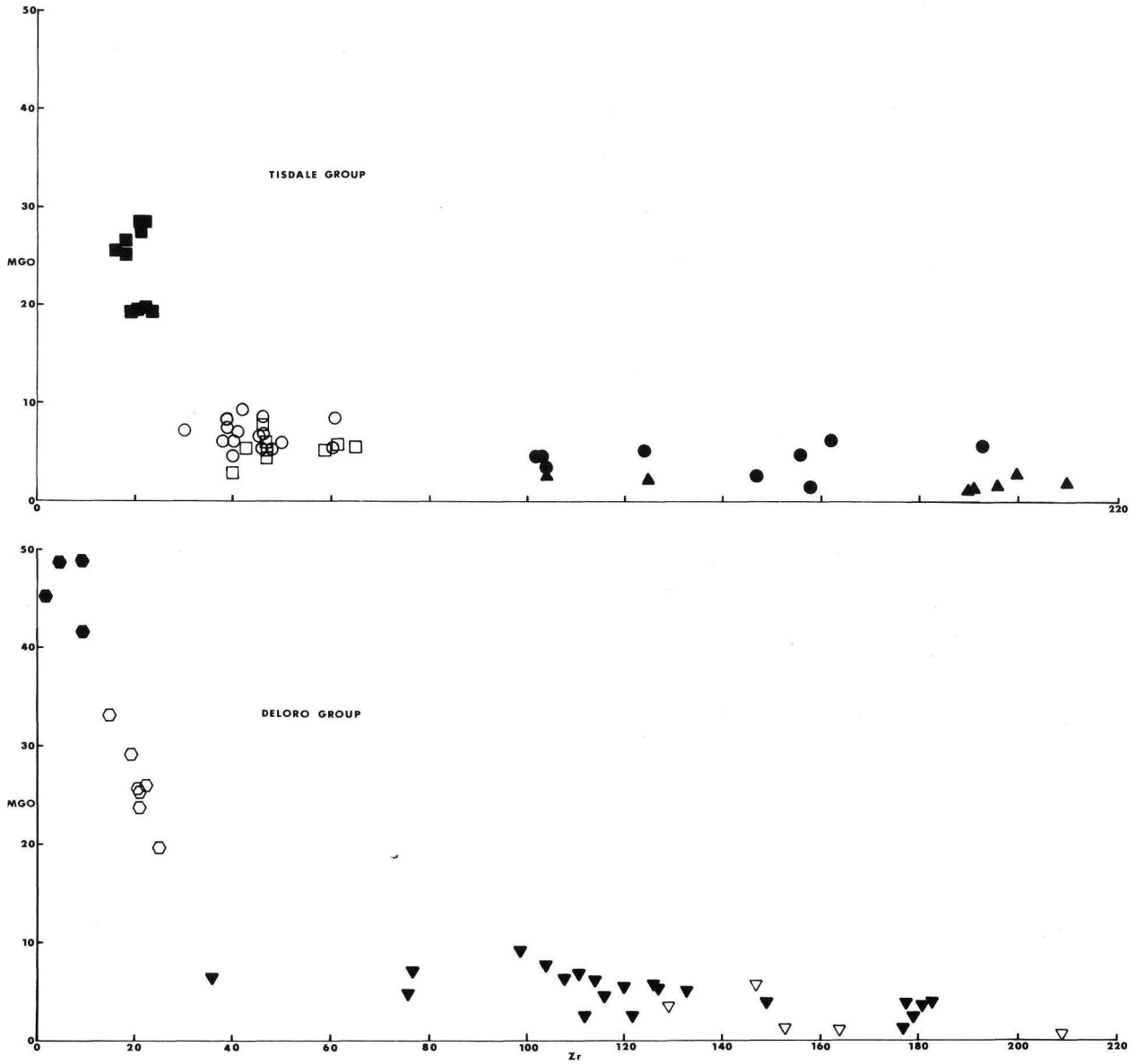
TISDALE GROUP
MGO
50
40
30
20
10
0
0
220
DELORO GROUP
MGO
50
40
30
20
10
0
0
20
40
60
80
100
120
140
160
180
200
220
Zr

FIGURE 12S

Sun (1976), Arndt et al., (1977) and Jolly (1978), but appear low when compared with Viljoen and Viljoen (1969) who reported an average value of 1.5. The average non-cumulate Ti/Zr ratio for the Goose Lake Formation is 129 and 128 for the Donut Lake Formation. These values are close to that reported by Nesbitt and Sun (1976). However, the peridotitic komatiitic cumulate rocks have a higher average Ti/Zr ratio of 157 accompanied by lower alumina values. The higher value suggests titanium fractionation during crystal settling (Rankama and Sahama, 1950; Wilkinson and Duggan, 1973). A plot of Al_2O_3 vs. FeO*/FeO* + MgO (Fig. 13) shows the komatiitic rocks fall to the left of the dividing line which separates the komatiitic and tholeiitic fields, however, the basaltic komatiites plot on both sides of the line suggesting a similarity to tholeiitic rocks of the same Al_2O_3 content. The difference between mafic tholeiitic rocks and basaltic komatiites in the Timmins area is lower values of FeO* and CaO in the latter relative to the former. Figures 12b and 13 suggest slight differences in alumina and iron at equivalent MgO values between the Donut Lake and Goose Lake Formations. The Donut Lake Formation, being slightly higher in alumina and lower in iron suggests that olivine is richer in MgO than FeO* and the alumina values are slightly higher due to the presence of chlorite in most thin sections. Figure 12b also indicates a gap in the MgO distribution between 14 and 8%. Arndt et al., (1977) found a gap between 19 and 14% MgO while Nisbet et al., (1977) have reported a gap between 20 and 16% MgO. The gaps in the MgO contents reported in the literature do not occur at the same interval suggesting that in fact there may be a break that is diagnostic of each komatiitic sequence of lavas in different greenstone belts.

Figure 13

LEGEND

TISDALE GROUP

○ Upper Schumacher Formation

■ Goose Lake Formation

DELORO GROUP

⬡ Donut Lake Formation

⬢ Dunite-Peridotite

Al_2O_3 vs. FeO*/(FeO* + MgO) Diagram

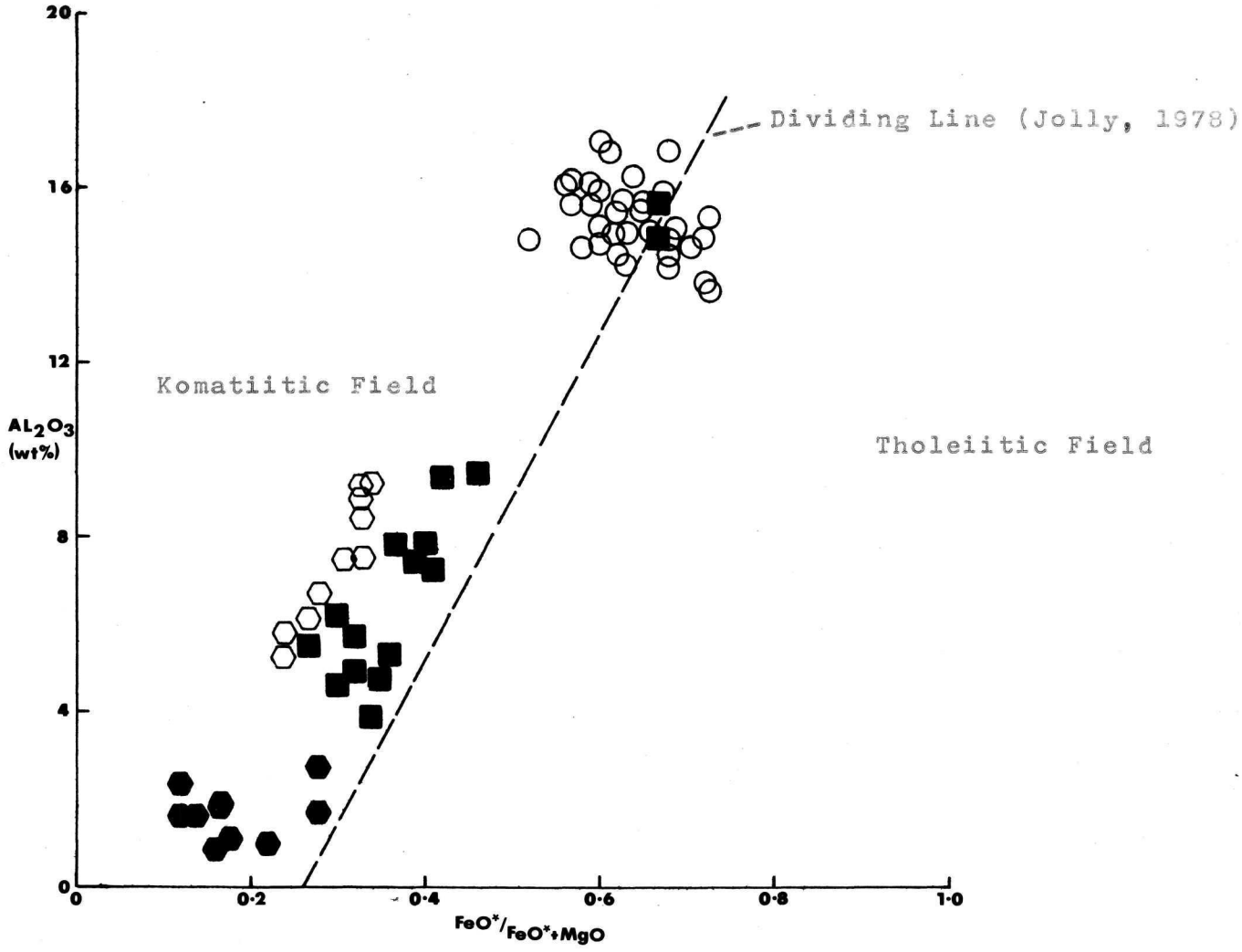

FIGURE 13

BASALTIC KOMATIITES AND THOLEIITES (LOWER SCHUMACHER FORMATION)

The Lower Schumacher Formation can be subdivided into two parts where the lower part is dominantly basaltic komatiite while the upper part is composed of tholeiitic rocks.

Generally, the Lower Schumacher Formation is enriched from the basalts to andesites in SiO_2, K_2O, TiO_2, P_2O_5, Zr, Zn, and Rb while being depleted in Al_2O_3, FeO*, MgO, CaO, MnO, S, and Ce (Fig. 12a-s). Na_2O, Ba, Cu and Ni are enriched from basalt to basaltic-andesite (6.5% MgO) but is depleted inthe andesites. Figure 13 indicates that the Lower Schumacher Fm. is dominantly basaltic komatiite in character while the samples falling on the right side of the dividing line are low TiO_2 tholeiites. Sample locations of the tholeiitic rocks place most at or near the top of the Lower Schumacher Fm., stratigraphically under the variolitic lava flows. Petrographically there is no difference between the two types of rocks. Figure 13 indicates a slightly higher FeO*/Feo* + MgO ratio for the tholeiitic rocks at an equivalent Al_2O_3 content. Figure 14 suggests a slightly higher TiO_2 value (1.05) while the basaltic komatiites average 0.8% TiO_2. The diagram also indicates a slightly higher zirconium content of 53 ppm for the tholeiites compared to 45 ppm for the basaltic komatiites. The increase in TiO_2 and Zr contents of the tholeiitic rocks suggests a slightly more fractionated rock in comparison with the basaltic komatiites. The average Ti/Zr ratio of the Lower Schumacher Formation is 115 similar to that reported by Nesbitt and Sun (1976) for their "low MgO metabasalts of the high-magnesium series." Magnesian values range from 7.1% in the basalts to 6.7% in the basaltic andesites to 5.6% in the andesites while FeO* ranges from 12.4% in the basalts, 11.5% in the basaltic andesites and 10.9% in the andesites. These values

Figure 14

LEGEND

TISDALE GROUP

▲ Krist Formation

○ Upper Schumacher Formation

● Variolitic Flows

□ Lower Schumacher Formation

■ Goose Lake Formation

DELORO GROUP

▽ Boomerang Formation

▼ Redstone Formation

⬡ Donut Lake Formation

⬢ Dunite-Peridotite

TiO_2 expressed in weight percent

Zr expressed in parts per million

TiO_2 vs. Zr Diagram

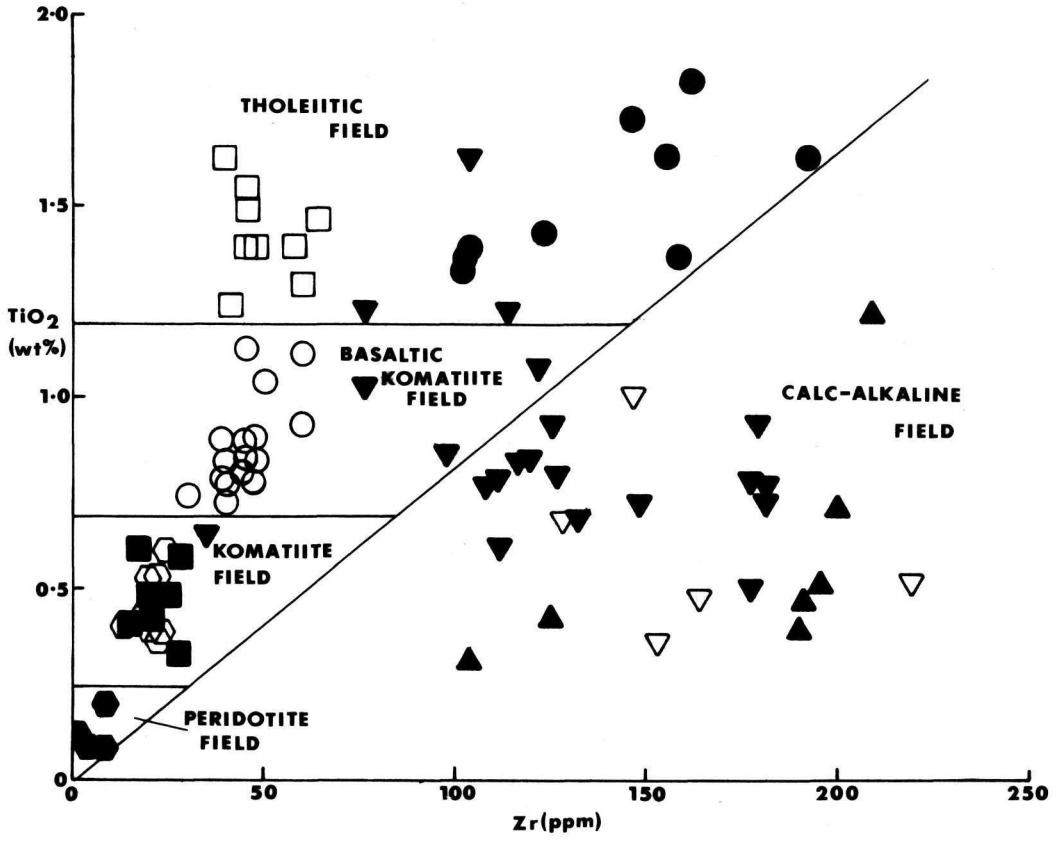

FIGURE 14

indicate no iron enrichment in this suite of rocks suggesting their affinity for the komatiite suite. Nickel values range from 71 ppm (basalts) to 63 ppm in the andesites.

VARIOLITIC LAVA FLOWS

A thin stratigraphic zone of variolitic flows occurs in the Schumacher Fm. between the basaltic komatiites (Lower Schumacher Fm.) and the tholeiites (Upper Schumacher Fm.) Whole rock analyses of the flows are presented in Appendix I. The variolitic flows range in composition from basalt to andesite. Figure 12a-s, indicates that SiO_2 and P_2O_5 become progressively enriched while MgO, Ba, Zr, Sr, Zn, Ni and Rb are depleted throught the variolitic flows. CaO, Na_2O, K_2O, MnO, Y, S, and Ce are all depleted in the basaltic andesite and are only slightly enriched in the basaltic andesites and are then depleted in the andesites. The basaltic variolitic flows contain high average concentrations of Ba, Zr, Sr, S, Na_2O, TiO_2, P_2O_5, Zn, Rb and Ce compared to both the underlying basaltic komatiites and the overlying tholeiites. The basaltic andesites and andesitic variolitic flows contain lesser amounts of these elements (Appendix I). The variolitic flows show a slight iron enrichment at 4.5% MgO and 16.4% FeO*. Generally, the refractive elements are concentrated while the ferromagnesian elements are slightly depleted. Average values of each variolitic class indicates abnormally high values of iron and titanium. Brooks (1977) suggested that these elements are concentrated in the matrix surrounding the varioles. Gelinas et al., (1976) reported that variolites formed by the separation of a tholeiitic magma into two immiscible liquids, a felsic phase forming the varioles and a mafic phase, the matrix. Chemical analyses of variolitic lavas from the Timmins area agrees with analyses presented by

Gelinas et al., (1976) but does not confirm their hypothesis. Their proposal has been criticized by Philpotts (1977) and Hughes (1977). Hughes (1977) maintains that varioles are products of metamorphic and metasomatic processes which accompany degradation in the prehnite-pumpellyite to low greenschist facies which accentuate and differentiate structures and textures in a uniform basalt. This theory does not take into account why most of the felsic elements become enriched. It also does not explain the restricted stratigraphic distribution of the variolites in the Timmins area. Gelinas et al., (1976) suggested that no alteration process can transform a basalt into discrete lenses of rhyolitic composition while preserving the skeletal morphology of quench crystals. Roedder and Weiblen (1970) working on the lunar highland rocks proposed that a late stage immiscibility developed in all lunar crystalline rocks. The two immiscibility silicate melts vary in composition in which the felsic component is similar to a potassic granite while the other approximates a pyroxenite. Data of individual analyses of Roedder and Weiblen (1970) and Massion and Van Groos (1973) are plotted with average analyses of variolitic flows from the Timmins area (Fig. 15). The plots of the average Timmins variolites agrees with the data plotted for Roedder and Weiblen (1970) and Massion and Van Groos (1973). An alternative hypothesis has been introduced by Green (1975) where he has described variolitic flows as plagioclase glomeroporphyroblasts which formed as quench features during extrusion. Green (1975) also stated that the variolitic flows occur at the transition from tholeiitic to calc-alkaline rocks ($SiO_2 \approx 55\%$). This is not true in the Timmins area where the variolitic flows occur between the intercalated basaltic komatiites and tholeiites (Lower Schumacher Fm.) and the tholeiitic suite

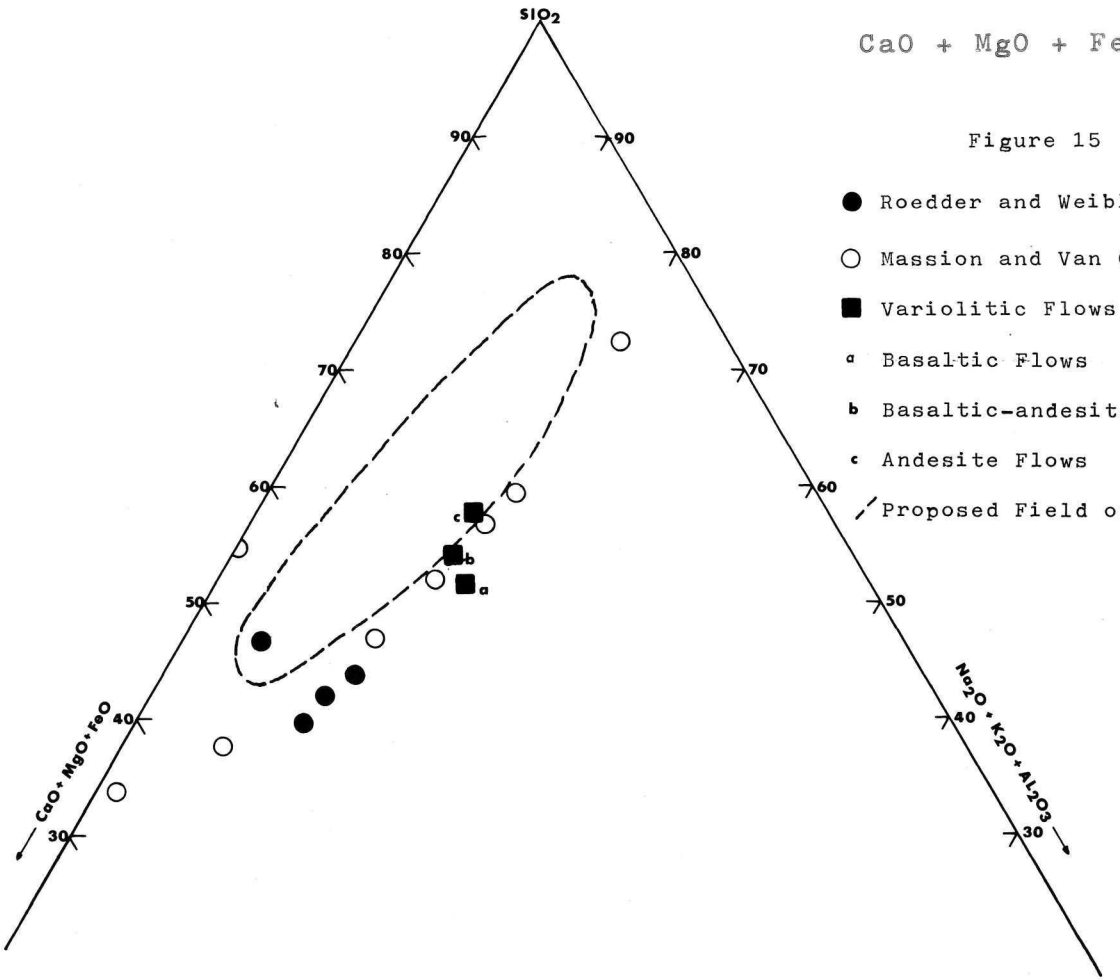

CaO + MgO + Feo* - SiO_2 - Na_2O + K_2O + Al_2O_3 Diagram.

Figure 15

- Roedder and Weiblen (1970)
- Massion and Van Groos (1973)
- Variolitic Flows Timmins Area
- a Basaltic Flows
- b Basaltic-andesite Flows
- c Andesite Flows
- Proposed Field of Immiscibility

(Upper Schumacher Fm.).

THOLEIITES
(UPPER SCHUMACHER FORMATION)

The Upper Schumacher Fm. is made up of a tholeiitic suite of basalts, basaltic andesites and andesites. Figure 12a-s indicates that SiO_2, Al_2O_3, Na_2O, Zr, Y, Sr and Zn are all enriched while MgO, K_2O, MnO, Ba, S, Cu, Ni, Rb and Ce are depleted throughout the suite. FeO*, CaO, TiO_2 and P_2O_5 are enriched in the basaltic andesite then depleted in the andesites.

Tholeiitic lavas are characterized by a marked iron enrichment in their intermediate members (Carmichael, 1964; Jolly, 1978). The tholeiitic suite in the Timmins area show a mild iron enrichment at 13.66% FeO* (AVE.) and 4.62% (AVE.) MgO (Fig. 12c). This suite of tholeiitic rocks is similar to that found by Jolly (1978) for the Blake River tholeiitic volcanic rocks. The Blake River suite exhibits an iron enrichment at 14.00% FeO* and 4.5% MgO (Fig. 16). Figure 12g also indicates a TiO_2 enrichment in the basaltic andesites of 1.45% (AVE.) at 4.62% (AVE.) MgO for the tholeiitic rocks in the Timmins area.

CALC-ALKALINE
REDSTONE FORMATION

The Redstone Fm. is a sequence of calc-alkaline volcanics ranging in composition from basalt, basaltic andesite, andesite and dacite. Chemical analyses are presented in Appendix I. Figure 12a-s, suggests that SiO_2, Na_2O, Zr and Ce are enriched while FeO*, MgO, CaO, Zn and Ni are depleted towards the dacitic compositions. Enrichment of Al_2O_3, TiO_2, P_2O_5 and S occurs in the basaltic andesite-andesite class. Figure 12g, indicates that TiO_2 is enriched (1.05%, AVE.) in the basaltic andesite at 6% (AVE.) Mgo while

Figure 16

MgO vs FeO*

Iron Enrichment Trend Lines

1. Magnesian Suite (Jolly, 1978)
2. Magnesian Tholeiite Suite (Jolly, 1978)
3. Dequisier 1st Cycle (Gelinas *et al*, 1977)
4. Baragar Traverse
5. Blake River Group Tholeiites (Jolly, 1978)
6. Tholeiitic Suite (Jolly, 1978)
7. Tholeiitic Trend Upper Schumacher Fm. Timmins Area.

FeO*- Total Iron

MgO vs. FeO* Diagram

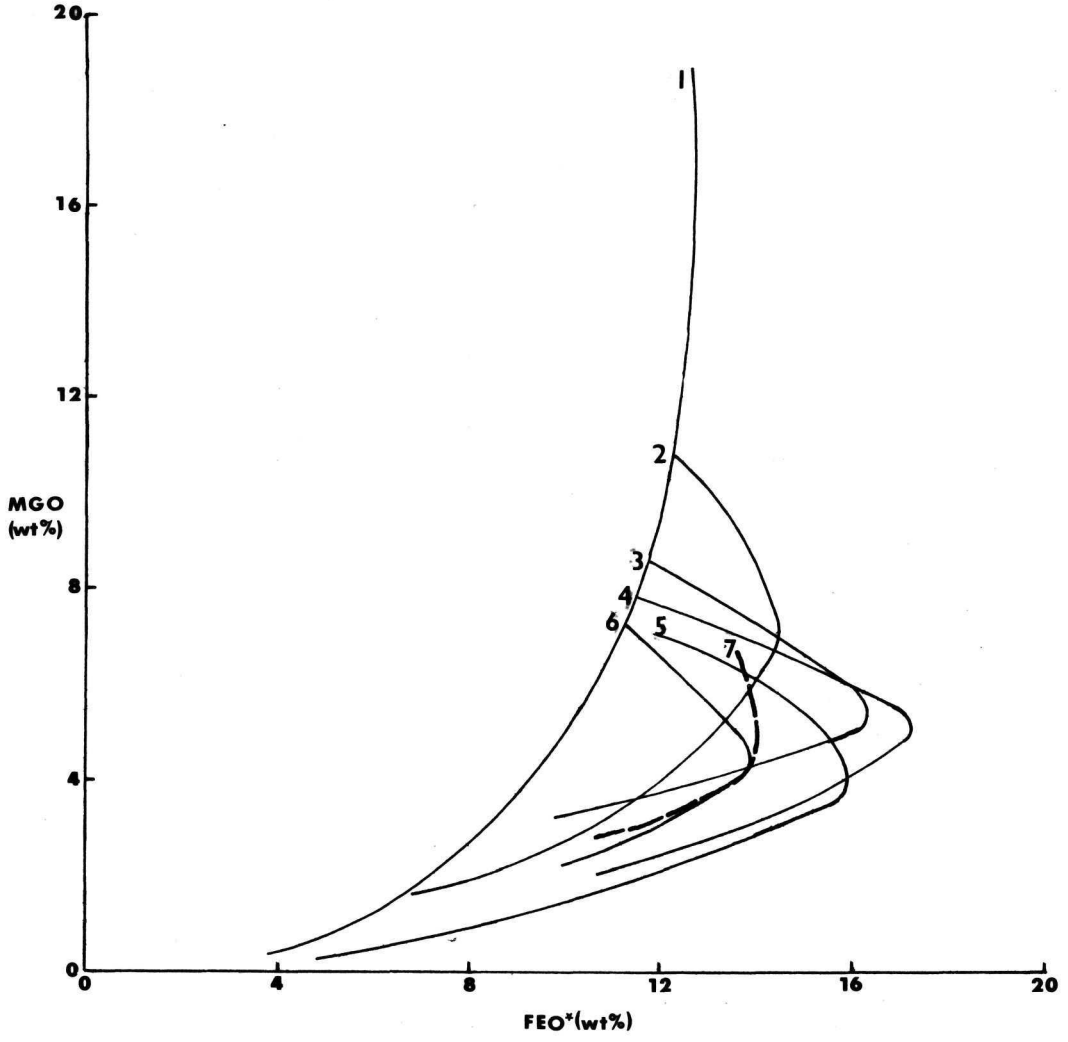

FIGURE 16

FeO* is systematically depleted throughout the suite (Fig. 12c). The titanium enrichment in the basaltic andesites is confirmed by the higher percentage of sphene observed in thin sections which suggests that ilmenite-magnetite may have fractionated out during the production of the basaltic andesites. The titanium enrichment suggests that the mafic sequence of the Redstone Fm. is basaltic komatiite-tholeiitic in character while the andesitic compositions are calc-alkaline in nature. The andesitic and dacitic rocks of this suite are commonly porphyritic which is rare in the tholeiitic rocks of the Timmins area, thus adding a felsic component to the rocks. Metasomatic processes have depleted the rocks in K_2O, Ba, Y, Cu and Rb(Fig.12e,j,l,n,q).

FELSIC CALC-ALKALINE
(BOOMERANG AND KRIST FORMATIONS)

The Krist and Boomerang Fms. are dominatly felsic pyroclastic sequences occuring stratigraphically at the top of the Deloro and Tisdale Groups north and south of the Destor-Porcupine Break. Analyses of the Boomerang and Krist Fms. are presented in Appendix I. The felsic calc-alkaline rocks make up a small percentage of the total amount of volcanic rock in the Timmins area. Figure 12a-s indicates that the Krist Fm. is a sequence of dacitic lavas while the Boomerang Fm. is dacitic to rhyolitic in composition. SiO_2, Rb and Ce are enriched while FeO*, TiO_2, MnO, Zn, Ni and MgO are depleted through this sequence of rocks. SiO_2, Na_2O, K_2O, Ba, Zr, Sr, Cu, Rb and Ce are enriched in the Krist Fm. Due to the close proximity of the Boomerang Fm. with the Destor-Porcupine Break, the reliability of the analyses representing original magmatic characteristics is questionable. The MgO-FeO* plot (Fig. 12c) exhibits a linear trend with no iron enrichment. This trend is similar to that reported by Green and Ringwood (1968), Smith and Carmichael (1968) and

Jolly (1975).

PERIDOTITES

Analyses of peridotites are presented in Appendix I. The peridotites contain between 41-48% MgO which is reflected in the abundance of normative olivine and orthopyroxene. Silica values range from 35-45% while there are low average amounts of Al_2O_3 (1.64%), CaO (1.25%) and TiO_2 (0.10%). The average Ti/Zr ratio of 99 for the peridotites from the Timmins area is within the values given by Nesbitt and Sun (1976). Olivine cumulate rocks have a Ti/Zr ratio of 363 suggesting strong titanium fractionation during crystal settling. The average CaO/Al_2O_3 ratio is 0.73 for the peridotites.

KEEWATIN AND TIMISKAMING-TYPE SEDIMENTARY ROCKS

Chemical analyses of the sedimentary rocks of the Timmins area are presented in Appendix I. Since each chemical analysis represents an individual bed the data indicates that the composition of each bed is different. Similar findings have been reported in other greywackes by Weber and Middleton (1961), Condie (1967) and Condie *et al.*, (1970). Table 4a suggests that the average composition of Keewatin type sedimentary rocks closely resembles that of quartz diorite or granodiorite.

TABLE 4a

Average Chemical Compositions of Sedimentary and Igneous Rocks

	(1)	(2)	(3)	(4)	(5)
SiO_2 (wt.%)	66.16	59.22	66.88	66.15	60.40
Al_2O_3	17.33	14.57	15.66	15.56	15.07
Fe_2O_3	5.01	10.64	4.21	5.16	7.31
MgO	2.55	3.84	1.57	1.94	3.39
CaO	2.57	6.06	3.56	4.65	8.01
Na_2O	3.60	3.46	3.84	3.90	3.80
K_2O	1.95	0.72	3.07	1.42	1.09
TiO_2	0.69	1.00	0.57	0.62	0.66
MnO	0.06	0.3	0.05	0.06	0.13
P_2O_5	0.08	0.18	----	----	0.18
Ni (PPM)	103	61	10	25	63
Rb	54	29	75	110	21
Sr	392	212	200	400	304
Zr	152	130	150	200	142
Al_2O_3/Na_2O	4.8	4.2	4.1	4.0	4.0

(1) AVE. Keewatin Seds, (2) AVE. Timiskaming Seds,
(3) AVE. Granodiorite, (4) AVE. Quartz Diorite,
(5) AVE. Calc-alkaline Andesite-Dacite (Timmins area)
(1), (2), (5) - Average from Timmins area
(3), (4) - Average major elements Nockolds (1954),
(3), (4) - Trace elements, Condie (1967)

The only difference between them is that the Keewatin-type greywackes have higher values of MgO and Ni which suggest a minor mafic rock source. This lends further support to the suggestion that the greywackes were derived from a distant source rather than locally. Also the thin laminated sharp based beds with well developed shale horizons all suggest a distal environment for the greywackes (Walker, 1967). The high Al_2O_3: Na_2O ratio for the Keewatin-type greywackes of 4.8 suggests that their apparent mineralogical and chemical maturity is controlled chiefly by the composition of source

materials and diagenetic processes rather than by the amount of weathering and erosion (Pettijohn, 1957; Condie, 1967).

The Timiskaming-type greywackes are chemically distinct from the Keewatin-type greywackes with lesser amounts of SiO_2, Al_2O_3, K_2O, Ni, Rb, Sr and Zr. This is directly reflected in the mineralogy by lesser amounts of quartz, feldspar and muscovite. The Timiskaming-type greywackes have higher amounts of FeO* and CaO. The CaO may in part be metasomatically controlled but the higher amount of pyrite in thin section influenced the iron content of the Timiskaming-type greywackes relative to the Keewatin-type greywackes. The Timiskaming-type greywackes are similar in composition to the felsic calc-alkaline rocks of the Timmins area. Average compositions of both are presented in Table 4a. The greywackes contain more FeO*, MgO, TiO_2, MnO and Ni suggesting a minor mafic component within the sediments. The Al_2O_3:Na_2O ratio of 4.2 is lower than that reported by Pettijohn (1957) for greywackes but is in agreement with values reported by Condie (1967) and Condie et al., (1970) for Precambrian greywackes of Wyoming and South Africa (Fig Tree Formation) respectively.

SUMMARY

The components of the ZTN ternary plot do not appear to suffer from metasomatic changes which are inherent in the AFM diagram. The volcanic rocks of the Tisdale and Deloro Groups are separated on the basis of the ZTN diagram into their respective volcanic series (Table 4). The chemical characteristics of each suite are summarized in Table 4b. The Donut Lake Fm. consists of peridotitic and pyroxenitic komatiites; both are chemically characterized by CaO/Al_2O_3 ratios of $\approx$ 1, Ti/Zr ratios $\approx$ 128, low Al_2O_3, low TiO_2 and high MgO values. The komatiites also show little or no

Table 4b

General Chemical Characteristics of the Different Formations of the Timmins Area

	Komatiite Goose Lake Fm.	Komatiite Donut Lake Fm.	Basaltic Komatiite Lower Schumacher Fm.	Variolitic Flows	Tholeiite Upper Schumacher	Felsic Calc-alkaline Krist Fm.	Felsic Calc-alkaline Boomerang Fm.	Calc-alkaline Redstone Fm.
Enrichment	SiO_2, Al_2O_3, Na_2O, K_2O, TiO_2, P_2O_5, Ba, Zr, Sr, S, Zn	SiO_2, Al_2O_3, CaO Na_2O, K_2O, TiO_2, Ba, Zr, Sr, Y, S, Cu,	SiO_2, K_2O, TiO_2, P_2O_5, Zr, Zn, Rb	SiO_2, P_2O_5	SiO_2, Al_2O_3, Na_2O, Zr, Sr, Y, Zn	SiO_2 , Na O, K_2O, Ba, Zr, Sr, Cu, Rb, Ce,	SiO_2 , Rb, Ce	SiO_2 , Na_2O, Zr, Ce
Depletion	Fe_2O_3, MgO, Y, Cu, Ni, Rb, Ce	Fe_2O_3 , MgO P_2O_5, Zn, Ni, Rb Ce,	Al_2O_3 , Fe_2O_3, MgO, CaO, MnO S, Ce,	MgO, Ba, Zr, Sr, Zn, Ni, Rb	MgO, K_2O, MnO, Ba, S, Cu, Ni, Rb, Ce	Fe_2O_3 , MgO, CaO, Y, S, Zn, Ni	Fe_2O_3, MgO, TiO_2, MnO, Zn, Ni,	Fe_2O_3, MgO, CaO, Zn, Ni,
Enrichment then Depletion	CaO,		Na_2O, Ba, Cu, Ni	Al_2O_3 , Fe_2O_3 TiO_2 Cu,	Fe_2O_3 , CaO, TiO_2 ,	Al_2O_3, TiO_2, MnO, P_2O_5	Al_2O_3, CaO, P_2O_5 , Na_2O, K_2O, Ba, Zr, Y, S, Cu	TiO_2 , P_2O_5 , S, Al_2O_3 , K_2O, Ba, Y, Cu, Rb
Depletion then Enrichment	MnO,		Sr, Y,	CaO, Na_2O, K_2O, MnO, Y, S, Ce				(Random Distribution) MnO, Sr,

Enrichment Then Depletion in: Basaltic Komatiites MgO = 6.7%
Tholeiites MgO = 4.5%
Variolitic Flows MgO = 4.5%

iron enrichment in the basaltic classes. The next sequence of lavas is the Redstone Fm. which is chemically identified as calc-alkaline with the mafic end members representing tholeiitic to basaltic komatiites. It is made up of basaltic to dacitic lavas which are commonly porphyritic. The mafic end members show a mild TiO_2 enrichment at 6.5% MgO. They do not exhibit iron enrichment. The Boomerang Formation is a minor felsic, generally pyroclastic calc-alkaline unit forming the top of the Deloro Group.

The Tisdale Group is composed of komatiitic, tholeiitic and felsic calc-alkaline rocks. Structurally, the basal unit, (Goose Lake Fm.) is a sequence of peridotitic, pyroxenitic and basaltic komatiites. The peridotitic komatiites occur as two restricted horizons within the formation. The peridotitic komatiites are not pillowed and no spinifex textured lavas were observed during field work. However, the Goose Lake and Donut Lake lavas exhibit polyhedral jointing indicative of extrusion (Arndt et al., 1977; Pyke, 1978). The unit is characterized by CaO/Al_2O_3 ratios of $\approx$ 1, Ti/Zr ratios of $\approx$ 127, low Al_2O_3, low TiO_2 and MgO values. These lavas show no iron enrichment. The most ultramafic peridotitic komatiites are cumulate rocks rich in olivine and pyroxene which have high Ti/Zr ratios of 157 suggesting strong titanium fractionation during crystal settling. The upper most sequences of the Goose Lake Fm. are composed of basaltic komatiites as suggested by samples 94 and 96. The Lower Schumacher Fm. is an intercalated sequence of basaltic komatiites and tholeiitic rocks. Generally, the lower part of the sequence is dominated by basaltic komatiites while the upper sequence is tholeiitic. The tholeiites in this section are somewhat lower in TiO_2 than the Upper Schumacher Fm, suggesting that the lavas are intermediate between the end member komatiites and tholeiites.

This association suggests that there may be a "genetic link" between the two end member types. The Lower Schumacher Fm. does not show iron enrichment even in the tholeiitic members, further suggesting a genetic link. The Upper Schumacher Fm. is a tholeiitic sequence of lavas whose chemical characteristics show iron enrichment at 4.6% MgO which is similar to that reported for the Blake River lavas by Jolly (1978). Separating the Lower and Upper Schumacher Fms. is a sequence of variolitic flows which exhibit felsic tholeiitic characteristics. Gelinas et al., (1976) reported variolites at a similar stratigraphic level in the Destor area. Although whole rock chemical analyses of the variolitic flows was done the felsic nature of the flows suggest that some sort of immiscible felsic component (varioles) separated from the magma source to produce the varioles. The mafic matrix is conversely enriched in the ferromagnesian elements. In thin section, the varioles contain feldspar, quartz, carbonate, chlorite, and epidote-clinozoisite suggesting that prior to alteration the varioles were felsic in comparison to the matrix. Analyses of variole and matrix by Brooks (1977) further suggests a mafic component for the matrix because Brooks analyses show 16-24% FeO*, 6-12% MgO and 1.3-1.8% TiO_2. Because of the complimentary chemical nature of the varioles and matrix it is believed that they originated from the same magma source. The mode of formation of the variolitic flows is uncertain. Gelinas et al., (1976) and Brooks and Gelinas (1975) suggested from petrographic and chemical data that the variolitic flows formed by immiscible-liquid splitting of a tholeiitic magma where the varioles have the composition of a low-K rhyolite and the matrix is a ferruginous basalt. Green (1975) reported that variolitic flows from the Knee Lake Greenstone Belt formed as plagioclase glomerophenocrysts during extrusion of the lavas

which suggests a quench texture feature. Several characteristics of the variolitic flows in the Timmins area are:

1. chemical distinctness between varioles and matrix;
2. chemical complementary nature between varioles (felsic) and matrix (mafic);
3. sharp contacts between varioles and matrix;
4. restricted stratigraphic position of variolitic flows;
5. long continuous nature of variolitic flows, traceable over long distances;
6. association of variolitic flows within tholeiitic sequences;
7. chemical distinctness of variolitic flows with surrounding tholeiitic lavas.

The irregularity of the varioles within the lava flows suggest some interaction between varioles and matrix prior to extrusion indicating that the varioles did not form as a quench texture.

Overlying the Upper Schumacher Fm. is the pyroclastic felsic calc-alkaline Krist Fm. It is similar in nature to the Marda Complex (Hallberg et al., 1977).

Intruded into the Redstone Fm. is a series of dunite-peridotite sills. Chemically, the dunite-peridotites are very high in MgO (41-48%) and low in Al_2O_3, CaO and TiO_2. They have Ti/Zr ratios of $\approx$ 99 and CaO/Al_2O_3 ratios of $\approx$ 0.73. Cumulate rocks have Ti/Zr ratios of $\approx$ 363 suggesting very strong and early titanium fractionation. The dunite-peridotites in the Timmins area are spatially associated with faulting suggesting a deep seated nature to the faults.

Stratigraphically above the volcanic rocks in the Timmins area are the Keewatin and Timiskaming-type sedimentary rocks which indicate distal and local source derivations respectively. The Keewatin-type rocks appear to have been

derived from rocks similar in composition to quartz diorite or granodiorite while the Timiskaming-type rocks are similar in composition to the felsic calc-alkaline rocks of the Timmins area. Sediment transport direction was from the south for the Keewatin-type sedimentary rocks (Carlson, 1967, Ferguson, 1968).

CHAPTER VI
PETROGENETIC SYNTHESIS

GENERAL STATEMENT

Petrographic relations, normative calculations and projections of the CAMS (calcium-aluminum-magnesium-silicon) tetrahedron (O'Hara, 1968) are used to establish a general framework for the crystallization and depth of fractionation of each of the three lava suites. The use of petrographic observations are limited due to the extent and pervassiveness of the metamorphic alteration.

KOMATIITIC LAVAS

The Goose Lake Fm. has previously been subdivided into: a) peridotitic komatiite, b) pyroxenitic komatiite and c) basaltic komatiite.

Petrographic evidence suggests that the peridotitic komatiites contain both accumulitic and fine-grained lavas; only the latter type are used because accumulitic lavas do not represent original magmatic compositions (Clarke, 1970). Normative calculations of the peridotitic komatiites indicate relatively small amounts of cpx (3-27%) to that of opx (6-36%) while olivine ranges between 32-46%. Plagioclase ranges between 10-18% but in thin section no feldspar was observed in the peridotitic komatiites. Magnetite ranges from 2-4% (Table 5). Petrographic examination of the rocks suggest that interstitial amounts of magnetite-ilmenite are of primary origin. Normative calculations for pyroxenitic komatiites show an increase in cpx (16-24%) and opx (7-53%) compared to the peridotitic komatiites while there is a decrease in olivine (1-30%). Similar modal relations were observed in komatiitic lavas of Munro Township, east of the study area by Arndt et al., (1977). Plagioclase also increases (17-26%) compared to peridotitic

komatiites. The presence of minor interstitial feldspar was observed in thin section. Magnetite-ilmenite ranges in value from 2-4% remaining relatively constant as the more ultramafic peridotitic komatiites. The basaltic komatiites show the first presence of normative quartz (0.22-14%) accompanied by a substantial increase in normative plagioclase (43-52%). Interstitial feldspar and quartz are observed in thin section, although the feldspar is altered by subsequent metamorphic events. Olivine is no longer present in the normative calculations but opx ranges between 23-29% while cpx ranges between 0.2-17%. The amount of normative magnetite-ilmenite (5-6%) is greater than in the more ultramafic komatiites. This increase in iron-titanium oxides in the basaltic komatiites is possibly due to lesser amounts of opx which would subdue iron enrichment in the more ultramafic lavas (Jolly, 1978). Arndt et al., (1977) has reported similar results from Munro Township. A summary of the normative mineral calculations are presented in Table 5. The CS-A-MS projection (Fig. 17) suggests a crystallization sequence for the Goose Lake Fm. ultramafic rocks as:

A.	peridotitic komatiite	ol + cpx + opx + plag + Fe - Ti oxides
B.	pyroxenitic komatiite	ol + cpx + opx + plag + Fe - Ti oxides
C.	basaltic komatiite	ol + plag + opx + cpx + Fe - Ti oxides

The peridotitic komatiites whose average value plots near the boundary of the opx + cpx fields suggests that both cpx and opx precipitate simultaneously until the psuedo-cotectic is reached at which time plagioclase joins the pyroxenes. The pyroxenitic komatiites have a similar crystallization sequence to that of the peridotitic komatiites. The only difference being that a slight increase in cpx precipitation

TABLE 5

AVERAGE NORMATIVE MINERAL PERCENTS

Formation	ol	opx	cpx	plag	mt+il	qtz
Goose Lake						
Peridotitic Komatiite (3)	36.07	18.07	20.76	16.62	3.41	0.0
Pyroxenitic Komatiite (6)	17.36	30.38	24.71	21.39	2.63	0.0
Basaltic Komatiite (2)	0.0	26.09	8.55	47.39	5.63	6.85
Upper Schumacher Fm.						
Tholeiitic (5)	8.28 (1)	26.75	13.91	40.81	6.26	3.39 (4)
Lower Schumacher Fm.						
Basaltic Komatiite (12)	10.26 (4)	23.36	19.81 (11)	45.36	4.83	4.19 (8)
Redstone Fm.	5.61 (1)	31.74	12.50 (2)	39.40	5.06	7.84 (2)
Basaltic Komatiite (3)						

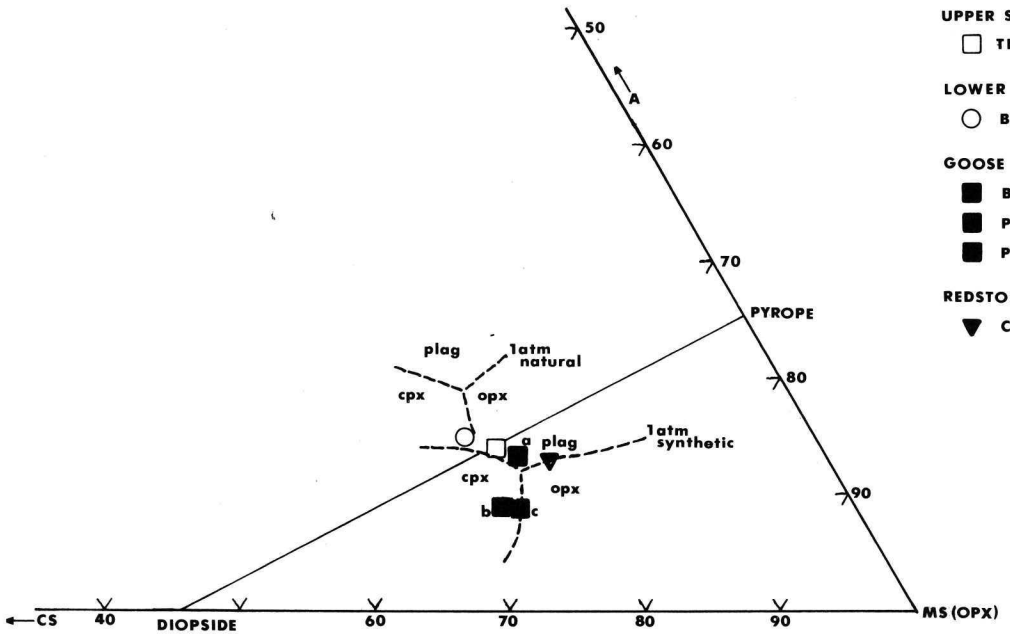

CS-A-MS PROJECTION

AVERAGE MAFIC ENDMEMBERS

UPPER SCHUMACHER FM

□ THOLEIITE

LOWER SCHUMACHER FM

○ BASALTIC KOMATIITE

GOOSE LAKE FM

■ BASALTIC KOMATIITE (a)

■ PYROXENITIC KOMATIITE (b)

■ PERIDOTITIC KOMATIITE (c)

REDSTONE FM

▼ CALCALKALINE

FIGURE 17

occurs before the bivariant is reached.

Generally, the ultramafic lavas appear to be controlled by olivine fractionation at low pressures while the komatiitic basalts are controlled by ol + opx during low pressure fractionation. Further support is given by Figure 12c which shows no iron enrichment in the komatiitic rocks. The iron must be used in the production of opx and minor olivine (Fo_{72-85}) which subdues the iron enrichment trend. Then in the basaltic komatiites plagioclase appears along with abundant Fe-Ti oxides both of which occur interstitially. This is similar to the findings of Pearce and Birkett (1974) and Arndt et al., (1977).

THOLEIITIC ROCKS

Most of the mafic end members of the tholeiitic suite are quartz normative. The average MgO content is 6% while normative opx (26.75%) and cpx (13.91%) are dominated by normative plagioclase (40.81%) (Table 5). Petrographic evidence suggesting calcic feldspar was originally present but exact determinations of the amount is difficult due to the pervasive metamorphism. The CS-A-MS projection (O'Hara, 1968; Fig. 17) suggests a crystallization sequence of: ol + plag + cpx + opx + Fe - Ti oxides for the tholeiitic rocks. Because only one sample contains normative olivine and the rest are quartz normative the Upper Schumacher Fm. is considered a highly fractionated tholeiitic sequence due to the lack of normative olivine in the norms. Jolly (1978) reported that olivine is no longer produced after 40% of the liquid has solidified which further supports that the tholeiitic rocks are of lage stage origin.

BASALTIC KOMATIITES

The basaltic komatiites normative mineral calculations

are presented in Table 5. The Lower Schumacher Fm. has a similar crystallization sequence to that of the Upper Schumacher Fm. which is: ol + plag + cpx + opx + Fe - Ti oxides (Fig. 17). One difference between the two is that the Lower Schumacher Fm. shows less iron enrichment (Fig. 12c). Also, Figure 13 suggests that the predominant lavas of the Lower Schumacher Fm. may be classified as basaltic komatiites.

CALC-ALKALINE ROCKS

The mafic end members of the Redstone Fm. appear to be basaltic komatiites as suggested in Figure 10. Average normative mineral calculations (Table 5) indicate that only one sample contains normative olivine (5.61%) while the other samples are quartz normative. Normative plagioclase averages 39.40% which is supported by petrographic observations where plagioclase occurs both in the matrix and as phenocrysts. The crystallization sequence of the Redstone Fm. as suggested by Figure 17 is: ol + plag + opx + cpx + Fe - Ti oxides. A similar crystallization sequence is reported by Jenson (1973) for mafic calc-alkaline rocks. The sequence indicates a reversal of opx + cpx which Jenson suggested is precipitated as pigeonite.

DEPTH OF FRACTIONATION

The hypothetical crystallization sequences discussed earlier in this chapter suggests that the volcanic rocks fractionated at at least two different depths. The crystallization sequence of the komatiitic rocks suggests that the partial melts originated at depths in excess of 100 km. and 30 kb. pressure (Clarke, 1970; Green, 1975; Nesbitt and Sun, 1976; Hawkesworth and O'Nions, 1977; Nisbet et al., 1977; Jolly, 1978). Further evidence is

the early appearance of opx in the crystallization sequence which Jolly (1978) stated is indicative of higher pressures.

The tholeiitic crystallization sequence suggests that fractionation took place at low pressures (1-10 kb.) If crystallization took place at greater pressures, opx would have appeared earlier in the sequence (Jolly, 1978).

The Redstone Fms mafic end members are basaltic komatiites rather than mafic calc-alkaline rocks. However, the crystallization sequence suggests shallow fractionation and is similar to the tholeiitic rocks. Possibly, the lack of exposed calc-alkaline mafic rocks suggest that the mafic end members observed in the Redstone Fm. are in fact parental material of which the calc-alkaline rocks were derived.

DISCUSSION OF THE VOLCANIC DEVELOPMENT OF THE TIMMINS AREA

North of the Destor-Porcupine Break, the basal sequence of lavas is comprised of a series of komatiitic flows that make up the Goose Lake Fm. Experimental melting relations of the lavas suggest that temperatures during extrusion were 1650°C. (Green, 1975). Because of the high extrusion temperature, the initial temperature during partial melting in the mantle must have been around 1950°C. (Cawthorn, 1975). The transport mechanism, as to how the melt reached or formed near surface fractionation chambers is uncertain. However, Ramberg (1972) and Cawthorn (1975) suggested that the mantle material undergoing original melting rose as a diapir. Because several samples of peridotitic komatiites in the Goose Lake Fm. contain basal cumulitic zones of olivine and pyroxene, the diapir must have been raised rapidly as crystal + liquid mush (Clark, 1972; Cawthorn, 1975; Nesbitt and Sun, 1976). These lavas were possibly derived from 35-55% initial partial melts from the mantle (Nesbitt and Sun, 1976; Nisbet *et al.*, 1977). The lavas were then extruded from shallow chambers. A sequence of peridotitic komatiites then followed by pyroxenitic komatiites was developed; finally a second sequence of peridotitic komatiites, perhaps representing a new aliquot of parental magma introduced from depth into the fractionating chamber.

The sequence is overlain by basaltic komatiites which make up a thin layer at the top of the Goose Lake Fm. and the lower part of the Lower Schumacher Fm. The generation of basaltic komatiites is believed to have originated from their own partial melt, not as another sequence of the more ultramafic komatiites (Nesbitt and Sun, 1976, Arndt *et al.* 1977), because the ultramafic komatiites follow a crystallization sequence of ol + opx + cpx while the basaltic komatiites show ol + plag + cpx. Nesbitt and Sun (1976)

also suggested that basaltic komatiites are derived from a primary melt with an MgO content of about 12%. These melts were produced at lower temperatures and lower degrees of partial melting with subsequent differentiation resulting in lower MgO contents. The upper part of the Lower Schumacher Fm. is a sequence of intercalated basaltic komatiites and low TiO_2 tholeiites. The intimate relations between the two lava types suggest that they were erupted simultaneously, possibly from the same magma chamber. When the two lava types are compared at approximately equivalent MgO contents, the basaltic komatiites carry lower TiO_2 values. The Ti/Zr ratio suggests that the tholeiites are slightly more fractionated due to magnetite-ilmenite removal. Similarities between the crystallization sequences and geochemistry of the two types suggests that the basaltic komatiites are genetically related with the tholeiitic rocks.

The evidence presented earlier suggests that the variolitic flows originated from a tholeiitic melt that has split into two immiscible liquids. Upon extrusion, the lavas are rapidly cooled which retains the identity of the two liquid compositions. This is similar to that proposed for late-stage lunar rocks in which the variolitic data plots very close to the proposed field of immiscibility (Wieblen and Roedder, 1973). Detailed studies of variolitic flows in other parts of the Abitibi Belt (Brooks and Gelinas, 1975; Gelinas *et al.*, 1976; Brooks, 1977) has had similar interpretations. Stratigraphically above the variolitic flows is a sequence of tholeiitic lavas which range from basalt to andesite. The presence of plagioclase and a slight iron enrichment indicate that they represent material derived from a low pressure and low PO_2 melt (Osborn, 1959, 1962). Also, the absence of normative olivine suggests that they were a late stage effusion (Jolly, 1978). The overlying

Krist Fm. is a sequence of felsic pyroclastic and tuffaceous rocks which represent a final late state emanation.

The evidence suggests that two partial melting events took place to produce the observed lavas in the Timmins area. The peridotitic lavas originated by large degrees of partial melting while the basaltic komatiites and tholeiitic lavas represent a low pressure continuously fractionated series.

The development of the lava sequence south of the Destor-Porcupine Break is dominantly of calc-alkaline affinity. Because only basaltic komatiites and calc-alkaline lavas are exposed south of the Destor-Porcupine Break in the study area, the two are considered to be products of a basaltic komatiitic magma, possibly derived from the same magma source that supplied the lavas to the north. Reviews by Green and Ringwood (1968), O'Hara (1968), Hyndman (1972) and Jolly (1978) suggested that both theoleiitic and calc-alkaline rocks can be derived from a shallow fractionating source. Evidence to support this contention is the presence of plagioclase phenocrysts in the lavas which would not have formed if the pressure was greater than 15 Kb.; instead alumina basalts would have formed which are not present in the study area (Green and Ringwood, 1968). The lack of iron enrichment in the calc-alkaline rocks of the study area suggests that the pO_2 was high enough to cause the precipitation of magnetite (Osborn, 1959; 1962). Development of the high pO_2 could have occurred by simple concentration of the volatiles in the magma due to continual fractionation which would decrease the volume of melt assuming that the lavas are extruded. This would concentrate the volatiles as the liquid phase decreased thus the melt would become "wet". Another possibility is that the margins of the magma chamber incorporated "wet" sialic material which upon

fractionation of the mafic rocks would increase the amount of volatiles in the magma.

During the waning stages of volcanism the residual melt continued to fractionate with the final emanations of the felsic pyroclastic and tuffaceous material. Field evidence, petrography and geochemical characteristics suggest a strong similarity between the Krist and Boomerang Fms. This may indicate that the rocks from both formations in the study area were deposited contemporaneously or that the waning stages of volcanism both north and south of the Destor-Porcupine Break produced exactly the same types of felsic pyroclastic rocks.

The consideration of the above discussion suggests the following sequence of events for the volcanogenic development of the Timmins area:

1) The initiation of 35-55% partial melting in the mantle at depths in excess of 100 km.
2) The melt rose rapidly, possibly as a diapir within a convecting mantle.
3) Within low pressure magma chambers, minor fractionation took place with the emanation of the ultramafic komatiites
4) Associated with sequences 1) and 2) was the development of minor partial melts which also rose to low pressure magma chambers to produce the basaltic komatiites, low TiO_2 tholeiites and normal tholeiites.
5) The grouping of the data on the variation diagrams (Fig. 12a-s) suggests that minor fractionation produced the basaltic komatiites and low TiO_2 tholeiites (olivine fractionation) and the normal tholeiites (plagioclase fractionation).
6) Prior to the effusion of the normal tholeiites,

the variolitic flows were erupted possibly from a satellite chamber.

7) The increase in PO_2 of the melt possibly caused by a decrease in magma volume produced the calc-alkaline lavas.

8) The termination of magma being introduced from depth associated with the residual melt of the chamber plus the high PO_2 conditions produced the felsic pyroclastic and tuffaceous material.

CONCLUSIONS

The Archean volcanic rocks of the Timmins area have been subdivided into komatiitic, tholeiitic and calc-alkaline suites based on Zr, TiO_2, and Ni. The three elements were used due to their relative immobility during subsequent metamorphic events.

The earliest lavas erupted belong to the komatiitic suite which, in the Timmins area, make up the Goose Lake and Donut Lake Fms. They can be further subdivided into peridotitic, pyroxenitic and minor basaltic komatiites. The peridotitic and pyroxenitic komatiites are characterized by low Al_2O_3, low TiO_2, high MgO, Ti/Zr ratios of about 129 and absence of iron enrichment in intermediate members. Stratigraphically above the Goose Lake Fm. is the Schumacher Fm. which has been subdivided into four sequences on the bases of the geochemistry. 1) The Lower Schumacher Fm. is dominantly a sequence of basaltic komatiites whose characteristics are low TiO_2, MgO 5-7% and no iron enrichment. 2) The upper part of the Lower Schumacher Fm. is an intercalated sequence of basaltic komatiites and low TiO_2 tholeiites. The low TiO_2 tholeiites are characterized by higher TiO_2 and FeO* contents relative to the basaltic komatiites. No iron enrichment is observed in the low TiO_2 tholeiites. 3) Separating the low TiO_2 tholeiites and the normal tholeiites are a series of variolitic flows that are used as marker horizons throughout the Timmins area. The variolitic flows represent a series of felsic tholeiitic flows whose chemistry suggests that they developed from a tholeiitic magma that separated into a complimentary felsic (variole) and mafic (matrix) phase. The variolitic basaltic flows have been enriched in the refractive elements relative to the andesitic flows. 4) The Upper Schumacher Formation is a series of tholeiitic rocks which are characterized by high TiO_2 and minor iron enrichment.

Overlying the Schumacher Fm. is a minor series of dacitic calc-alkaline rocks, the Krist Fm. The formation is a series of intercalated pyroclastic and brecciated material showing high Al_2O_3 and no iron enrichment. Stratigraphically above the Krist Fm. are the Keewatin-type sedimentary rocks which are composed of an intercalated sequence of greywacke and slate. Chemical data indicates that these rocks were derived from a source area with a composition similar to that of granodiorite or quartz diorite. Petrographic, geochemical and field evidence suggests they were derived from a distal source, ultimately transported and deposited in the study area by turbidity currents. Unconformably overlying the Keewatin-type sedimentary rocks are the Timiskaming-type sedimentary rocks. The Timiskaming-type rocks are a sequence of basal polymictic conglomerate overlain by intercalated greywacke and slate. These rocks approximate the composition of the felsic calc-alkaline rocks in the Timmins area. Petrographic, geochemical and field evidence suggests the rocks were derived locally.

South of the Destor-Porcupine Break, a sequence of ultramafic volcanic rocks (Donut Lake Fm.) are exposed 25 km. south of Timmins. However, its relationship to the Redstone Fm. in the study area is unclear. The Donut Lake Fm. is a sequence of peridotitic and pyroxenitic komatiites. These lavas are characterized by slightly lower Al_2O_3 and slightly higher FeO* than the Goose Lake Fm. The Donut Lake Fm. also shows low TiO_2, high MgO, Ti/Zr ratios of 128 and absence of iron enrichment. The lowest section exposed south of the Destor-Porcupine Break in the study area is the Redstone Fm. which is dominantly a calc-alkaline sequence of basaltic andesites to dacites. The formation is moderately high in Al_2O_3 in its felsic end members. Most flows are porphyritic. The mafic flows are commonly pillowed.

Mafic rocks in the Redstone Fm. are basaltic komatiites in composition. Above the Redstone Fm. is the felsic calc-alkaline Boomerang Fm. This unit is dacitic to rhyolitic in composition and is dominantly pyroclastic rocks. The first recognizable deformation observed in the Timmins area is prelithification deformation. Localized disturbances observed in the sedimentary rocks are: smallscale folding, draping, disruption of bedding, flame structures and scouring. Field evidence suggests that deformation was contemporaneous with sedimentation because disturbed horizons are directly overlain by undisturbed beds. Several unconformities are observed in the Timmins area and the map pattern suggests that they are extensive and possibly regional.

The development of the tectonic history of the Timmins area is based on the structural relationships between deformational events and is therefore time sequential.

The first phase of tectonic deformation (D_1) was the development of isoclinal F_1 folds of which the original attitude is uncertain. Associated with the major F_1 folds are a series of parasitic folds that developed on the flanks of the major F_1 structures. The major F_1 structures are cut by the Burrows Benedict fault to the east. A subparallel bedding foliation, S_1, accompanied the F_1 folding in both the Keewatin and Timiskaming-type sedimentary rocks. Bedding, pillow tops and continuous variolitic flows were used to outline the major F_1 structures.

The second phase of tectonic deformation (D_2) was the development of a penetrative S_2 strain slip foliation whose orientation is axial planar to the F_2 folds. The F_2 folding refolded the F_1 structures to produce the Porcupine Syncline. Field observations and map patterns suggest the Porcupine Synclinal axial trace is continuous to the west. Deformation of the Porcupine Syncline produced mesoscopic

F_2 folds in the sedimentary rocks whose axial trace parallels the major F_2 structure. The plunge of the parasitic F_2 folds ranges between 17-44° NE. Associated with the plunge of the F_2 folds is a stretching lineation L_1, that developed in the S_2 plane of foliation. The attitude of the L_1 lineation is 47° NE plunging at 40°. The interference pattern developed between the major F_1 and F_2 structures in the Timmins area produced the observed map pattern. The pervasive S_2 foliation in the Timmins area developed due to regional low grade (greenschist facies) metamorphism associated with this deformational event. The S_2 foliation is observed south of the Destor-Porcupine Break.

The third phase of tectonic deformation (D_3) was recorded as sub-horizontal S_3 crenulation cleavage which developed in the plane of the S_2 foliation. The axial plane attitude of the S_3 crenulation cleavage is 023/27° ESE. The S_3 crenulation cleavage is observed south of the Destor-Porcupine Break. No mesoscopic folds were observed associated with this deformation. Evidence indicates the S_3 crenulation cleavage overprints the S_3 foliation.

The fourth phase of tectonic deformation (D_4) is characterized by a series of large (3-4 km.) wavelength F_4 folds that refolded the F_2 axial plane. The general attitude of the F_4 folds is north-west. The F_4 macrostructures are accompanied by a S_4 subvertical crenulation cleavage which developed in the plane of the S_2 foliation. The S_4 crenulation cleavage developed in the sedimentary rocks whose attitude is 101/47 NE and 099/45 SW. The F_4 folding refolded the F_2 axial plane. The S_2 foliation was not metamorphically modified by the D_4 deformation.

The sequence of events observed in the Timmins area indicates that the intensity of the deformational events decreased with time.

REFERENCES

Arndt, N. T., Naldrett, A. T., and Pyke, D. R., 1977, Komatiitic and iron-rich tholeiitic lavas of Munro Township, northeast Ontario: Jour. Petrol., v. 18, n. 2, p. 319-369.

Bass, M. N., 1961, Regional tectonics of part of the southern Canadian Shield: Jour. Geol., v. 69, p. 668-702.

Blatt, H., 1967, Original characteristics of clastic quartz grains: Jour. Sed. Petrol., v. 37, p. 401-424.

Bright, E. G., 1973, Timmins area. Annual field trip guidebook: Ont. Div. Mines Geological Branch, pp. 67.

Brooks, C., 1977, Archean variolites: source of iron in the Precambrian environment: Can. Jour. of Earth Sci., Comm., v. 14, n. 3, p. 511-513.

_____, and Gelinas, L., 1975, Immiscibility in ancient and modern volcanism: Carnegie Inst. Washington, Yearbook, v. 74, p. 240-247.

Burrows, A. G., 1911, The Porcupine gold area: Ont. Bur. Mines, v. 20, pt. 2, accompanied by map 20E, scale 1 inch to 1 mile.

_____, 1912, The Porcupine gold area, second report: Ont. Bur. Mines, v. 21, pt. 1, p. 205-249. Accompanied by map 21a, scale 1 inch to 1 mile.

_____, 1915, The Porcupine gold area; third report: Ont. Bur. Mines, v. 24, pt. 3, p. 1-57. Accompanied by map 24d, scale 1 inch to 2000 feet.

_____, 1924, The Porcupine gold area, fourth report: Ont. Dept. Mines, v. 33, pt. 2. Accompanied by map 33a, scale 1 inch to 2000 feet (1925).

_____, and Rogers, W. R., 1910, Map of the Porcupine gold area. Districts of sudbury and Nipissing, Ontario: Ont. Dept. Mines, map 19c, scale 1 inch to 1 mile.

Carlson, H. D., 1967, Geology of Ogden, Deloro and Shaw Townships: Ont. Dept. Mines, open file report 5012. Accompanied by maps p. 341, p. 342, and p. 343, scale 1 inch to ¼ mile.

Carmichael, I. S. E., 1964, The petrology of Thingmuli, a tertiary volcano in eastern Iceland: Jour. Petrol., v. 5, p. 435-460.

Carnevali, J., 1976, Structural analysis of the Timmins-South Porcupine area, Ontario: Unpublished M. Sc. Thesis, University of Waterloo.

Cawthorn, R. G., 1975, Degrees of melting in mantle diapirs and the origin of ultrabasic liquids: Earth Planet. Sci. Lett., v. 27, p. 113-120.

Clarke, D. B., 1970, Tertiary basalts of Baffin Bay: possible primary magma from the mantle: Contr. Mineral. Petrol., v. 25, p. 203-224.

Condie, K. C., 1967, Geochemistry of early Precambrian greywackes from Wyoming: Geochim. Cosmochim. Acta , v. 31, p. 2135-2149.

_____, Mackie, J. E., and Reimea, T. O., 1970, Petrology and geochemistry of early Precambrian greywackes from the Fig Tree Group, South Africa: Geol. Soc. Am. Bull., v. 81, p. 2759-2776.

Cooper, J. R., 1943, Flow structure in the Beria Sandstone and Bedford Shale of central Ohio: Jour. Geol., v. 51, p. 190-203.

Dalrymple, G. B. and Hirooka, K., 1965, Variation of the potassium, argon, and calulated age in a late Cenozoic basalt: Jour. Geophys. Research, v. 70, p. 5291-5296.

Davies, J. F., 1977, Structural interpretation of the Timmins mining area, Ontario: Can.Jour. of Earth Sci., v. 14, n. 5, p. 1046-1053.

Donaldson, J. A. and Jackson, G. D., 1965, Archaean sedimentary rocks of north Spirit Lake area, north-western Ontario: Can. Jour. of Earth Sci., v.2 , n. 6, p. 622-647.

Dunbar, W. R., 1948, Structural relations of the Porcupine ore deposits: in Structural geology of Canadian ore deposits. Can. Mining and Met. Symposium, p. 442-456.

Durney, D. W., 1972, Deformation history of the western Helvetic Nappes, Volais, Switzerland: Unpublished Ph. D. Thesis, Univ. of London, London.

Evans, B. W., 1977, Metamorphism of alpine peridotites and serpentinite: Ann. Rev. Earth Planet. Sci., v. 5, p. 397-447.

_____, and Moore, J. G., 1968, Mineralogy as a function of depth in the prehistoric Makaopuhi tholeiitic lava lake, Hawaii: Contr. Minerol. Petrol., v. 17, p. 85-115.

Ferguson, S. A., 1956-1958, Tisdale Township and parts of Whitney and Deloro Townships: Ont. Dept. Mines, Prelim. maps P. 5- P. 12, scale 1 inch to 500 feet (1959-1960).

_____, 1960-1961, Tisdale Township, District of Cochrane, subsurface plans: Ont. Dept. Mines, Prelim. maps. P. 106-P. 112, scale 1 inch to 500 feet (1961).

_____,1962, Tisdale Township, District of Cochrane, geological cross-sections of mine workings and drilling sections by mining companies: Ont. Dept. Mines, Prelim. maps p. 171-173, scale 1 inch to 500 feet (1963).

_____,1966, The relationship of mineralization to stratigraphy in the Porcupine and Red Lake areas, Ontario: in The relationship of mineralization to Precambrian stratigraphy in certain areas of Ontario and Quebec, Geol. Ass. Can., Spec. pap. no. 3, p. 99-119.

_____, et al., 1968, Geology and ore deposits of Tisdale Township: Ont. Dept. Mines Geological Rept. 58.

Flannagan, F. J., 1969, U.S. geological survey standard - II. First compilation of data for the new U.S.G.S. rocks: Geochim. Cosmochim. Acta , v. 33, p. 81-120.

Floyd, P. A., and Winchester, J. A., 1975, Magma type and tectonic setting discrimination using immobile elements: Earth Planet. Sci. Let., v. 27, p. 211-218.

Frost, B. R., 1967, Limits to the assemblage forsterite + anorthite as inferred from peridotite hornfelses, Icicle Creek, Washington: Am. Mineral., v. 61, p. 732-750.

Gast P. W., 1968, Trace element fractionation and origin of tholeiitic and alkaline magma types: Geochim. Cosmochim. Acta , v. 32, p. 1057-1086.

Gelinas, L., Brooks, C., and Trzcienski, W., 1975, Archean variolites-quenched immiscible liquids: Can. Jour. Earth Sci., v. 13, p. 210-236.

George, P. T., 1967, Centennial field excursion, northwestern Quebec and northern Ontario: Can. Mining Met., p. 101-134.

_____, Pyke, D. R., Fisher, D. F. and Ransom, D. M., 1975, Precambrian economic geology of the Timmins area: in Waterloo '75, Field Excursion Guidebook, Part A. Joint meeting of Geol. Ass. Can., Mineral Ass. Can., Geol. Soc. Am. , (North Central Section) Edited by P. G. Telford, p. 63-96.

Ginn, R. M., Savage, W. S., Thompson, R., Thompson, J. E., and Fenwick, K. G., 1964, Timmins-Kirkland Lake sheet, Cochrane, Sudbury and Timiskaming Districts: Ont. Dep. Mines, Geol. Compilation Ser., map 2046, scale 1 inch to 4 miles. Geology and compilation 1961 and 1962.

Goodwin, A. M., et al., 1972, The Superior Province: in tectonic styles in Canada; Geol. Ass. Can., Spec. pap. 11, Edited by R. A. Price and R. T. W. Douglas, p. 527-623.

Grant, R. W. E., 1977, Geochemistry of metavolcanic rocks of the Timmins Region northeastern Ontario: Unpublished M. Sc. Thesis, Laurentian University, Sudbury, Ontario.

Graton, L. C., McKinstry, H. E., et al., 1933, outstanding features of the Hollinger geology: Can. Mining Met. Trans., v. 36, p. 1-20.

Green, D. H.,1975, Genesis of Archean peridotitic magmas and constraints on Archean geothermal gradients and tectonics: Geology, v. 3, p. 15-18.

_____, and Ringwood, A. S., 1968, Genesis of the calc-alkaline igneous rock suite: Contr. Mineral. and Petrol., v. 18, p. 105-162.

Green, N. L., 1975, Archean glomeroporphyritic basalts: Can. Jour. Earth Sci., v. 12, p. 1770-1784.

Griffis, A. T., 1962, A geological study of the McIntyre mine: Can. Mining Met. Trans., v. 65, p. 47-54.

Hallberg, J. A., Carter, D. N., and West, K. N., 1976, Archean volcanism and sedimentation near Meekathara, W. Australia: Precambrian Res., v. 3, p. 577-595.

_____,Johnston, C., and Bye, S.m., 1976, The Archean Marda Complex, W. Australia: Precambrian Res., v. 3, p. 11-136.

Hart, S. R., 1969, K, Rb, CS contents and K/Rb, K/CS ratios of fresh and altered submarine basalts: Earth Planet. Sci. Letters, v. 6, p. 295.

_____, Gunn, B. M., and Watkins, N.D., 1971, Intralava variations of alkalis elements in Icelandic basalt: Am. Jour. Sci., v. 270, p. 315-318.

_____, Nalwalk A. T., 1970, K, Rb SC, and Sr relationships in submarine basalts from the Puerto Rico Trench: Geochim. Cosmochin. Acta , v. 34, pp. 145.

Hawkesworth, C. J., and O'Nions, R. K., 1977, The petrogenesis of some Archean volcanic rocks from Southern Africa: Jour. Petrol., v. 18, pt. 3, p. 487-520.

Hogg, N., 1950, The Porcupine gold area: Can. Mining Jour., v. 71, p. 102-106.

Holmes, T. C., 1968, Dome Mines Limited: in: Geology and ore deposits of Tisdale Township, S. A. Ferguson, Ont. Dept. Mines, Geol. Rept. 58.

Hughes, C. J., 1977, Archean variolites - quenched immiscible liquids: Discussion. Can. Jour. Earth Sci., v. 14, p. 137-139.

Hurst, M. E., 1936, Recent studies in the Porcupine area: Can. Mining Met. Trans., v. 39, p. 448-458. Accompanied by sketch map.

_____, 1939, Porcupine area, District of Cochrane, Ontario. Third Edition; Ont. Dept. Mines, map 47a, scale 1 inch to 2,000 feet. Geology 1935, 1936, 1937.

_____, 1942, Gold deposits of Porcupine, Ontario: in: Ore deposits as related to structural features. Princeton University Press. Princeton, New Jersey, U.S.A. Edited by N. H. Newhouse, p. 196-199.

Hyndman, D. W., 1972, Petrology of igneous and metamorphic rocks: McGraw Hill Book Company, New York.

Irvine, T. N., and Baragar, W. R. A., 1971, A guide to the chemical classification of the common volcanic rocks: Can. Jour. Earth Sci., v. 8, p. 523-548.

Jakes, P., and White, A. J. R., 1972, Major and trace element abundances in volcanic rocks of orogenic areas: Geol. Soc. Amer. Bull., v. 83, p. 29-40.

Jenson, L. S., 1973, Lightning River Area, District of Cochrane: Ont. Div. Mines, Misc. Paper 56, p. 133-138.

Jolly, W. T., 1975, Subdivision of the Archean lavas of the Abitibi area, from Fe-Mg-Ni-Cr relations: Earth Planet. Sci. Let., v. 27, p. 200-210.

_____,1978, Development and degradation of Archean lavas, Abitibi area, Canada, in light of major element geochemistry: In Press.

_____, and Smith R. E., 1972, Degradation and metamorphic differentiation of the Keweenawan tholeiitic lavas of Northern Michigan: Jour. Petol., v. 13, p. 273-309.

Jones, W. A., 1968, Hollinger Consolidated Gold Mines Limited: in: Geology and ore deposits of Tisdale Township. S. A. Ferguson, Ont. Dept. Mines, Geol. Rept. 58.

Kerr, P. F., 1959, Optical mineralogy: McGraw Hill Book Company, New York.

Liou, J. G., Kuniyoshi, S., and Ito, K., 1974, Experimental studies of the phase relations between greenschist and amphibolite in a basaltic system: Am. Jour. Sci., v. 274, p. 613-632.

MacDonald, J. G., 1967, Variations within a Scottish Lower Carboniferous lava flows; Jour. Geol., v. 3, p. 34-45.

Massion, P. T., and Koster Van Groos, A. F., 1973, Liquid immiscibility in silicates: Nat. Phys. Sci., v. 245, p. 60-63.

McLaughlin, D. B., 1956, Keewatin-Timiskaming unconformity at Porcupine, Ontario: Geol. Soc. Am. , Bull., v. 67, p. 939-940.

Miller, W. G., 1907, Lake Abitibi gold deposits: Ont. Bur. Mines, v. 16, pt. 1, p. 219-220.

Miyashiro, A., 1961, Evolution of metamorphic belts: Jour. Petrol., v. 2, p. 277-311.

_____, and Shido, F., 1975, Tholeiitic and calc-alkaline series in relation to the behaviors of titanium, vanadium, chromium and nickel: Am. Jour. Sci., v. 275, p. 265-277.

Moore, E. S., 1953, The structural history of the Porcupine gold area, Ontario: Roy. Soc. Can. Trans., Third Ser., Sect. IV, v. 47, p. 39-53.

Naquis, M., and Hussain, S. M., 1973, Relation between trace element composition of the chitaldrug metabasalts, Mysore, India, and the Archean mantle: Chem. Geol., v. 11, p. 17-31.

Nesbitt, R. W., and Sun, S., 1976, Geochemistry of Archean spinifex-textured peridotites and magnesian and low-magnesian tholeiites: Earth Planet. Sci. Let., v. 31, p. 433-453.

Nisbet, E. G., Bickle, M. J., and Martin, A., 1977, The mafic and ultramafic lavas of the Belingwe Greenstone Belt, Rhodesia: Jour. Petrol., v. 18, pt. 4, p. 521-566.

Nockolds, S. R., 1954, Average chemical compositions of some igneous rocks: Geol. Soc. Am. Bull., v. 65, n, 10, p. 1007-1032.

Nold, J. K., and Erickson, K. P., 1967, Changes in K-feldspar staining methods and adaptations for field use: Am. Mineral., v. 52, p. 1575-1576.

O'Hara, M. J., 1968, The bearing of phase equilibria studies in synthetic and natural systems on the origin and evolution of basic and ultrabasic rocks: Earth Sci. Rev., v. 4, p. 69-133.

Osborn, E. F., 1959, Role of oxygen pressure in the crystallization and differentiation of basaltic magma: Am. Jour. Sci., v. 257, p. 609-647.

_____, 1962, Reaction series for subalkaline igneous rocks based on different oxygen pressure conditions: Am. Mineral., v. 47, n. 3 and 4, p. 211-226.

Parks, W. A., 1899, The Nipissing-Algoma Boundary: Ont. Bur. Mines, v. 8, pt. 2, p. 175-196. Accompanied by map 8c, scale 1 inch to 8 miles.

Pearce, T. H., and Birkett, T. C., 1974, Archean meta-volcanic rocks from Thackeray Township, Ontario: Can. Jour. Earth. Sci., v. 12, p. 509-519.

Pettijohn, F. J., 1957, Sedimentary rocks: Harper and Row, 2nd Edition. New York.

Philpotts, A. R., 1977, Archean variolites-quenced immiscible liquids: Discussion, Can. Jour. Earth Sci., v. 14, p. 139-144.

Philpotts, J. A., Schnetzler, C. C., 1970, Phenocryst-matrix partition coefficients for K, Rb, Sr and Ba, with applications to anorthosite and basalt genesis: Geochim. Cosmochim. Acta , v. 34, p. 307-322.

Pyke, D. R., 1974, Timmins Area, Districts of Cochrane and Timiskaming: Ont. Div. Mines, Prelim. map P 941, Geol. Ser. Scale 1 inch to 1 mile. Geology and compilation 1973.

_____, 1975a, Volcanic and sedimentary stratigraphy of the Timmins area: in: Waterloo '75, Field Excursion Guidebook, Part A. Joint meeting of Geol. Ass. Can., Mineral. Ass Can., Geol.Soc. Am. , (North Central Section). Edited by P. G. Telford, p. 68-74.

_____, 1975b, On the relationship of gold mineralization and ultramafic volcanic rocks in the Timmins area, Northeastern Ontario: Ont. Div. Mines, Miscellaneous Paper 62.

_____, 1978, Geology of the Peterlong Lake Area, Districts of Timiskaming and Sudbury: Ont. Geol. Sur., Report 171.

_____, Ayres, L. D., and Innes, D. G., 1973, Timmins-Kirkland Lake Sheet, Cochrane, Sudbury and Timiskaming Districts: Ont. Div. Mines, Geol. Comp. Ser., map 2205, scale 1 inch to 4 miles. Compilation 1971, 1972.

Ramberg, H., 1972, Mantle diapirism and its tectonic and magmatic consequences: Phys. Earth Plan. Int., v. 5, p. 45-60.

Ramsay, J. G., 1967, Folding and fracturing of rocks: McGraw Hill, Toronto.

Rankama, K., and Sahama, Th. G., 1950, Geochemistry: University of Chicago Press, Chicago.

Roberts, R. G., Carnevali, J., and Harris, J. D., 1978, The volcanic-tectonic setting of gold-quartz vien systems in the Timmins District, Ontario: Geol. Surv. Can., Current Research, Part B, Paper 78-1B.

Roedder, E., and Weiblen, P. W., 1970, Silicate liquid immiscibility in lunar magmas, evidenced by melt inclusions in lunar rocks: Science 167, v. 10, p. 641-644.

Sato, M., and Wright, T. L., 1966, Oxygen fugacities directly measured in volcanic gases: Science, v. 153, p. 1103-1105.

Smith, A. L. and Carmichael, I. S. E., 1968, Quaternary lavas from the Southern Cascades, Western U.S.A.: Contrib. Mineral. Petrol., v. 19, p. 212-238.

Smith, R. E., 1968, Redistribution of major elements in the alteration of some basic lavas during burial metamorphism: Jour. Petrol., v. 9, p. 191-219.

_____, 1969, Zones of progressive regional burial metamorphism in part of the Tasman Geosyncline, Eastern Australia: Jour. Petrol., v. 10, pp. 144.

Smith, R. E., and Smith S. E., 1976, Comments on the use of Ti, Zr, Y, Sr, K, P and Nb in classification of basaltic magmas: Earth Planet. Sci. Let., v. 32, p. 114-120.

Spry, A., 1969, Metamorphic textures: Pergamon Press, Toronto.

Tabatabai, M., 1978, Petrography and geochemistry of McArthur Township Area,Ontario: Unpublished M. Sc. Thesis, Brock University.

Trommsdorff, V., and Evans, B. W., 1972, Progressive metamorphism of antigorite schist in the Bergell tonalite aureole (Italy): Am. Jour. Sci., v. 272, p. 423-437.

Turner, C. C., and Walker, R. G., 1973, Sedimentary, stratigraphy and crustal evolution of the Archean Greenstone Belt near Sioux Lookout, Ontario: Can. Jour. Earth Sci., v. 10, p. 817-845.

Turner, F. S., 1968, Metamorphic petrology, mineralogical and field aspects: McGraw Hill, Toronto.

Twenhofel, W. H., 1950, Principles of sedimentation: McGraw Hill, Toronto.

Walker, R. G., 1967, Turbidite sedimentary structures and their relationship to proximal and distal depositional environments: Jour. Sed. Petrol., v. 37, p. 25-43.

Watkins, N. D., Gunn, B. M., and Coy-yll, R., 1970, Major and trace element variations during the initial cooling of an Icelandic lava: Am. Jour. Sci., v. 268, p. 24-49.

_____, and Haggerty, S. E., 1967, Primary oxidation variation and petrogenesis in a single lava: Contr. Mineral. Petrol., v. 15, p. 251-271.

Weber, J. N., and Middleton, G. V., 1961, Geochemistry of the turbidites of Normanskill and Charny Formations: Geochim. Cosmochim. Acta , v. 22, p. 200-243.

Wieblen, P. W., and Roedder, E., 1973, Petrology of melt inclusions in Apollo samples 15598 and 62295, and of clasts in 67915 and several lunar soils: Proceedings of the fourth lunar science conference (supplement 4, Geochim. Cosmochim. Acta , v. 1, p. 681-703.

Wilkinson, J. F. G., and Duggan, N. T., 1973, Some tholeiites from the Inverell Area, New South Wales, and their bearing on low pressure tholeiite fractionation: Jour. Petrol., v. 14, pt. 2, p. 339-348.

Williams, P. F., 1972, Development of metamorphic layering and cleavage at Bermagui, Australia: Am. Jour. Sci., v. 272, p. 1-47.

Winkler, H. G. F., 1974, Petrogenesis of metamorphic rocks: 3rd Edition, Springer-Verlag, New York.

Vallance, T. G., 1965, on the chemistry of pillow lavas and the origin of spilites: Mineral. Mag., v. 34, p. 471-481.

Viljoen, M. J., and Viljoen, R. D., 1969, The geology and geochemistry of the lower ultramafic unit of the Onverwacht Group and a proposed new class of igneous rock: Geol. Soc. South Africa Spec. Pub., v. 2, p. 55-85.

APPENDIX I

Presentation of chemical analyses and normative calculations.

	Timiskaming Sedimentary Rocks				Keewatin Sedimentary Rocks		
SAMPLE NO.	122	130	128	134	117	124	120
MAJOR OXIDES (Wt.%)							
SIO2	50.65	50.79	65.75	59.40	62.10	63.06	65.72
AL203	14.07	12.72	14.30	19.04	15.71	15.44	15.31
FE203	14.38	10.57	4.93	5.50	5.24	2.69	5.53
MGO	3.94	4.49	2.59	3.13	3.24	0.85	2.45
CAO	6.46	9.76	0.71	1.69	1.49	4.92	1.60
NA20	2.70	2.55	4.52	0.98	3.95	5.35	3.33
K20	0.09	0.25	1.71	2.75	1.93	0.84	1.84
TIO2	1.59	0.62	0.60	0.79	0.73	0.37	0.72
MNO	0.28	0.49	0.06	0.00	0.18	0.00	0.05
P205	0.21	0.10	0.21	0.11	0.04	0.01	0.14
LOI	6.67	9.60	2.86	4.79	3.62	6.12	2.71
TOTAL	100.73	101.96	98.24	98.20	98.23	99.66	99.39
TRACE ELEMENTS (PPM)							
Ba	63.1	224.4	530.2	640.9		242.1	492.6
Ce	49.4	47.9	72.4	92.9		134.5	78.3
Cu	187.3	104.9	34.4	46.8		33.5	75.5
Ni	29.1	60.6	92.7	156.3		32.1	119.8
Rb	0.1	22.3	63.1	82.3		24.7	56.3
S	432.0	609.9	101.6	1188.1		26.7	1836.1
Sr	149.8	195.9	289.9	353.1		343.1	478.3
Y	17.0	16.6	21.1	19.7		8.1	18.1
Zn	80.1	104.0	119.1	93.1		43.2	80.8
Zr	108.1	110.2	172.6	164.4		105.2	185.5
NORMATIVE MINERALS							
Q	8.24	6.44	25.66	32.52	21.28	17.79	29.84
OR	0.53	1.48	10.11	16.25	11.41	4.96	10.87
AB	22.84	21.57	38.24	8.29	33.42	45.26	28.17
AN	26.00	22.51	2.15	7.67	7.13	15.63	7.02
NE							
C			4.22	11.64	4.51		5.27
CPX	3.97	21.14				7.26	
OPX	25.87	15.34	11.87	13.68	13.69	0.81	12.22
OL							
MT	4.48	3.07	3.04	3.32	3.23	2.71	3.22
IL	3.02	1.18	1.14	1.50	1.39	0.70	1.37
RU	0.02	0.01	0.01	0.01	0.01		0.01
AP							
U.T.M. GRID REFERENCE	816681	833686	832687	843713	819689	816680	821687

Krist Formation

SAMPLE NO.	144	143	147	148	140	139	146	142	145	141
MAJOR OXIDES (Wt.%)										
SI02	47.33	53.28	60.52	60.79	62.91	64.31	63.84	63.68	64.57	65.18
AL203	12.06	12.70	17.26	17.30	16.03	18.51	16.89	12.41	16.38	14.09
FE203	7.23	6.71	4.51	4.93	5.34	3.49	3.53	4.37	3.38	3.80
MGO	3.43	2.48	1.76	2.33	2.67	1.36	1.01	2.06	0.82	1.29
CAO	15.84	12.37	4.86	4.01	1.53	2.72	4.64	6.27	3.44	3.80
NA20	2.14	2.84	5.20	4.55	5.03	4.03	4.42	5.51	5.67	6.34
K20	0.28	0.37	1.25	1.27	2.21	1.84	1.31	0.55	1.09	1.10
TI02	0.29	0.30	1.16	1.16	0.68	0.48	0.37	0.40	0.32	0.44
MNO	0.92	0.00	0.06	0.04	0.26	0.00	0.01	0.06	0.04	0.18
P205	0.12	0.11	0.25	0.21	0.08	0.16	0.18	0.18	0.22	0.08
LOI	9.62	9.75	5.16	4.85	4.23	3.73	4.53	6.64	4.53	5.05
TOTAL	99.86	100.91	101.99	101.44	101.59	100.64	100.72	102.14	100.46	101.35
TRACE ELEMENTS (PPM)										
Ba		143.9	313.7		383.6	334.7	340.7	138.7		202.1
Ce		60.2	103.2		158.3	172.1	94.2	122.8		79.2
Cu		19.1	94.4		17.3	15.3	13.8	21.1		11.2
Ni		50.1	68.4		14.5	16.9	13.1	83.4		7.6
Rb		4.2	32.5		52.0	29.5	40.5	17.2		29.7
S		695.2	2646.1		165.5	132.9	198.5	23.7		37.6
Sr		294.8	454.0		630.3	729.3	592.0	310.1		632.4
Y		10.7	15.0		7.9	7.8	7.8	9.9		6.1
Zn		69.7	59.5		72.1	75.9	40.4	66.3		39.1
Zr		104.6	209.3		199.9	196.1	190.5	125.7		191.8
NORMATIVE MINERALS										
Q	2.13	9.91	15.17	16.16	15.48	24.91	20.51	16.11	17.83	14.97
OR	1.65	2.19	7.39	7.51	13.06	10.87	7.74	3.25	6.44	6.50
AB	18.10	24.03	43.99	38.49	42.55	34.09	37.39	46.61	47.97	53.63
AN	24.10	20.80	20.05	18.52	7.07	12.45	21.85	7.50	15.63	6.73
NE										
C				1.65	2.77	5.32	0.19		0.14	
CPX	37.22	30.42	1.99					18.59		9.68
OPX			6.75	9.83	12.56	6.73	6.20	0.95	5.59	2.34
OL										
MT	2.60	2.61	3.86	3.86	3.16	2.87	2.71	2.75	2.64	2.81
IL	0.55	0.57	2.21	2.21	1.29	0.91	0.70	0.76	0.61	0.84
RU			0.01	0.01	0.01	0.01		0.01		0.01
AP										
U.T.M. GRID REFERENCE	802686	802687	763671	762668	810695	810696	765671	801688	766670	810695

	Upper Schumacher Formation									
SAMPLE NO.	269	256	265	161	267	230	277	233	234	266
MAJOR OXIDES (Wt.%)										
SIO2	45.54	45.60	45.83	45.70	45.32	47.55	48.07	49.69	49.28	47.56
AL2O3	14.72	14.80	13.43	12.33	14.14	13.36	13.82	14.28	13.79	13.78
FE2O3	16.12	16.12	14.36	15.03	12.18	13.90	14.36	14.62	11.10	12.90
MGO	6.94	7.02	5.25	5.13	4.65	3.95	4.58	5.71	4.70	5.06
CAO	7.54	6.81	8.36	10.02	11.28	10.52	8.64	2.65	10.23	9.49
NA2O	0.85	0.67	2.19	1.88	0.44	1.78	0.09	2.44	3.24	0.15
K2O	0.71	0.71	1.41	0.20	0.76	0.23	1.20	0.04	0.05	0.41
TIO2	1.30	1.35	1.08	1.27	1.10	1.41	1.26	1.39	1.28	1.15
MNO	0.85	0.71	0.80	0.11	0.18	0.00	0.92	0.18	0.14	0.08
P2O5	0.09	0.09	0.11	0.09	0.10	0.06	0.10	0.13	0.12	0.13
LOI	4.85	6.53	8.15	8.63	9.58	6.81	6.51	4.22	8.21	11.06
TOTAL	99.55	100.41	100.99	100.38	99.73	99.57	99.54	99.33	102.14	101.76
TRACE ELEMENTS (PPM)										
Ba	283.6				172.0	88.1	246.6	36.6	45.6	218.0
Ce	30.2				38.3	27.7	47.3	47.4	21.0	35.0
Cu	38.1				207.8	37.9	65.5	197.1	263.1	106.1
Ni	123.4				121.2	58.0	65.5	73.9	96.0	92.4
Rb	13.8				13.4	2.7	16.8	00.0	2.0	4.1
S	192.2				674.4	30.4	111.9	127.3	391.9	33.2
Sr	39.0				76.0	59.6	52.4	54.8	112.7	121.1
Y	15.5				10.5	8.7	14.4	11.0	10.9	11.9
Zn	83.2				60.6	59.5	67.7	87.7	50.9	65.3
Zr	46.1				42.9	46.9	47.3	46.8	59.1	61.3
NORMATIVE MINERALS										
Q	2.10	4.14		1.12	6.20	4.94	10.90	5.01	1.16	12.04
OR	4.20	4.20	8.33	1.18	4.49	1.36	7.09	0.24	0.30	2.42
AB	7.19	5.67	18.53	15.90	3.72	15.06	0.76	20.64	27.41	1.27
AN	34.24	33.20	22.64	24.60	34.35	27.77	33.75	27.88	22.93	35.70
NE										
C		0.76								
CPX	2.15		15.23	20.66	17.58	20.35	7.14	3.57	22.56	8.83
OPX	38.40	39.55	14.14	22.86	18.96	17.81	27.20	31.92	14.42	25.42
OL			8.28							
MT	4.06	4.13	3.74	4.02	3.77	4.22	4.00	4.19	4.03	3.84
IL	2.47	2.57	2.05	2.42	2.09	2.68	2.40	2.64	2.44	2.19
RU	0.02	0.02	0.01	0.02	0.01	0.02	0.02	0.02	0.02	0.01
AP										
U.T.M. GRID REFERENCE	809672	773678	805676	830749	806674	804702	804697	807699	807697	805675

Upper Schumacher Formation

SAMPLE NO.	176	232	248	202	198	231	199	175	244	253
MAJOR OXIDES (Wt.%)										
SIO2	52.23	50.12	50.32	52.88	54.02	51.25	54.45	53.50	55.48	54.37
AL203	14.53	15.61	11.72	13.20	14.79	13.02	13.85	13.89	14.43	13.84
FE203	12.64	11.71	18.61	18.05	12.86	17.47	13.23	9.33	9.87	12.98
MGO	6.30	5.17	2.12	3.72	4.35	2.61	3.04	2.94	3.17	2.61
CAO	6.96	6.67	8.42	7.77	7.52	5.14	5.68	8.18	7.57	6.12
NA20	4.48	3.68	0.00	0.00	3.42	2.22	4.73	3.81	3.93	0.00
K20	0.14	0.04	0.35	0.21	0.36	0.05	0.24	0.06	0.04	0.17
TIO2	1.38	1.36	1.32	1.54	1.23	1.51	1.33	1.44	1.14	1.24
MNO	0.11	0.13	0.00	0.16	0.18	0.08	0.16	0.04	0.00	0.09
P205	0.11	0.12	0.52	0.17	0.12	0.50	0.15	0.18	0.09	0.19
LOI	2.95	6.61	7.74	3.80	2.96	7.64	4.31	6.47	6.28	7.80
TOTAL	101.84	101.22	101.12	101.50	101.81	101.50	101.16	102.00	99.85	99.40
TRACE ELEMENTS (PPM)										
Ba		62.5				20.9				
Ce		18.2				38.9				
Cu		92.8				6.2				
Ni		127.6				68.3				
Rb		00.0				1.0				
S		34.7				379.7				
Sr		87.5				65.3				
Y		16.8				30.5				
Zn		79.2				94.1				
Zr		65.0				40.2				
NORMATIVE MINERALS										
Q		1.57	18.91	19.53	5.49	13.78	4.31	8.94	9.52	29.45
OR	0.83	0.24	2.07	0.24	2.13	0.30	1.42	0.35	0.24	1.00
AB	37.90	31.13			28.93	18.78	40.01	32.23	33.25	
AN	19.12	25.95	30.93	35.38	23.93	22.24	15.84	20.61	21.61	29.12
NE										
C						1.16				2.98
CPX	12.20	5.30	6.47	1.75	10.60		9.67	15.78	12.92	
OPX	16.11	24.99	28.17	33.14	22.48	30.39	19.99	10.04	13.65	23.64
OL	7.21									
MT	4.18	4.15	4.09	4.41	3.90	4.36	4.10	4.26	3.83	3.97
IL	2.63	2.59	2.51	2.93	2.34	2.87	2.53	2.74	2.17	2.36
RU	0.02	0.02	0.02	0.02	0.02	0.02	0.02	0.02	0.01	0.02
AP										
U.T.M. GRID REFERENCE	841724	806700	784679	757708	753711	805701	754711	841727	782675	780688

Variolitic Flows

SAMPLE NO.	174	270	268	243	246	271	228	247	229
MAJOR OXIDES (Wt.%)									
SIO2	49.55	50.68	50.35	49.17	51.92	52.40	52.81	52.69	53.61
AL203	14.12	14.63	12.88	13.49	14.51	13.49	13.24	10.81	11.48
FE203	16.58	19.00	18.59	15.45	16.56	12.34	14.04	18.29	8.58
MGO	5.55	2.39	5.73	4.39	4.92	4.15	4.24	3.08	1.30
CAO	6.58	3.77	5.88	7.48	7.18	6.78	5.18	6.64	10.73
NA20	2.93	3.28	0.00	0.95	0.00	2.68	3.31	0.00	3.07
K20	0.25	0.06	0.03	0.03	0.03	0.03	0.05	0.22	0.04
TIO2	1.54	1.62	1.70	1.49	1.37	1.22	1.26	1.27	1.23
MNO	0.19	0.19	0.04	0.19	0.16	0.20	0.05	0.24	0.13
P205	0.18	0.46	0.10	0.18	0.13	0.14	0.14	0.57	0.41
LOI	3.12	5.38	6.07	8.61	4.43	7.70	7.62	6.88	10.21
TOTAL	100.58	101.35	101.38	101.45	101.21	101.68	101.94	100.68	100.79
TRACE ELEMENTS (PPM)									
Ba	612.6	49.0	81.1	51.5	21.9	49.3	49.5	92.0	0.0
Ce	965.4	14.4	11.4	19.3	23.1	25.7	44.9	20.1	59.0
Cu	33.7	4.0	105.0	47.2	67.7	94.3	44.8	3.5	48.7
Ni	46.4	15.3	36.5	47.3	62.7	58.4	57.4	3.4	15.3
Rb	120.6	0.7	0.0	0.0	0.0	0.0	0.0	0.0	0.0
S	385.1	22.7	62.3	349.5	96.4	160.8	180.2	1179.4	704.3
Sr	196.9	81.6	82.5	144.5	284.7	58.4	68.4	29.2	167.7
Y	29.7	30.4	10.2	19.1	21.8	22.6	15.0	20.8	31.9
Zn	107.5	112.3	85.8	72.4	87.3	68.9	81.0	153.4	46.0
Zr	193.3	147.6	162.9	156.7	124.0	102.4	103.0	104.7	158.7
NORMATIVE MINERALS									
Q	1.00	9.14	17.88	12.84	19.11	10.77	8.56	22.96	14.48
OR	1.48	0.35	0.18	0.18	0.18	0.18	0.30	1.30	0.24
AB	24.79	27.75		8.04		22.67	28.00		25.97
AN	24.63	15.70	28.52	32.44	34.77	24.68	21.11	28.84	17.42
NE									
C		3.41	2.39		1.73				
CPX	5.77			2.96		6.77	3.10	0.33	25.57
OPX	33.27	32.07	39.54	30.05	34.98	23.07	27.84	33.34	
OL									
MT	4.41	4.54	4.64	4.34	4.16	3.94	4.00	4.02	3.96
IL	2.93	3.10	3.23	2.83	2.61	2.32	2.40	2.42	2.34
RU	0.02	0.02	0.02	0.02	0.02	0.02	0.02	0.02	0.02
AP									
U.T.M. GRID REFERENCE	839729	809671	807673	783673	782677	811672	802704	782678	803703

Lower Schumacher Formation

SAMPLE NO.	107	169	106	90	201	83	89	172	173	164
MAJOR OXIDES (Wt.%)										
SIO2	45.58	47.73	48.68	47.78	50.34	46.26	49.46	48.82	49.50	48.86
AL2O3	15.24	15.77	15.54	16.19	14.06	13.90	14.73	13.49	14.74	13.53
FE2O3	13.47	12.38	14.63	13.79	11.74	11.24	14.76	14.31	13.37	13.23
MGO	5.79	8.42	9.01	8.17	7.67	5.52	7.19	7.83	7.47	5.72
CAO	15.69	11.03	7.73	4.58	10.95	11.44	7.48	9.74	10.07	11.76
NA2O	0.00	2.57	1.27	2.00	3.28	1.41	2.25	0.32	0.55	1.17
K2O	0.05	0.10	0.33	0.06	0.29	0.24	0.05	0.11	0.18	0.04
TIO2	0.69	0.82	0.77	0.50	0.66	0.77	0.84	0.84	0.85	0.84
MNO	0.95	0.10	0.86	1.28	0.03	0.00	0.09	0.04	0.00	0.23
P2O5	0.07	0.06	0.07	0.08	0.07	0.03	0.09	0.10	0.07	0.13
LOI	4.18	2.75	3.78	7.17	2.54	8.48	4.48	2.95	4.91	6.26
TOTAL	101.70	101.73	101.87	101.59	101.63	99.28	101.41	98.54	101.69	101.77
TRACE ELEMENTS (PPM)										
Ba	83.6	50.6	20.0					68.8		22.6
Ce	35.2	27.3	16.6					61.9		23.9
Cu	13.4	67.0	14.2					70.1		94.1
Ni	46.1	90.5	77.9					95.6		56.3
Rb	00.0	0.6	6.9					3.5		0.0
S	43.4	29.2	12.2					69.3		2565.3
Sr	146.8	68.5	56.7					203.4		70.1
Y	5.0	13.0	11.9					13.6		11.8
Zn	47.3	69.4	64.2					62.8		82.3
Zr	40.6	46.0	42.2					38.9		47.9
NORMATIVE MINERALS										
Q	2.30		1.13	4.90		3.01	1.53	7.74	7.22	5.71
OR	0.30	0.59	1.95	0.35	1.71	1.42	0.30	0.65	1.06	0.24
AB		21.74	10.74	16.92	27.75	11.93	19.03	2.71	4.65	9.90
AN	41.42	31.19	35.71	22.20	22.78	30.88	29.93	35.04	37.21	31.54
NE										
C				4.70						
CPX	60.22	19.07	1.80		25.66	21.38	5.49	10.55	10.20	21.73
OPX	18.72	4.66	42.60	40.69	2.89	18.57	36.24	34.60	32.31	21.96
OL		17.69			14.77					
MT	3.18	3.36	3.29	2.90	3.13	3.29	3.39	3.39	3.41	3.39
IL	1.31	1.56	1.46	0.95	1.26	1.46	1.60	1.60	1.62	1.60
RU	0.01	0.01	0.01	0.01	0.01	0.01	0.01	0.01	0.01	0.01
AP										
U.T.M. GRID REFERENCE	832681	835737	832683	796644	755708	788658	786646	838734	839731	830751

	Lower Schumacher Formation									
SAMPLE NO.	81	109	91	168	105	167	272	166	108	213
MAJOR OXIDES (Wt.%)										
SIO2	46.82	51.12	48.54	49.57	49.85	48.87	47.56	49.83	51.38	51.39
AL203	13.82	14.52	15.77	14.91	14.96	13.79	13.89	15.00	14.47	13.84
FE203	11.21	14.92	13.47	13.22	14.45	12.00	10.81	13.61	12.39	13.71
MGO	3.65	5.88	7.70	7.14	6.26	4.26	6.14	8.00	6.87	7.31
CAO	11.35	8.37	7.28	6.55	5.97	10.31	11.03	7.20	9.44	7.58
NA20	2.99	3.40	1.04	3.19	3.53	2.49	1.02	0.46	2.48	3.59
K20	0.39	0.18	0.04	0.21	0.07	0.89	0.03	0.04	0.18	0.08
TIO2	0.92	1.02	0.48	0.95	0.90	0.76	0.79	0.88	0.74	0.84
MNO	0.07	0.29	0.08	0.47	0.59	0.87	0.00	0.61	0.30	0.04
P205	0.07	0.12	0.07	0.04	0.14	0.06	0.09	0.08	0.11	0.11
LOI	8.04	1.76	4.11	4.39	5.32	5.05	10.51	5.55	2.36	2.82
TOTAL	99.33	101.57	98.59	100.64	102.04	99.34	101.87	101.28	100.73	101.31
TRACE ELEMENTS (PPM)										
Ba		63.5				257.1	23.6	160.5	40.3	
Ce		27.8				0.0	23.8	28.7	65.1	
Cu		220.4				90.3	120.3	172.6	46.0	
Ni		60.6				104.4	93.1	85.5	75.6	
Rb		0.0				11.7	0.2	2.6	0.0	
S		31.4				199.8	78.1	35.2	4.9	
Sr		52.6				33.4	83.6	167.7	75.7	
Y		13.3				12.7	10.3	8.4	9.4	
Zn		46.3				59.0	83.6	78.1	62.8	
Zr		50.4				40.1	46.3	60.7	41.0	
NORMATIVE MINERALS										
Q			6.44			0.91	6.82	11.19	2.14	
OR	2.30	1.06	0.24	1.24	0.41	5.26	0.18	0.24	1.06	0.47
AB	25.29	28.76	8.80	26.99	29.86	21.06	8.63	3.89	20.98	30.37
AN	23.13	23.82	35.66	25.73	24.76	23.81	33.22	35.20	27.81	21.40
NE										
C			0.94					1.30		
CPX	27.60	14.21		5.40	3.30	22.69	17.41		15.19	12.86
OPX	4.75	22.36	39.01	28.58	30.03	15.95	21.41	39.00	27.00	23.24
OL	4.07	4.51		3.54	3.22					5.86
MT	3.51	3.65	2.87	3.55	3.48	3.28	3.32	3.45	3.25	3.39
IL	1.75	1.94	0.91	1.81	1.71	1.45	1.50	1.67	1.41	1.60
RU	0.01	0.01	0.01	0.01	0.01	0.01	0.01	0.01	0.01	0.01
AP										
U.T.M. GRID REFERENCE	787656	833679	793642	834740	817665	834739	812671	832740	832679	771693

Lower Schumacher Formation

SAMPLE NO.	170	222	110	206	88	95	163	171	242	209
MAJOR OXIDES (Wt.%)										
SIO2	48.27	46.09	49.27	51.60	50.05	50.13	52.69	52.46	49.68	52.72
AL2O3	14.28	13.03	14.50	14.35	15.61	13.83	14.59	15.26	13.98	15.31
FE2O3	10.95	11.12	11.11	8.54	15.59	14.07	10.28	9.47	10.11	13.50
MGO	6.77	4.41	5.89	7.20	6.63	6.41	6.09	6.77	6.81	6.76
CAO	9.01	11.82	10.83	10.39	2.76	5.85	9.34	10.07	8.60	2.57
NA2O	1.69	0.00	0.00	3.80	2.93	3.05	4.10	0.84	0.00	3.50
K2O	0.08	0.41	0.16	0.13	0.05	0.11	0.26	0.47	0.03	0.03
TIO2	0.71	0.73	0.75	0.79	0.93	0.79	0.75	0.70	0.82	1.08
MNO	0.18	0.20	0.60	0.11	0.04	0.03	0.15	0.18	0.11	0.16
P2O5	0.15	0.15	0.09	0.13	0.10	0.03	0.16	0.10	0.04	0.12
LOI	9.37	13.74	8.82	3.26	5.50	6.98	3.67	3.80	10.53	5.94
TOTAL	101.46	101.70	102.00	100.30	100.17	101.28	102.07	100.12	100.70	101.69
TRACE ELEMENTS (PPM)										
Ba	37.6	142.4	41.0				47.3	54.7		
Ce	53.5	27.9	48.9				34.1	55.0		
Cu	10.6	81.9	58.6				98.3	37.0		
Ni	70.7	56.3	60.1				85.0	46.7		
Rb	0.0	5.2	0.2				2.4	2.0		
S	21.5	385.4	45.6				40.5	89.0		
Sr	48.0	99.5	45.0				81.0	62.1		
Y	9.2	15.0	11.3				15.3	5.1		
Zn	67.9	86.5	54.0				63.9	56.1		
Zr	39.3	48.3	45.6				217.2	30.4		
NORMATIVE MINERALS										
Q	5.01	11.10	13.04		7.50	1.95		11.39	15.93	8.64
OR	0.47	2.42	0.89	0.77	0.30	0.65	1.54	2.78	0.18	0.18
AB	14.30			32.15	24.79	25.80	34.68	7.11		29.61
AN	31.13	34.33	39.11	21.71	13.04	23.71	20.63	36.47	38.04	11.97
NE										
C					5.95					5.13
CPX	10.40	19.57	11.66	23.66		4.28	20.38	10.56	3.59	
OPX	26.84	16.53	24.17	8.77	38.73	33.89	12.26	24.37	28.64	35.23
OL				6.25			4.96			
MT	3.20	3.23	3.26	3.32	3.52	3.32	3.26	3.19	3.36	3.74
IL	1.35	1.39	1.43	1.50	1.77	1.50	1.43	1.33	1.56	2.05
RU	0.01	0.01	0.01	0.01	0.01	0.01	0.01	0.01	0.01	0.01
AP										
U.T.M. GRID REFERENCE	836736	800705	834678	768709	778636	794665	830750	837735	783669	769707

			Lower Schumacher Formation		
SAMPLE NO.	160	211	210	245	200
MAJOR OXIDES (Wt.%)					
SIO2	51.17	49.84	54.25	55.54	51.09
AL203	13.15	12.29	14.16	13.20	13.30
FE203	11.11	12.76	10.65	15.37	8.96
MGO	4.64	4.46	6.32	5.21	4.66
CAO	11.20	9.29	7.11	7.09	10.53
NA20	0.00	0.00	3.76	0.79	0.00
K20	0.08	0.45	0.65	0.04	0.14
TIO2	1.04	1.08	0.78	1.08	0.79
MNO	0.14	0.03	0.16	0.20	0.19
P205	0.07	0.13	0.06	0.13	0.12
LOI	5.59	10.86	3.98	2.67	9.27
TOTAL	98.18	101.18	101.88	101.32	99.04
TRACE ELEMENTS (PPM)					
Ba	114.7			19.3	
Ce	32.4			19.3	
Cu	162.4			20.1	
Ni	106.4			63.0	
Rb	3.3			3.5	
S	85.2			7.7	
Sr	72.0			188.6	
Y	12.0			22.8	
Zn	84.0			97.7	
Zr	46.5			60.6	
NORMATIVE MINERALS					
Q	17.73	16.93	2.09	18.85	19.46
OR	0.47	2.66	3.84	0.24	0.83
AB			31.81	6.68	
AN	35.63	32.19	19.83	32.34	35.86
NE					
C					
CPX	16.28	10.97	12.44	1.67	12.93
OPX	18.00	22.77	24.04	33.62	16.83
OL					
MT	3.68	3.74	3.30	3.74	3.32
IL	1.98	2.05	1.48	2.05	1.50
RU	0.01	0.01	0.01	0.01	0.01
AP					
U.T.M. GRID REFERENCE	830749	771707	769705	782676	754709

Goose Lake Formation

SAMPLE NO.	188	192	186	103	187	185	99	102
MAJOR OXIDES (Wt.%)								
SIO2	41.61	41.15	42.04	44.45	43.80	42.67	43.67	44.06
AL203	3.52	3.96	4.36	5.08	4.59	4.91	5.41	5.82
FE203	15.68	12.27	15.60	10.83	13.09	15.54	12.32	11.33
MGO	27.18	25.70	26.12	26.33	25.40	24.34	23.74	23.97
CAO	2.61	4.45	3.26	5.82	6.33	5.07	9.21	8.43
NA20	0.11	0.73	0.97	0.53	0.25	0.28	0.67	0.21
K20	0.01	0.01	0.02	0.02	0.06	0.02	0.04	0.02
TIO2	0.48	0.47	0.52	0.33	0.39	0.55	0.39	0.39
MNO	0.11	0.13	0.07	0.00	0.19	0.177	0.11	0.20
P205	0.05	0.02	0.03	0.04	0.05	0.00	0.04	0.02
LOI	10.14	11.71	8.22	7.80	6.22	7.46	6.49	6.18
TOTAL	101.52	100.60	101.21	101.23	100.35	101.00	102.09	100.63
TRACE ELEMENTS (PPM)								
Ba			0.0	72.1	46.1	0.0	12.4	44.9
Ce			70.5	36.8	40.1	37.6	37.1	37.8
Cu			19.8	24.1	29.7	17.0	47.6	143.9
Ni			1631.4	1584.8	1558.5	1693.6	1298.6	1431.4
Rb			0.0	0.0	3.5	2.1	0.5	0.0
S			273.9	38.8	98.8	430.2	66.4	31.0
Sr			0.0	7.9	0.0	1.7	5.1	0.3
Y			2.5	0.7	7.4	5.9	2.5	2.0
Zn			59.2	64.9	62.7	51.2	68.8	81.2
Zr			22.3	21.8	20.8	18.1	18.3	16.4
NORMATIVE MINERALS								
Q								
OR	0.06	0.06	0.12	0.12	0.35	0.12	0.24	0.12
AB	0.93	6.18	8.21	4.48	2.11	2.37	5.67	1.78
AN	9.08	7.50	7.48	11.42	11.22	12.08	11.63	14.87
NE								
C								
CPX	2.85	11.28	6.83	13.72	15.92	10.45	27.11	21.45
OPX	36.55	32.74	19.90	26.51	26.52	29.05	6.46	21.24
OL	38.31	18.25	46.86	34.59	34.85	35.73	41.55	32.06
MT	2.87		2.93	2.65	2.74	2.97	2.74	2.74
IL	0.91	0.23	0.99	0.63	0.74	1.05	0.74	0.74
RU	0.01		0.01			0.01		
AP								
U.T.M. GRID REFERENCE	757724	756733	756728	821659	757726	756729	821658	821661

Goose Lake Formation

SAMPLE NO.	151	104	193	152	191	100	94	96
MAJOR OXIDES (Wt.%)								
SIO2	43.82	46.51	46.08	46.09	48.47	46.92	49.68	54.47
AL203	8.96	7.52	7.11	7.20	6.58	8.81	14.48	14.55
FE203	15.73	12.62	12.90	13.34	12.29	14.23	15.06	9.75
MGO	19.21	18.92	17.71	18.63	16.21	15.23	6.58	4.36
CAO	8.27	8.92	7.34	10.54	9.06	8.85	10.21	5.44
NA20	0.97	1.42	0.00	1.09	0.00	0.00	1.65	3.00
K20	0.03	0.09	0.03	0.03	0.03	0.11	0.93	0.05
TIO2	0.49	0.45	0.44	0.40	0.52	0.50	1.14	0.92
MNO	0.18	0.17	0.14	0.13	0.07	0.00	0.22	1.17
P205	0.08	0.03	0.09	0.05	0.07	0.05	0.18	0.09
LOI	3.66	4.59	6.49	3.96	5.13	5.21	1.46	6.42
TOTAL	101.39	101.24	98.33	101.46	98.41	99.99	101.58	100.23
TRACE ELEMENTS (PPM)								
Ba	40.7	20.1	21.3	56.7				
Ce	20.7	28.5	33.5	31.6				
Cu	52.9	5.2	43.8	11.8				
Ni	950.0	824.8	820.8	937.9				
Rb	1.0	0.0	0.0	1.6				
S	62.4	391.9	3393.7	41.5				
Sr	7.8	1.4	0.0	4.8				
Y	0.9	3.0	1.0	6.2				
Zn	66.0	79.8	54.1	64.2				
Zr	23.2	22.9	21.3	19.6				
NORMATIVE MINERALS								
Q							0.22	13.26
OR	0.18	0.53	0.18	0.18	2.64	0.65	5.50	0.30
AB	2.20	12.01		9.22	0.18		13.96	25.38
AN	15.33	13.87	19.30	14.66	17.86	23.71	29.35	26.08
NE								
C								
CPX	42.71	24.34	13.35	30.15	21.54	16.18	16.82	0.27
OPX	7.58	13.71	53.13	10.16	47.78	49.89	28.82	23.35
OL	24.26	29.00	2.56	30.00		1.00		
MT	2.83	2.83	2.81	2.75	2.93	2.90	3.83	3.51
IL	0.86	0.86	0.84	0.76	0.99	0.95	2.17	1.75
RU	0.01	0.01	0.01	0.01	0.01	0.01	0.01	0.01
AP								
U.T.M. GRID REFERENCE	831754	821662	760773	831753	756731	821659	796663	795662

	Boomerang Formation				
SAMPLE NO.	1	63	138	93	137
MAJOR OXIDES (Wt.%)					
SIO2	50.18	56.42	67.09	70.79	69.44
AL203	15.31	11.54	14.20	15.87	12.96
FE203	10.58	5.32	4.11	3.73	3.01
MGO	5.12	3.14	0.62	1.19	1.02
CAO	3.37	9.71	1.86	2.53	2.93
NA20	3.21	2.94	4.65	2.65	2.37
K20	1.35	0.99	2.27	1.39	2.18
TIO2	0.89	0.61	0.48	0.36	0.45
MNO	0.22	0.06	0.01	0.12	0.05
P205	0.11	0.28	0.25	0.05	0.24
LOI	8.63	9.43	3.18	2.55	3.68
TOTAL	98.96	100.44	98.72	101.23	98.21
TRACE ELEMENTS (PPM)					
Ba	338.8	271.0	292.4	334.8	451.4
Ce	60.0	79.0	157.5	133.9	137.4
Cu	54.1	34.5	60.6	25.0	39.6
Ni	90.6	78.6	21.0	50.8	31.9
Rb	22.8	23.2	64.4	50.3	62.0
S	256.7	22.5	22.4	10.7	69.3
Sr	104.4	258.3	127.3	254.1	206.8
Y	15.7	12.6	24.3	14.3	18.2
Zn	94.1	63.1	70.2	62.5	21.6
Zr	147.4	129.9	219.3	153.7	164.2
NORMATIVE MINERALS					
Q	5.41	14.78	25.17	41.17	39.00
OR	7.98	5.85	13.42	8.21	12.88
AB	27.16	24.87	39.34	22.42	20.05
AN	16.00	15.36	7.60	12.23	12.97
NE					
C	2.70		1.31	5.52	1.95
CPX		25.48			
OPX	26.79	1.38	5.90	7.00	5.16
OL					
MT	3.47	3.06	2.87	2.70	2.83
IL	1.69	1.16	0.91	0.68	0.86
RU	0.01	0.01	0.01		0.01
AP					
U.T.M. GRID REFERENCE	752625	850661	847678	793638	843683

	Redstone Formation									
SAMPLE NO.	22	25	45	56	35	30	39	31	37	5
MAJOR OXIDES (Wt.%)										
SIO2	48.84	49.71	46.88	49.70	50.55	51.33	50.85	51.26	54.19	52.91
AL203	16.11	14.08	15.47	14.34	14.80	15.42	13.42	14.07	15.92	17.58
FE203	13.44	14.64	15.57	11.97	9.76	12.46	11.59	11.62	9.85	11.34
MGO	6.26	6.84	8.26	5.53	4.60	6.41	7.20	5.54	5.10	6.49
CAO	8.38	10.79	4.60	6.98	10.86	5.56	7.88	4.99	8.31	0.39
NA20	2.23	0.98	0.70	2.71	2.17	2.89	0.55	4.19	2.21	4.23
K20	1.09	0.45	0.05	0.49	0.19	0.43	0.15	0.27	0.48	0.76
TIO2	0.61	1.19	0.78	1.13	0.96	0.75	1.50	0.85	0.81	0.88
MNO	0.19	0.14	0.03	0.16	0.13	0.04	0.22	0.19	0.00	0.01
P205	0.10	0.17	0.17	0.26	0.09	0.21	0.25	0.16	0.12	0.19
LOI	3.66	0.78	7.67	8.28	7.52	5.36	8.33	6.70	4.79	4.98
TOTAL	100.90	99.76	100.18	101.56	101.64	100.85	101.92	99.84	101.77	99.76
TRACE ELEMENTS (PPM)										
Ba	207.0	171.6	36.3	203.2	134.5	208.3	0.0		122.1	
Ce	27.9	26.5	46.2	32.5	24.1	43.7	47.5		41.8	
Cu	25.7	134.5	93.7	47.5	14.8	51.9	4.2		38.6	
Ni	117.4	86.5	145.2	119.4	93.6	182.7	212.4		99.6	
Rb	24.0	3.9	2.0	13.6	4.3	10.1	2.9		10.2	
S	36.4	164.2	22.6	100.1	58.5	54.5	23.8		110.8	
Sr	86.9	132.6	65.4	84.6	245.8	253.0	48.8		204.6	
Y	16.2	15.4	7.8	16.7	12.4	12.2	8.2		10.2	
Zn	72.9	74.9	117.8	74.5	37.1	103.1	93.2		87.7	
Zr	36.7	77.4	98.9	114.8	76.1	111.1	104.3		120.1	
NORMATIVE MINERALS										
Q		4.61	10.67	4.04	6.65	4.04	14.52	1.21	10.31	8.46
OR	6.44	2.66	0.30	2.90	1.12	2.54	0.89	1.60	2.84	4.49
AB	18.87	8.29	5.92	22.93	18.36	24.45	4.65	35.45	18.70	35.78
AN	30.72	32.68	21.71	25.51	30.07	26.21	33.69	18.78	32.09	0.70
NE										
C			6.30			0.59				9.54
CPX	8.53	16.46		6.18	19.32		3.10	4.11	6.93	
OPX	23.24	28.86	43.13	26.45	14.39	33.45	30.61	27.62	22.30	31.48
OL	5.61									
MT	3.06	3.90	3.31	3.81	3.57	3.26	4.35	3.41	3.35	3.45
IL	1.16	2.26	1.48	2.15	1.83	1.43	2.85	1.62	1.54	1.67
RU	0.01	0.01	0.01	0.01	0.01	0.01	0.02	0.01	0.01	0.01
AP										
U.T.M. GRID REFERENCE	800615	803623	813636	834611	828611	801626	811626	797629	815615	754607

	Redstone Formation									
SAMPLE NO.	40	43	33	34	36	44	38	42	4	57
MAJOR OXIDES (Wt.%)										
SIO2	52.42	53.24	54.64	54.24	55.70	55.59	56.12	56.56	58.34	57.44
AL203	14.49	15.59	15.80	15.90	15.80	14.57	14.91	19.82	15.81	15.16
FE203	10.35	10.42	9.25	8.89	10.22	8.53	9.48	5.47	9.19	8.57
MGO	5.45	5.29	5.07	4.75	4.10	4.73	5.83	2.47	3.83	3.65
CAO	6.96	4.33	6.07	5.07	8.45	5.73	5.29	3.52	4.38	5.22
NA20	1.55	3.54	3.85	1.52	0.27	4.04	1.53	0.72	4.50	2.92
K20	0.81	0.05	0.82	2.67	0.22	0.19	0.36	4.68	0.14	0.44
TIO2	0.88	0.88	0.74	0.75	0.79	0.62	0.71	1.02	0.75	0.67
MNO	0.17	0.78	0.03	0.00	0.11	0.00	0.11	0.27	0.15	0.13
P205	0.18	0.14	0.18	0.18	0.14	0.14	0.20	0.11	0.26	0.20
LOI	7.91	7.19	2.35	6.72	3.67	7.28	3.89	6.48	3.52	3.64
TOTAL	101.17	101.44	98.80	100.70	99.44	101.43	98.43	101.13	100.85	98.03
TRACE ELEMENTS (PPM)										
Ba		0.0		604.6	30.0	101.8	88.8	555.9	127.7	123.0
Ce		58.6		36.3	51.9	84.1	37.8	56.2	92.0	66.4
Cu		20.6		68.0	15.8	6.5	9.5	8.8	32.6	60.7
Ni		187.3		115.8	99.8	105.7	136.7	100.0	112.0	76.4
Rb		0.0		66.8	2.3	4.0	11.8	100.2	21.5	13.1
S		23.0		43.3	93.1	21.1	7.9	3830.6	4.3	135.1
Sr		139.7		66.4	181.7	181.3	82.3	48.0	72.6	157.9
Y		9.2		24.2	9.2	13.0	12.1	28.7	14.1	15.0
Zn		108.2		55.1	68.6	74.3	73.6	153.2	104.5	72.3
Zr		126.5		127.0	116.0	133.0	108.5	122.4	177.4	149.1
NORMATIVE MINERALS										
Q	12.23	9.41	4.70	12.47	23.20	8.68	20.62	21.14	11.77	17.59
OR	4.79	0.30	4.85	15.78	1.30	1.12	2.13	27.66	0.83	2.60
AB	13.11	29.95	32.57	12.86	2.28	34.18	12.94	6.09	38.07	24.70
AN	30.18	20.57	23.40	23.98	41.07	21.05	24.94	16.75	20.03	24.59
NE										
C		2.17		1.72	0.06		2.86	7.43	0.91	0.86
CPX	2.63		4.58			5.36				
OPX	25.95	26.99	22.57	23.42	23.90	20.45	27.19	11.43	21.63	20.35
OL										
MT	3.45	3.45	3.25	3.26	3.32	3.07	3.20	3.20	3.26	3.15
IL	1.67	1.67	1.41	1.43	1.50	1.18	1.35	1.94	1.43	1.27
RU	0.01	0.01	0.01	0.01	0.01	0.01	0.01	0.01	0.01	0.01
AP										
U.T.M. GRID REFERENCE	809629	799633	815619	817616	815616	799636	814615	801630	752610	833612

				Redstone Formation		
SAMPLE NO.	303	55	11	12	28	29
MAJOR OXIDES (Wt.%)						
SIO2	56.86	57.74	60.18	59.77	60.12	66.00
AL203	14.17	15.69	15.60	15.55	16.40	16.02
FE203	5.15	8.60	8.92	6.58	4.16	3.11
MGO	3.32	2.04	1.93	3.69	2.25	1.18
CAO	4.31	4.52	3.07	4.27	2.21	3.68
NA20	6.70	0.63	5.37	3.27	3.06	5.84
K20	0.15	1.92	0.08	0.24	2.47	1.24
TIO2	0.71	0.85	0.73	0.67	0.56	0.49
MNO	0.40	0.17	0.06	0.06	0.01	0.02
P205	0.16	0.25	0.19	0.23	0.08	0.14
LOI	6.40	6.60	3.06	4.71	7.56	3.43
TOTAL	98.33	99.02	99.18	99.04	99.38	101.15
TRACE ELEMENTS (PPM)						
Ba	5.9	163.9		0.0	692.1	319.1
Ce	54.3	27.2		55.5	101.9	84.8
Cu	6.0	16.8		5.9	12.3	225.7
Ni	81.3	29.1		87.2	82.6	29.5
Rb	3.7	43.0		6.7	83.7	43.8
S	3.2	11.6		0.0	11.9	72.3
Sr	220.1	72.5		243.4	105.1	284.8
Y	13.8	18.3		19.6	22.3	10.8
Zn	16.0	33.7		16.0	53.0	14.4
Zr	181.3	179.7		183.1	112.2	177.6
NORMATIVE MINERALS						
Q	3.71	29.76	14.40	22.21	23.08	17.58
OR	0.89	11.35	0.47	1.42	14.60	7.33
AB	56.68	5.33	45.43	27.66	25.89	49.40
AN	8.14	20.79	13.99	19.68	10.44	13.83
NE						
C		4.95	1.55	2.69	4.86	
CPX	9.99					2.90
OPX	8.92	15.95	16.50	17.16	9.85	4.19
OL						
MT	3.20	3.41	3.23	3.15	2.99	2.89
IL	1.35	1.62	1.39	1.27	1.07	0.93
RU	0.01	0.01	0.01	0.01	0.01	0.01
AP						
U.T.M. GRID REFERENCE	802588	833610	798574	804589	799624	804627

Donut Lake Formation

SAMPLE NO.	235	19	264	266	224	228	226	230	232	18
MAJOR OXIDES (Wt.%)										
SIO2	40.48	42.45	41.02	41.21	41.62	42.38	42.95	43.82	43.54	51.49
AL203	4.50	5.41	6.01	5.85	6.59	8.35	6.85	7.81	8.56	8.56
FE203	10.01	10.95	11.47	10.88	11.32	12.63	12.27	12.58	12.88	10.53
MGO	28.93	30.70	26.23	26.37	22.96	23.59	22.64	23.27	22.24	19.05
CAO	4.02	5.41	4.99	10.89	5.92	5.83	5.74	6.61	6.63	7.39
NA20	0.00	0.50	0.43	0.15	0.33	0.00	0.59	0.00	0.17	0.46
K20	0.02	0.02	0.04	0.02	0.04	0.02	0.11	0.02	0.04	0.06
TIO2	0.35	0.43	0.38	0.33	0.33	0.52	0.36	0.49	0.49	0.58
MNO	0.00	0.15	0.00	0.03	0.07	0.00	0.06	0.00	0.00	0.02
P205	0.09	0.01	0.03	0.02	0.04	0.04	0.08	0.06	0.08	0.01
LOI	9.30	6.70	8.14	6.69	11.35	7.10	17.41	6.40	5.90	1.85
TOTAL	97.70	102.72	99.34	102.43	100.58	100.47	99.06	101.05	100.53	100.01
TRACE ELEMENTS (PPM)										
Ba	0.0		0.4		28.6		77.6	38.1	47.7	124.2
Ce	42.0		10.4		5.9		9.3	8.0	20.3	0.0
Cu	5.6		3.2		18.6		3.7	3.5	77.0	23.9
Ni	1958.7		1654.4		1408.9		1546.4	1303.7	1207.0	976.3
Rb	0.0		0.0		0.0		0.6	0.7	0.0	0.0
S	42.0		1110		56.0		1288.0	47.0	54.0	1315.0
Sr	2.3		0.0		33.4		11.7	5.3	23.6	34.7
Y	4.7		2.9		1.1		0.2	7.5	3.5	5.5
Zn	43.4		47.8		59.0		56.2	35.2	54.1	29.2
Zr	14.8		19.5		22.5		21.4	22.5	21.7	25.6
NORMATIVE MINERALS										
Q										1.04
OR	0.12	0.12	0.12		0.24	0.12	0.65	0.12	0.24	0.35
AB		4.23	2.62		2.79		4.99		1.44	3.89
AN	12.22	12.45	14.51		16.38	22.72	15.70	21.24	22.47	21.11
NE										
C										
CPX	5.69	11.40	7.64		10.20	4.67	9.83	8.96	7.96	12.42
OPX	27.74	10.37	28.76		26.32	31.22	26.06	33.47	30.69	56.24
OL	39.95	54.53	32.28		30.58	31.29	31.44	27.68	28.55	
MT	2.68	2.80	2.28		2.65	2.93	2.70	2.89	2.89	3.02
IL	0.67	0.82	0.86		0.63	0.99	0.68	0.93	0.93	1.10
RU		0.01	0.01			0.01		0.01	0.01	0.01
AP										
U.T.M. GRID REFERENCE	731369	734372	730374	731373	733372	730370	732371	731370	731368	733374

	Dunite-Peridotite									
SAMPLE NO.	7	9	13	19	18	16	8	17	21	20
MAJOR OXIDES (Wt.%)										
SIO2	28.95	31.07	29.99	34.10	33.74	38.77	34.16	38.97	33.12	36.58
AL2O3	0.81	0.89	1.14	0.71	1.64	1.38	1.92	1.63	2.34	1.48
FE2O3	12.29	9.81	5.40	8.60	8.54	7.49	5.36	8.25	15.41	16.00
MGO	39.60	39.28	34.71	39.68	38.13	39.83	37.06	37.32	36.05	36.88
CAO	0.43	0.17	0.07	1.21	1.52	0.47	3.88	1.58	1.18	0.04
NA2O	0.03	0.03	0.31	0.75	0.49	0.51	0.15	0.00	0.04	0.00
K2O	0.01	0.01	0.01	0.01	0.01	0.01	0.02	0.02	0.02	0.01
TIO2	0.07	0.07	0.03	0.05	0.14	0.11	0.09	0.07	0.18	0.06
MNO	0.06	0.05	0.20	0.05	0.06	0.01	0.30	0.20	0.00	0.00
P2O5	0.01	0.01	0.04	0.01	0.02	0.01	0.03	0.07	0.01	0.03
LOI	17.13	16.80	29.60	14.32	13.88	12.49	17.78	13.97	10.41	10.49
TOTAL	99.39	98.19	101.49	99.47	98.17	101.09	100.83	102.07	98.75	101.57
TRACE ELEMENTS (PPM)										
Ba	0.0	0.0				0.0			33.9	
Ce	67.0	75.9				67.6			21.7	
Cu	9.4	20.2				13.5			11.4	
Ni	2175.0	2428.8				2405.8			1869.0	
Rb	0.0	0.4				3.1			3.7	
S	37.9	152.2				146.2			100.8	
Sr	0.0	0.0				7.2			0.0	
Y	0.0	0.0				0.0			0.0	
Zn	8.4	35.6				46.0			47.3	
Zr	9.1	4.8				2.0			9.5	
NORMATIVE MINERALS										
Q										
OR			0.06			0.06				
AB			2.62			4.31				
AN			0.09			1.45				
NE										
C			0.59							
CPX						0.64				
OPX			1.75			9.32				
OL			65.21			71.09				
MT			2.22			2.33				
IL			0.06			0.21				
RU										
AP										
U.T.M. GRID REFERENCE	769596	769584	814603	804609	809611	809607	775592	809603	804613	804611

APPENDIX II
GEOCHEMISTRY

SAMPLING AND SAMPLE PREPARATION

Sampling of all the formations in the study area is based on several criteria: 1) sampling was done on the chilled margins of the volcanic rocks, or fine grained lavas were chosen if flow contacts were not exposed, 2) all extensively altered, sheared or carbonatized rocks were avoided, 3) sampling of the variolitic flows was achieved in most cases from pillow centres where the concentration of varioles is less, 4) most porphyritic, agglomeratic, brecciated, lapilli tuff or tuffs of the felsic rocks were sampled using the matrix material where possible. Most samples weighed from 0.5 to 3 kg. Rock samples were slabbed for thin sectioning and the remaining fresh chips were dried and ground in a tungsten-carbide shatter box to less than 200 mesh. Analytical methods are outlined as follows:

I. Loss on ignition

Method:

1) dry sample in oven for 1-2 hours, above 100°C.
2) dry ceramic crucible on hot plate or in oven above 100°C.
3) let both stand in dessicator until room temperature is attained
4) weigh crucible and 1.0000gram of sample
5) heat in muffle furnace at1100°C for 30 minutes
6) remove crucible, and place in dessicator until at room temperature
7) reweigh crucible and the change in weight is calculated as a weight percent of the sample.

II Major Oxide Glass Disc Preparation

Method:

1) 1.0000 gm. of sample is mechanically mixed with 10.0000 gms. of flux (90% lithium tetraborate + 10% lithium carbonate) plus the difference in weight of flux occurred by the sample during the loss on ignition process to preserve the 10:1 weight ratio

2) this mixture is placed in a platinum crucible and heated to 1100^{o}C for 30 minutes in a muffle furance, the crucible is swirled several times to ensure homogeneity and complete dissolution of the sample

3) the mixture is then poured into a non-wetting platinum mold and placed on ceramic beads over a bunsen burner and allowed to cool slowly or until no convection cells are visible in the sample, turn the bunsen burner off and allow to cool, the disc is ready to analyize

III Trace Element Powder Pack Preparation

Method:

1) dry sample, and weigh out 15.0000 gms.

2) add 2.0000gms. of binding agent and mechanically mix

3) pour sample into aluminium powder dish and press with more than 20 tons per sq. inch pressure for 30 seconds

The samples were then analysed using a Phillips Sequential X-Ray Fuorescence analysis system PW 1420 with the counts and time recorded on a data cassette and printer. The data were analysedby a Burrows 6700 computer for major oxides (not "mac" corrected) and trace elements ("mac" corrected).

Fourteen U.S.G.S. standards were used for the calibration of the Phillips PW 1420 in order to determine the unknown samples.

The U.S.G.S. standards used are listed below.

RGM-1	Rhyolite
AGV-1	Andesite
BCR-1	Basalt
BHVO	Basalt
DTS-1	Dunite
PCC-1	Peridotite
PPB	(3.5 gms. PCC) + (4.0 gms. BCR-1)
P-B	(½ PCC) + (½ BHVO)
GSP-1	Granodiorite
G-2	Granite
SCO	Cody Shale
QLO	Quartz Latite
STM	Kyanite Schist
SDC	Biotite-Muscovite Shist

The Phillips PW 1420 parameters used for the analysis of the major elements are listed below.

Major Element Parameters

Element	Det.	Coll.	Crystal	2θPk.	2θBkg.	Count Time	LL	Window	KV	MA
Si	Flow	coarse	PET	109.42	108.70	4	250	500	50	45
Al	Flow	coarse	PET	145.48	144.37	10	200	800	50	45
Fe	Flow	fine	LiF200	57.52	56.50	4	150	750	50	45
Mg	Flow	coarse	TLAP	45.37	44.83	20	250	700	50	45
Ca	Flow	coarse	LiF200	113.35	114.85	2	50	600	50	45
Na	Flow	coarse	TLAP	55.27	55.05	20	300	400	50	45
K	Flow	coarse	LiF200	136.94	135.60	10	300	400	50	45
Ti	Flow	coarse	LiF200	86.30	85.20	10	250	700	50	45
Mn	Flow	fine	LiF200	56.65	56.84	20	150	750	50	45
P	Flow	coarse	GE	141.16	140.54	10	200	800	50	45

Major element analyses performed on the standard rocks are presented below in graph form.

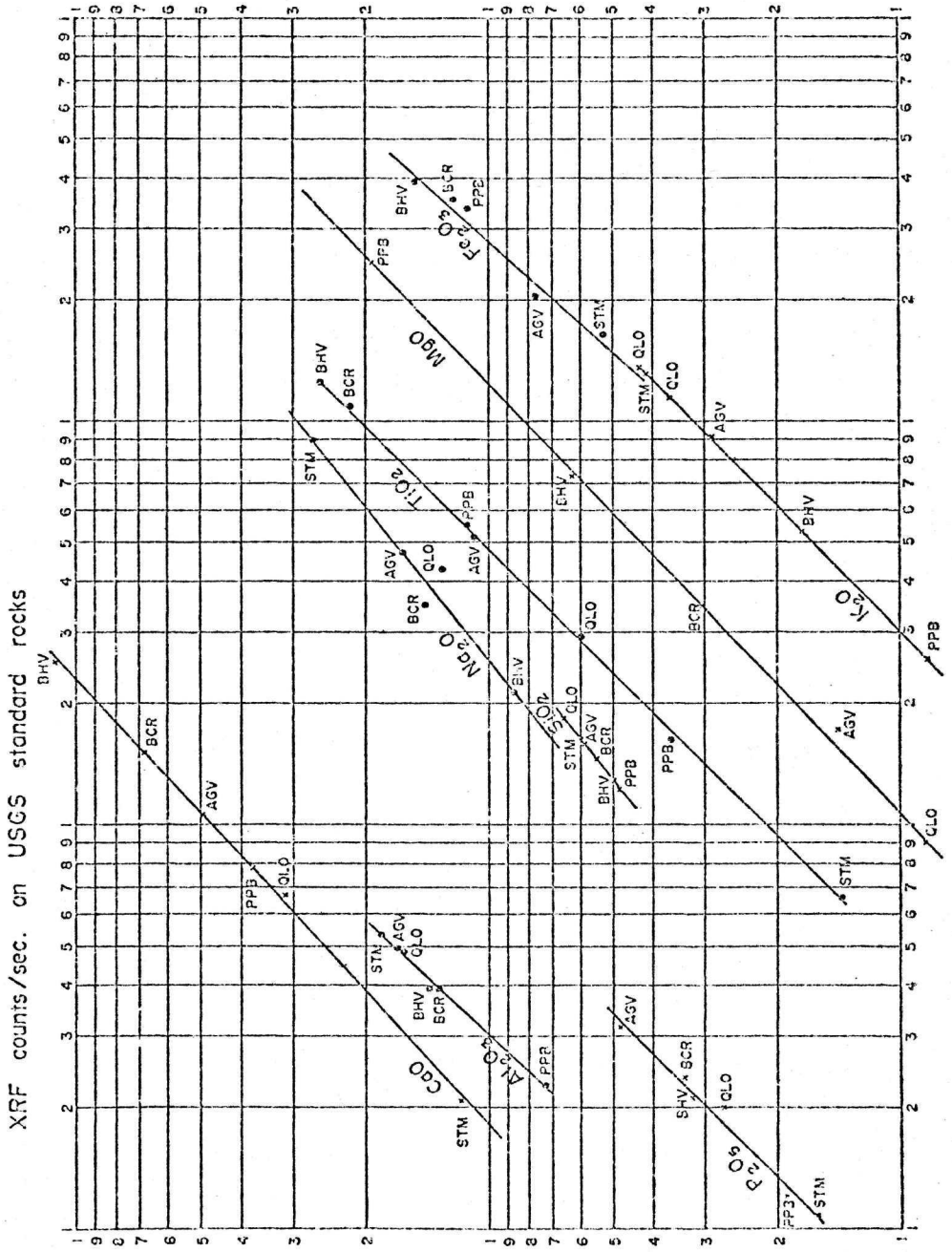

The results of the statistical tests carried out on the standard rocks for the major elements produced a standard limit of error for each element which are listed below, and expressed as % amount present.

To maintain proper precision limits for the unknown samples, a minimum of 3 U.S.G.S. standards were rerun after 12 unknown samples.

% Amount Present

$SiO_2 = \pm 1.0$

$Al_2O_3 = \pm 1.0$

$Fe_2O_3 = \pm 0.2$

$TiO_2 = \pm 0.1$

$K_2O = \pm 0.05$

$Na_2O = \pm 0.30$

$MgO = \pm 0.05$

$MnO = \pm 0.05$

$CaO = \pm 0.20$

$P_2O_5 = \pm 0.05$

The Phillips PW 1420 parameters used for analysis of the trace elements are presented below.

Minor Element Parameters

Element	Det.	Coll.	Crystal	2θPk.	2θBkg.	Count Time	LL	window	KV	MA
Ba	Scint.	fine	LiF200	11.02	11.50	20	250	500	50	45
Ce	Scint.	fine	LiF200	10.22	9.22	40	250	500	50	45
Cu	Scint. flow	coarse	LiF200	45.10	45.60	40	300	400	60	45
Ni	Scint. flow	coarse	LiF200	48.78	48.00	40	250	500	60	45
Rb	Scint.	fine	LiF200	26.30	26.57	20	300	400	50	45
S	flow	coarse	Ge	109.20	110.79	20	200	800	50	45
Sr	Scint.	fine	LiF200	25.12	24.75	20	250	500	50	45
Y	Scint.	fine	LiF200	23.72	23.50	20	250	500	60	45
Zn	Scint. flow	coarse	LiF200	41.90	41.20	40	300	400	60	45
Zr	Scint.	fine	LiF200	22.48	22.95	20	300	400	50	45

Trace element analysis of the standard rocks are presented below in graph form.

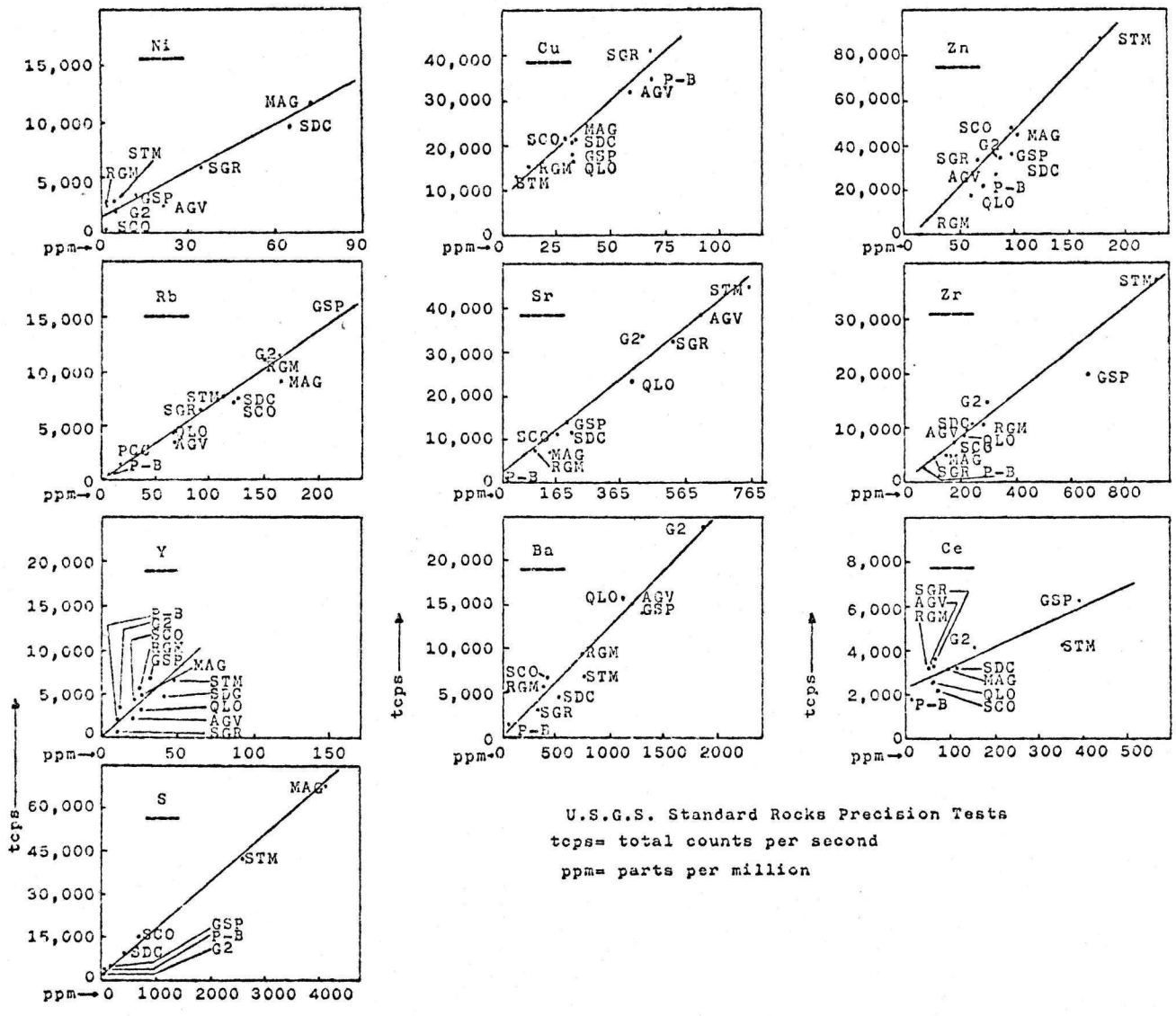

U.S.G.S. Standard Rocks Precision Tests
tcps= total counts per second
ppm= parts per million

The statisical tests of the standard rocks for the trace elements are presented below where, r= correlation coefficient, s(x,y)= standard limit of error and y= least squares solution of the equation of the line.

Nickel	Copper	Zinc
r=0.99	r=0.93	r=0.94
s(x,y)=10.79	s(x,y)=8.66	s(x,y)=14.39
y=0.12x-17.28	y=0.11x-42.65	y=0.07x+23.02

Rubidium	Strontium	Zirconium
r=0.97	r=0.98	r=0.97
s(x,y)=18.40	s(x,y)=50.12	s(x,y)=47.76
y=0.30x+5.30	y=0.33x-18.01	y=0.13x+78.20

Yttrium	Barium	Cerium
r=0.74	r=0.98	r=0.91
s(x,y)=9.33	s(x,y)=129.73	s(x,y)=54.56
y=0.09x+6.38	y=1.57x+58.02	y=3.46x-167.13

A minimun of 9 U.S.G.S. standards were rerun after 12 unknown samples to maintain proper precision limits.